COMPARATIVE FEEDING BIOMECHANICS AND BEHAVIORAL PERFORMANCE OF FEEDING IN THE FAMILY KOGIIDAE AND *TURSIOPS TRUNCATUS* (ODONTOCETI, CETACEA)

A Thesis

by

BRIAN EDWARD BLOODWORTH

Submitted to the Office of Graduate Studies of
Texas A&M University
in partial fulfillment of the requirements for the degree of

MASTER OF SCIENCE

May 2006

Major Subject: Wildlife and Fisheries Sciences

COMPARATIVE FEEDING BIOMECHANICS AND BEHAVIORAL PERFORMANCE OF FEEDING IN THE FAMILY KOGIIDAE AND *TURSIOPS TRUNCATUS* (ODONTOCETI, CETACEA)

A Thesis

by

BRIAN EDWARD BLOODWORTH

Submitted to the Office of Graduate Studies of
Texas A&M University
in partial fulfillment of the requirements for the degree of

MASTER OF SCIENCE

Approved by:

Chair of Committee,	Christopher D. Marshall
Committee Members,	Daniel F. Cowan
	Markus Horning
	Jane M. Packard
	Raymond J. Tarpley
Head of Department,	Robert D. Brown

May 2006

Major Subject: Wildlife and Fisheries Sciences

ABSTRACT

Comparative Feeding Biomechanics and Behavioral Performance of Feeding in
the Family Kogiidae and *Tursiops truncatus* (Odontoceti, Cetacea). (May 2006)
Brian Edward Bloodworth, B.S., Texas A&M University at Galveston
Chair of Advisory Committee: Dr. Christopher D. Marshall

Hyolingual biomechanics and kinematics in three species of two odontocete genera were investigated to compare adaptations and performance of divergent feeding strategies. Ram and suction feeding are two ends of a continuous spectrum that is poorly-studied in odontocetes. Comparative anatomy identified characters associated with feeding patterns of morphologically dissimilar and evolutionary distant genera. Hyolingual investigations included measurements of hyolingual muscle vectors and hyoid surface area/robustness. ANOVA's revealed *Kogia* basihyal and thyrohyal surface areas were significantly greater than *T. truncatus*. However, most predicted muscle tension values were not significantly different between genera. The presence of lateral gape occlusions, broad basihyal and thyrohyals near the caudal oral cavity, and a broad, short tongue were likely responsible for *Kogia*'s effective suction mechanism. These features were absent, or reduced, in *T. truncatus*.

The feeding kinematics of dwarf and pygmy sperm whales (*Kogia sima* and *K. breviceps*), and bottlenose dolphins (*Tursiops truncatus*) were characterized and compared incorporating the Ram-Suction Index (RSI). Mean RSI data support a suction feeding strategy for the phylogenetically basal *Kogia* (-0.67; S.D.±0.29) and a ram feeding strategy for the more-derived *Tursiops* (0.94; S.D.±0.11). *Tursiops* displayed two ram-based feeding behaviors, closed gape approach, where gape increased near food items, and open gape approach, where gape was at least 50% of maximum in the first video field. Four feeding phases were identified in both odontocetes: preparatory, jaw opening, gular depression, and jaw closing. The mean *Kogia* feeding cycle duration (470 ms; S.D.±139) was significantly shorter ($P<0.003$) than all *Tursiops* groups (pooled: 863 ms; S.D.±337, closed gape approach: 662 ms; S.D.±207, open gape approach: 1211 ms; S.D.±207). *Kogia* mean maximum gape angle (39.8˚; S.D.±18.9), mean maximum opening, and closing gape angle velocities (293˚/s; S.D.±261 and 223˚/s; S.D.±121, respectively) were significantly greater ($P<0.005$) than pooled *Tursiops* mean maximum gape angle (24.8˚; S.D.±6.6), mean maximum opening and closing gape angle velocities (84˚/s; S.D.±56 and 120˚/s; S.D.±54, respectively). Negative *Kogia* RSI values were correlated with increasing maximum hyoid depression and retraction, wide gape angle, and rapid opening gape velocity. Kinematic data support functional hypotheses that odontocetes generate suction by rapid depression of the hyoid and tongue.

ACKNOWLEDGEMENTS

I thank several individuals and organizations for their assistance in the studies conducted. My committee chair and advisor, Dr. Christopher D. Marshall provided me with the opportunities to conduct this research. My committee members, Daniel Cowan, Jane Packard, Markus Horning, and Raymond Tarpley were also invaluable in their constructive critique of these studies. I thank Nélio Barros, Petra and David Cunningham-Smith, Charles Manire, and the volunteer staff of Mote Marine Laboratory and the Dolphin and Whale Hospital in Sarasota, Florida. Without their assistance in all aspects of these studies, this thesis would not have been possible. Daniel Cowan and the staff and volunteers of the Texas Marine Mammal Stranding Network were likewise instrumental in providing specimens for the anatomical portion of this thesis. Dudley Wigdahl and the zoological staff of SeaWorld of Texas also provided essential opportunities for videography of bottlenose dolphins. I acknowledge the Southeast United States Stranding Network of the National Marine Fisheries Service for the opportunity to conduct this research. Funding was provided by the Texas Institute of Oceanography, Department of Marine Biology at Texas A&M University at Galveston, Texas A&M University Regents Fellowship to BEB and the Erma Lee and Luke Mooney Graduate Travel Grant.

I sincerely thank my loving wife Michelle, without whose support this project may not have reached fruition. My mom and dad, Janice and Kenneth, were both critical in helping me complete this degree.

TABLE OF CONTENTS

LIST OF FIGURES

LIST OF TABLES

CHAPTER I

INTRODUCTION

1.1 Statement of Problem

Odontocete (toothed whale) feeding behavior has been studied for over 50 years and produced a wealth of information on a variety of predatory aspects. Such work has focused on diet (e.g., Slijper 1962, Barros and Odell 1990, Cockcroft and Ross 1990*a*, Werth 2000*b*), behavior (e.g., Herman 1980, Bel'kovich 1991, Wells et al. 1999, Connor et al. 2000, Gannon et al. 2005), distribution and movement patterns (e.g., Slijper 1962, Kenney 1990, Forcada 2002), and physiology (e.g., Pabst et al. 1999, Clarke 1978, 2003, Stewart 2002). Additionally, the morphological and evolutionary diversity of odontocete taxa supports widely different feeding strategies (e.g., Berta and Sumich 1999). However, few studies have addressed the functional morphology or biomechanics of odontocete feeding to validate functional hypotheses of how these strategies operate (e.g., Werth 2000*b*). The goals of this thesis are to characterize and compare the biomechanical and behavioral aspects of prey capture in two widely-dissimilar odontocete genera, *Kogia* (pygmy and dwarf

---

This thesis follows the style of *Marine Mammal Science*.

sperm whale) and *T. truncatus* (bottlenose dolphins). Results will clarify odontocete feeding strategies in an ecological and evolutionary context.

The feeding strategy of *Kogia* is of particular interest due to their basal phylogenetic position within Odontoceti and relatively distant evolutionary relationship to delphinids (Milinkovitch et al. 1994, Berta and Sumich 1999, Geisler and Sanders 2003). In addition, *Kogia* possess characteristics typical of odontocetes that presumably use suction. The snout is blunt and the mouth is short, with reduced dentition; few, if any, teeth are present in the maxillae. The gracile, under slung mandibles contain up to 16 pairs of fang-like teeth (Handley 1966, Ross 1978, Caldwell and Caldwell 1989) that are likely advantageous in retaining squid in the mouth. As in other potential suction feeding odontocetes, *Kogia* are primarily teuthophagous (Pinedo 1987, Klages et al. 1989, Dos Santos and Haimovici 2001, Wang et al. 2002). The derived oral morphology in other species would appear to physically restrict the feeding mode to obligatory suction feeding. For example, male strap-toothed beaked whales (*Mesoplodon layardii*) possess single pairs of mandibular teeth that grow over the maxillae and constrain the jaws beyond a minimal gape that would make ram-based prey capture difficult (Heyning and Mead, 1996). The throat grooves and enlarged hyolingual musculature of ziphiids, physeterids, and kogiids are presumably adaptations for increasing oral volume related to suction feeding (Clarke et al. 1968, Reidenberg and Laitman 1994, Heyning and Mead 1996, Werth 2005). Robust hyolingual musculature is also present in the short-finned pilot whale

(*Globicephala melas*; Werth 1992, Reidenberg and Laitman 1994), which is the only odontocete in which a kinematic feeding investigation has validated the use of suction (Werth 2000*a*).

1.2 *Kogia* Life History

1.2.1 Morphology

Kogia is a poorly-known genus most closely related to sperm whales (*Physeter macrocephalus*), but separated into its own family (Kogiidae; Rice 1998) based upon cranial morphology (Gill 1871, Schulte 1917, Heyning 1989, Bianucci and Landini 1999) and genetic distance (Árnason et al. 1993, Milinkovitch et al. 1994, Ross et al. 2003). Kogiidae is composed of two morphologically similar species, the dwarf sperm whale (*K. sima*) and pygmy sperm whale (*K. breviceps*). Both species are robustly built, counter-shaded dark-gray dorsolaterally and cream ventrally, with a light crescent pigmentation on either lateral meatus termed the “false gill” (Hubbs 1951, Yamada 1954, Hale 1963, Ross 1978). The two species are accurately differentiated by cranial characters, such as dorsal cranial fossa slope, sagittal septum slope, condylobasal length, and mandibular symphasis length (Yamada 1954, Handley 1966, Ross 1978, Nagorsen 1985, Huckstadt and Antezana 2001). External characters, such as dorsal fin height and placement, tooth count, presence of throat grooves, total body length, melon shape, and eye placement allow for rapid but less accurate species diagnosis (Yamada 1954, Handley 1966, Ross 1978, Leatherwood and Reeves 1983, Nagorsen 1985, Caldwell and Caldwell

1989, Wynne and Schwartz 1999, Huckstadt and Antezana 2001). Although not recognized as separate species until 1966 (Yamada 1954, Handley 1966), data from stranded *K. sima* and *K. breviceps* have helped clarify *Kogia* life history. *Kogia sima* are born at approximately 1.0 m (Handley 1966, Ross 1978) and may reach 2.7 m (Handley 1966, Ross 1978) and 280 kg (Leatherwood et al. 1988). *Kogia breviceps* are generally larger; length at birth averages1.2 m (Caldwell and Golley 1965, Caldwell et al. 1971*b*, Ross 1978) and individuals may reach 4.25 m in length (Caldwell et al. 1971*b*) and 417 kg (Tomilin 1957). Sexual maturity is attained at 2.1-2.2 m for both *K. sima* sexes, while *K. breviceps* females become mature at 2.7-2.8 m versus 2.7-3.0 m for males (Ross 1978). Conception and parturition have been proposed to occur from autumn to spring for *K. breviceps* (Caldwell et al. 1971*a, b,* Ross 1978, Leatherwood and Reeves 1983, Nagorsen 1985, Leatherwood et al. 1988, Caldwell and Caldwell 1989, Wynne and Schwartz 1999). However, the paucity of data on free-ranging *Kogia* (Baird et al. 1993) leaves this area unresolved and life expectancy, movement patterns and ecological parameters are virtually unknown.

1.2.2 Abundance and Diet

Kogia life history is sparsely described primarily due to the genera's deep-water distribution, cryptic coloration (Balance and Pitman 1998, Mullin and Fulling 2004), inconspicuous surface blows (Leatherwood et al. 1988) and long dive durations (Scott et al. 2001, pers. obs.). Shipboard observations from the eastern tropical Pacific indicate that *K. sima* remains generally pelagic while *K. breviceps* is more-common in continental shelf and slope waters (Robert Pittman pers. comm.). However, Ross (1978) suggested an inverse occurrence in South Africa based on proportions of nearshore versus offshore prey in the stomachs of stranded specimens. In the Gulf of Mexico (GOM), *Kogia* are present year-round in water depths of 400-3500 m, but are most-frequently observed in regions of 400-1000 m (Mullin et al. 1994, Davis et al. 1998, Baumgartner et al. 2001). These areas include locations of frequent upwelling events that concentrate zooplankton biomass and cephalopod prey along the continental shelf (Davis et al. 1998). *Kogia* stomach content analyses support deep-water cephalopods as the staple diet, with myctophid fishes and shrimps as secondary prey (Fitch and Brownell 1968, Ross 1978, 1984, Pinedo 1987, Klages et al. 1989, McAlpine et al. 1997, Wang et al. 2002). Stomach contents (Gaskin 1967, Fitch and Brownell 1968, Nagorsen 1985), hemoglobin oxygen binding capacity (Lenfant 1969), and long dive durations (Scott and Cordaro 1987, pers. obs.) support a deep-diving ability in *Kogia*.

1.2.3 Distribution

Strandings and shipboard sightings confirm a worldwide temperate and tropical *Kogia* distribution. *Kogia* have been reported in the Pacific from Chile (Sanino and Yaňez 1996) north to Mexico (Vidal et al. 1987) and Canada (Nagorsen 1985), west through Hawaii (Nitta 1991), Guam (Kami and Lujan 1976), New Caledonia (Sylvestre 1988), Japan (Yamada 1954), and Australia

(Hale 1962). In the Atlantic, *Kogia* occur along the Brazilian coast (Pinedo 1987), in the Caribbean Sea (Caldwell et al. 1973), and near the United States and Canada (McAlpine et al. 1997). This range extends eastward to Senegal (Maigret and Robineau 1981), the Azores (Martins et al. 1985), Spain (Abollo et al. 1998), and northern Europe, as well as the Mediterranean Sea (Baccetti et al. 1991). In the Indian Ocean, stranded *Kogia* have been documented from South Africa (Ross 1978), Oman (Gallagher and van Bree 1980), India (Owen 1867), and Australia (Hale 1963). When sighted in the GOM, *Kogia* are usually solitary, but may form groups of up to eight individuals (Mullin et al. 1994, Baumgartner et al. 2001). These association data support limited *Kogia* inter- and intra-specific interactions (Balance and Pitman 1998) and little or no reliance on groups for feeding and anti-predatory strategies. However, there are few published *Kogia* field studies and most individual-based information has come from live stranded specimens.

1.2.4 *Kogia* in Captivity

Kogia are difficult to maintain in captivity. Sylvestre (1983) reported that of 33 rehabilitation attempts in the United States, all died within one month. Mote Marine Laboratory (MML) in Sarasota, Florida has engaged in the most extensive and successful rehabilitations of live stranded *Kogia*, but have not yet been able to permanently maintain or release them. The longest captive durations for *K. sima* and *K. breviceps* were at MML, where subjects involved in this thesis study survived for 21 and 15 months, respectively. Necropsies of unsuccessful *Kogia* rehabilitations have identified gastrointestinal ruptures, blockages, torsions or impactions and stress-induced cardiomyopathy as most-frequent causes of death (Manire et al. 2004). These findings support veterinary observations that *Kogia* are acutely affected by dietary and environmental changes (Manire et al. 2004). Although rehabilitations of *Kogia* at MML have not yet led to their release or permanent maintenance, this facility provides unique research opportunities to address basic biological questions in Kogiidae.

1.3 *Tursiops truncatus* Life History

Bottlenose dolphins (*T. truncatus*) are generally regarded as the most-thoroughly studied cetaceans to date (Wells and Scott 2002, Bernd Würsig pers. comm.) and have been the subjects of extensive observation. Atlantic bottlenose dolphins are countershaded light-gray to nearly black dorsolaterally and cream to pink ventrally. Body size is robust, with recorded total lengths up to 400 cm, but normally only reaching 300 cm (Fraser 1974, Leatherwood et al. 1988, Cockcroft and Ross 1990*b*, Mead and Potter 1990). Depending upon population, neonates are born at 84 to 140 cm (Wells and Scott 2002) during a calving season generally in late-spring to early-summer (Leatherwood et al. 1988, Scott et al. 1990, pers. obs.). Sexual maturity is reached at 5 to13 years (> 230 cm) for females and 9 to 14 years (> 235 cm) for males (Ross and Cockcroft 1990*b*). Females may be reproductive for up to 48 years of age (Wells and Scott 1999) and produce a calf every 3-6 years (Connor et al. 2000).

Bottlenose dolphins are known to be highly-social odontocetes, typically forming groups of 2-15, but groups in excess of 1000 individuals have been documented (Scott et al. 1990, Wells and Scott 2002). *Tursiops truncatus* occurs worldwide in nearshore and pelagic habitats throughout temperate and tropical marine waters (Wells and Scott 2002). Foraging strategies for bottlenose dolphins are also known to be diverse and many behavioral strategies have been documented, such as: beaching in pursuit of prey (Hoese 1971, Rigley 1983), crater-feeding (Rossbach and Herzing 1997), cooperatively herding fish (Leatherwood 1975, Hamilton and Nishimoto 1977), and interacting with commercial fishery gear (Leatherwood 1975, Fertl and Leatherwood 1997).

1.4 Feeding Kinematics, Behavior and Anatomy

Cetaceans have evolved highly-derived feeding behaviors relative to terrestrial mammalian taxa. Even among cetaceans, feeding adaptations are diverse and are exemplified in the comparison of the suborders Mysticeti (baleen whales) and Odontoceti (toothed whales). Due to their extreme modifications of the oral apparatus, mysticetes have received more scientific attention regarding their feeding biomechanics than odontocetes, which share more similarities in the structure and function of the oral apparatus with terrestrial mammalian taxa than mysticetes (e.g. Pivorunas 1977, Lambertsen 1983, Orton and Brodie 1987, Lambertsen et al. 1995, Lambertsen and Hintz 2004). The stereotypical image of an odontocete is that of narrow, long-snouted delphinids such as bottlenose dolphins, which chase down prey with a clap-trap type of jaw containing numerous homodont teeth (Winge 1921, Howell 1930, Slijper 1962, Norris and Møhl 1983, Heyning 1989, Rommel 1990). However, non-delphinids possess a wider morphological diversity than delphinids (Gaskin 1976). In contrast to the stereotypical odontocete image, many odontocetes possess blunt rostra, reduced dentition (Norris and Møhl 1983, Heyning and Mead 1996, Werth 2000*a*), feed on squid (teuthophagous), and may use suction as their primary mode of prey capture. Examples of such odontocetes include: pilot whales (*Globicephala*; Brown 1962, Werth 2000*a*), harbor porpoises (*Phocoena phocoena*; Kastelein et al. 1997), beaked whales (Ziphiidae; Heyning and Mead 1996), and sperm whales (Physeteridae and Kogiidae; Caldwell et al. 1966, Werth 2005). Elongated rostra are likely not supportive of suction feeding due to the relatively short distances over which negative intraoral pressures are exerted on the water column (Wainwright, 2001), reducing their utility to most delphinids. However, the underlying biomechanics of odontocete feeding have not been systematically investigated. Although there is a wealth of information on odontocete anatomy, there are surprisingly far fewer behavioral investigations to test functional hypotheses based on anatomical studies alone. A rare example of this are negative pressure measurements of suction feeding in captive *P. phocoena* (Kastelein et al. 1997).

The hyoid is the basis of the functional complex associated with mammalian suction feeding (Thexton et al. 1998, Werth 2000*b*). Fishes exploit their dense environment to draw prey into the mouth by rapid hyoid depression, cranial elevation and/or opercular expansion (e.g., Lauder 1985, Edmonds et al. 2001, Sanford and Wainwright 2002). In mammals, effective suction is a result of the hyoid complex and its associated musculature drawing the tongue caudoventrally to rapidly increase oral cavity volume (e.g., German et al. 1992, Thexton et al. 1998, German and Crompton 1996, Thexton et al. 2004). Functional changes, such as increased robustness of the hyoid and its muscles, are advantageous for generating powerful suction forces (Werth 1992). Enlarged hyoids and hyolingual muscles and the presence of throat grooves in *Kogia* suggests a powerful suction capability that could be among the best-developed of odontocetes (Caldwell and Caldwell 1989, Werth 1992, Reidenberg and Laitman 1994). The objective of hyolingual anatomy investigations was to identify dissimilar morphologies in hyoid osteology and myology between *Kogia* and *T. truncatus* to clarify the functional biomechanics of their presumed suction and ram feeding mechanisms.

With the cooperation of MML, the rare opportunity was available to conduct a detailed kinematic investigation of *Kogia* feeding behavior using two species that were kept alive in captivity for more than one year each (Manire et al. 2004). The objective of this study was to characterize the feeding performance and suction capability of *Kogia.* The feeding performance of a presumed ram-based feeder, *T. truncatus*, was also investigated for comparison. Anecdotal observations and morphological data suggest that *Kogia* and *T. truncatus* fall on opposite ends of the ram-suction spectrum. Motion analysis of feeding events allow for the calculation of specific kinematic variables, such as feeding cycles, gape and gular movements that define a feeding event. This analysis also permits measurement of the degree of ram or suction that occurs in a feeding event. Ram and suction are two ends of a feeding continuum frequently studied in aquatic vertebrates and have been addressed by numerous investigators (e.g., Lauder 1985, Aerts 1990, Norton and Brainerd 1993, Motta and Wilga 2001, Wainwright et al. 2001, Carroll et al. 2004). However, such indices have not been applied to odontocetes. Their divergent feeding behaviors and distant evolutionary relationship make *Kogia* and *T. truncatus* interesting candidates for comparative investigations of odontocete feeding performance. Results of these experiments can provide insight into the function of a feeding mode and its utility to diet and habitat use.

1.5 Specific Aims

1. *Investigate hyolingual adaptations in Kogia as suction feeders versus T. truncatus as ram feeders.* This will be accomplished through anatomical dissections of hyolingual myology, hyoid morphometry, and subsequent biomechanical modeling. It is hypothesized that *Kogia* hyolingual muscles are significantly larger and potentially capable of generating greater maximum tensions than *T. truncatus* that would result in more negative intra-oral pressures. It is further hypothesized that *Kogia* stylohyals, thyrohyals, and basihyals are more robust or have a greater

surface area than *T. truncatus* to provide greater attachment area to enlarged hyolingual muscles.

2. *Characterize hyolingual and oral movements associated with Kogia suction and T. truncatus ram feeding*. This will be accomplished by kinematic analysis of feeding in captive *Kogia* and *T. truncatus* subjects. It is hypothesized that *Kogia* prey ingestion occurs primarily by suction feeding. *Tursiops truncatus* is hypothesized to primarily be a ram feeder and utilize significantly different hyolingual kinematics than *Kogia*.

CHAPTER II

MATERIALS AND METHODS

2.1 Hyolingual Anatomy

2.1.1 Specific Aim 1

Investigate hyolingual adaptations in *Kogia* as suction feeders versus *T. truncatus* as ram feeders. It was hypothesized that *Kogia* hyolingual muscles are capable of significantly greater estimated maximum tensions than *T. truncatus* to produce a more forceful hyoid retraction and depression during suction feeding events. To address this, heads of necropsy specimens were dissected and hyolingual muscles excised. Muscle length, mass, width, and height (at center of mass) were measured with vernier calipers and cross-sections photographed for measurement with Image J (NIH, Bethesda, MD). Data were used to calculate predicted maximum tetanic forces for interspecies comparisons. It was also hypothesized that *Kogia* stylohyals, basihyals, and thyrohyals are more robust and exhibited greater surface areas than *T. truncatus* to increase attachment area for hyolingual muscles. This hypothesis was tested by removing and cleaning hyoid bones from necropsy specimens. Photographs of thyrohyals and basihyals were analyzed using Image J to measure ventral surface area. Stylohyal lengths and maximum widths (at the mid-length) were measured with vernier calipers and a ratio taken as an index of stylohyal robustness. *Kogia* and *T. truncatus* surface area and stylohyal ratios were compared by ANCOVA analyses and interspecies differences characterized.

2.1.2 Salvage Collection

The investigation of *Kogia* and *Tursiops* hyolingual anatomy was conducted using salvage material from five *K. sima*, four *K. breviceps* and six *T. truncatus* heads collected from code 2 or 3 stranded specimens with the assistance of the Texas Marine Mammal Stranding Network (TMMSN) and Mote Marine Laboratory (MML) under NOAA Southeast Regional Office Salvage Permit Number SER02-259 to Dr. Christopher Marshall. Life history data from collected specimens are summarized in Table 1. Heads were decapitated during necropsies, and in some cases, transected through the sternohyoideus, thyrohyoideus, cricothyroideus, and sternothyroideus. However, when possible, all hyolingual muscles were retained by the disarticulation of ribs and transecting the ventral cervical musculature and blubber to free the head and sternum from the body. Heads were frozen at -7º to -25º C until thawed for hyolingual dissection.

Table 1. Stranding parameters of specimens used in hyolingual anatomy studies.

Stranding identification	Species	Sex	Condition code	Total length (cm)	Total mass (kg)	Stranding location
GA1120	*K. sima*	F	3	210	unk.	Galveston Island, Texas
MML-0232	*K. sima*	F	2	165.5	47.7	Anna Maria Island, Florida
MML-0233	*K. sima*	F	2	227	66.8	Anna Maria Island, Florida
PA636	*K. sima*	M	2	234	182	Matagorda, Texas
PA716	*K. sima*	F	3E	233	121	Port Aransas, Texas
CMA-01-04B	*K. breviceps*	M	2	141	43.3	Indian Rocks Beach, Florida
PI159	*K. breviceps*	M	3	303	unk.	King Park, Willacy county, Texas
SP371	*K. breviceps*	M	2	317	~454	Texas-Louisiana border
SP378	*K. breviceps*	M	2	270	307	Bolivar, Texas
GA1214	*T. truncatus*	F	3E	248	102	Rollover Pass, Gilcrest Texas
GA1248	*T. truncatus*	M	2	235.5	142	Texas
GA1289	*T. truncatus*	F	2	209	79.5	Crystal Beach, Texas
PA680	*T. truncatus*	F	2	233	105.5	Fishery by-catch; Aransas County, Texas
PA692	*T. truncatus*	M	3	269	211	Mustang Island, Texas
PO432	*T. truncatus*	F	2	232	112	Galveston, Texas

2.1.3 Hyolingual Myology

Dissections of large heads were conducted at the TMMSN's Galveston Necropsy Laboratory while smaller heads, muscles, and hyoids were processed at the Ecological Morphology Laboratory at Texas A&M University at Galveston. Heads were thawed at room temperature or under refrigeration until the blubber softened, at which time features such as teeth, tongue, and cheek morphology, color patterns, blowhole asymmetry, and scar patterns were noted and photographed. To prevent decomposition, iodine was applied to heads before thawing continued.

Hyolingual myology investigations began with classic dissections of extrinsic lingual and hyoid muscles to identify insertions and origins. Muscles of interest included hyoid muscles (sternohyoideus, mylohyoideus, thyrohyoideus, geniohyoideus, stylohyoideus, and interhyoideus) and the tongue's extrinsic muscles (genioglossus, hyoglossus, and styloglossus). The sternothyroideus was measured as a potential laryngeal retractor. Muscle angles were measured relative to the palatal plane (horizontal) *in situ* to assist vector analysis of the hyolingual complex and to calculate potential depressive and retractive tensions of each muscle or muscle groups in biomechanical models of *Kogia* and *T. truncatus* feeding. This was accomplished by placing a protractor along a given muscle and the specimen's long axis. The angle of a muscle's line of pull relative to the body was measured three times at different locations for right and left muscles and a mean calculated. Individual muscles were then removed for cross-sectional area measurements.

2.1.4 Muscle Characterization

Physiological cross-sectional area (PCSA) was obtained following procedures adapted from Spector et al. (1980), Powell et al. (1984), and Loeb and Gans (1986) and morphological cross-sectional area (MCSA) from Gordon (1984) and Huber and Motta (2004). However, following several unsuccessful attempts to measure muscle fiber length in dissected specimens, fiber length was assumed to be equal to muscle length. This assumption was based on data from mammalian strap muscles (McMahon 1984). Each muscle's PCSA was determined following Spector et al. (1980), Powell et al. (1984), and Loeb and Gans (1986):

$$\text{PCSA} = (\text{muscle mass})^*(\cos\theta)/(\text{FL})^*(\text{muscle density})$$

where cos θ was the mean fiber angle relative to a muscle's line of pull, FL was the mean fiber length (cm), and muscle density was assumed to be 1.056 g/cm^3 (Mendez and Key 1960, Murphy and Beardsley 1974). Muscle height and width were also collected. *In situ* muscle angles in the transverse plane were also collected.

The MCSA of each muscle was obtained by photographing a muscle in cross-section at its center of mass with a Nikon Coolpix 885 digital camera. A metric ruler was included for scale. The perimeter was traced from digital photographs three times in Image J and a mean of each muscle's surface area (MCSA) was calculated. Estimated physiological and morphological maximum tetanic tension (PMTT and MMTT, respectively) from PCSA and MCSA were calculated following procedures adapted from Spector et al. (1980), Powell et al. (1984), and Loeb and Gans (1986):

$$\text{PMTT or MMTT} = (\text{CSA})^*(\text{specific tension})$$

where specific tension was assumed to be 22.5 N/cm^2 (Roy et al. 1982, Spector et al. 1980). PMTT (more representative of *in situ* condition) and muscle lines of pull relative to the palatal plane formed vectors in the biomechanical model. Vectors were used to identify the amount of depressive and retractive tension available for hyolingual motion during a feeding event. The overall resultant vector of depressive and retractive tension components was used to identify initial hyolingual movement in response to simultaneous muscle contraction.

2.1.5 Hyoid Osteology

To test the hypothesis that *Kogia* basihyal and thyrohyal surface areas were greater than *T. truncatus*, hyoids were removed, cleared of tissue, and dried for morphometric analysis. The ventral aspects of basihyals and thyrohyals with metric scale were photographed and the perimeter of each bone outlined three times with Image J to calculate a mean ventral surface area for muscle attachment. Each stylohyal was similarly cleared of tissue and dried. The length and maximum width at the mid-length were measured with vernier calipers. A stylohyal robustness index was developed by dividing the width by the length. The tympanohyal, stylohyal, and epihyal arc of rotation in the palatal plane was measured by protractor from digital images of the hyoid in its basal and fully depressed/retracted positions.

2.1.6 Statistical Analyses

Myological and osteological data were grouped by species or genus and analyzed. Comparisons included *K. sima* to *K. breviceps* and *Kogia* to *T. truncatus*. To compensate for scaling effects of body size, Analysis of Covariance (ANCOVA) ($\alpha \leq 0.05$) was used to identify significant differences in cross-sectional area and maximum tetanic tension using total length or mass as covariates (SPSS Statistical Software package 11.0). The most-reliable scaled means were standardized to the total body length that produced the greatest r^2 value. To identify differences in right versus left muscles and hyoid dimensions, one-way Analysis of Variance (ANOVA) ($\alpha \leq 0.05$) identified differences between

Kogia species and *T. truncatus*. Where three or more data points were available for each muscle's PMTT or MMTT, normality was met in all *K. sima*, *K. breviceps*, pooled *Kogia*, and *T. truncatus* groups, with the exception of *K. breviceps* genioglossus MMTT (0.018), pooled *Kogia* hyoglossus MMTT (0.048) and styloglossus PMTT (0.030), and *T. truncatus* geniohyoideus PMTT (0.012).

2.2 Behavioral Performance

2.2.1 Specific Aim 2

Characterize hyolingual and oral movements associated with *Kogia* suction and *T. truncatus* ram feeding. It was hypothesized that *Kogia* ingested prey primarily by suction in several distinct stages while *T. truncatus* was primarily a ram-based feeder and utilized significantly different hyolingual kinematics. To compare and contrast *Kogia* feeding behavior with that of *T. truncatus*, feeding performance trials of captive *Kogia* and *T. truncatus* were conducted. Underwater video of feeding sequences was recorded and addressed by motion analysis. Kinematic variables associated with feeding were measured and compared in and between *Kogia* and *T. truncatus*.

2.2.2 Subjects

One female *K. sima* calf ("Simone") and one female *K. breviceps* calf ("Ami") were subjects of behavioral performance investigations at MML (Sarasota, Florida USA). Data were also collected from two adult male *T. truncatus* subjects at SeaWorld of Texas (San Antonio, Texas USA). Both kogiids stranded and were taken to MML for rehabilitation, where they became the only kogiids to survive for more than one year in a captive setting (Manire et al. 2004). At the time of feeding trials, “Ami” was 10 - 11 months old, weighed 126.5 kg and was 203 cm in total body length. “Simone” was 10 - 12 months of age, had a mean weight of 60 kg and was 160 cm in mean total body length. *Tursiops truncatus* subjects included “Kai,” who was 26 years old, 344 kg and 308 cm in total body length, and “Clicker,” who was over 30 years old, 195 kg and 249 cm in total body length. A total of 236 minutes of footage was collected from *Kogia* feeding trials. A total of 85 minutes of footage was collected from *T. truncatus* feeding trials. All investigations of *Kogia* and *T. truncatus* were approved by Texas A&M University Laboratory Animal Care (AUP#2003-72), SeaWorld, and MML’s Institutional Animal Care and Usage Committee.

2.2.3 Feeding Trials

Feeding performance experiments with *Kogia* were performed during two, two-day sessions at fixed four-hour daytime feeding intervals over three months. Trials were conducted in an eight-meter wide circular pool maintained at a depth of 1.5 meters (Fig. 1A). Subjects were recorded feeding from a lateral perspective using a Sony Handycam Vision DCR-TRV900 or DCR-TRV950 (Shinagawa-Ku, Japan) in an Equinox (Portage, MI USA) underwater housing. Video footage was recorded at 60 fields per second at a shutter speed of 1/500 second. *Kogia sima* subjects were recorded feeding on whole opalescent inshore squid (*Loligo opalescens*) that rested loosely in a trainer’s hand, mantle towards subjects, until drawn into the subjects’ mouths. To standardize camera-

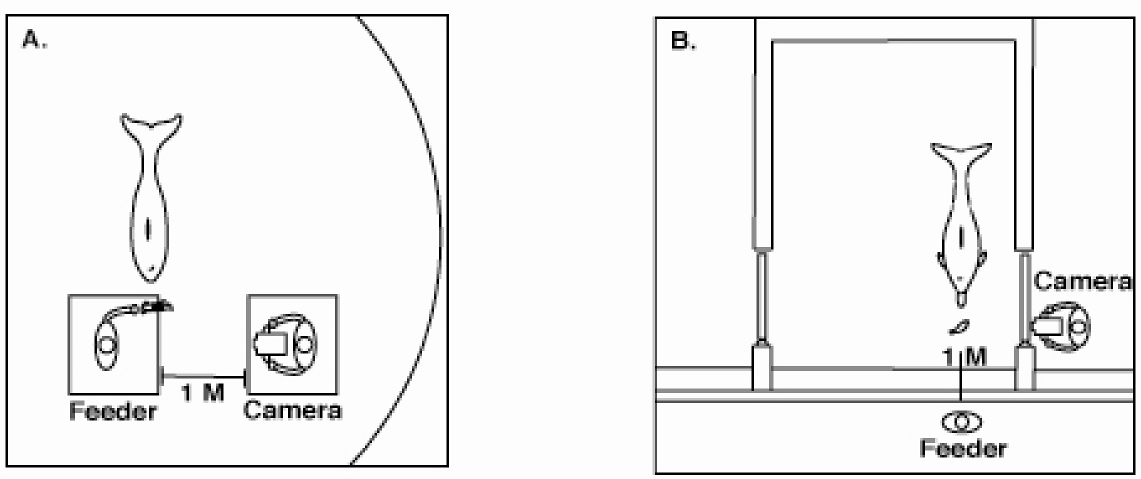

Figure 1. Experimental setup. (A.) *Kogia* at MML and (B.) *Tursiops truncatus* at SeaWorld of Texas. All videotaping was conducted from the lateral perspective. Note one-meter squares for *Kogia* videotaping to maintain relatively constant distance to subject.

to-subject distance, the feeder and camera were stationed in one-meter quadrants placed one meter apart. Subjects were offered food until they no longer showed interest. No *K. breviceps* subjects were in captivity during the study period. Footage of *K. breviceps* was provided subsequent to “Ami’s” death and sequences that met the orientation and landmark criteria of clarity were analyzed.

Tursiops truncatus feeding performance trials were conducted during four, one-day sessions over five months. Subjects were held in a four-meter deep pool and their lateral perspective was videotaped through a metal grated door (Fig. 1B). Subjects were fed herring at a fixed location, one meter from the camera. Herring were held underwater, head towards subjects, by a trainer outside of the pool until subjects approached within two meters, at which time food was released. Feeding trials occurred between 1000 and 1600 hours to minimize variation in light conditions. Natural landmarks such as the center of the eye were identified and, when possible, high-contrast zinc oxide dots were placed on facial and pectoral regions to assist in the identification of homologous landmarks during the digitizing process of data analysis (Fig. 2A and C).

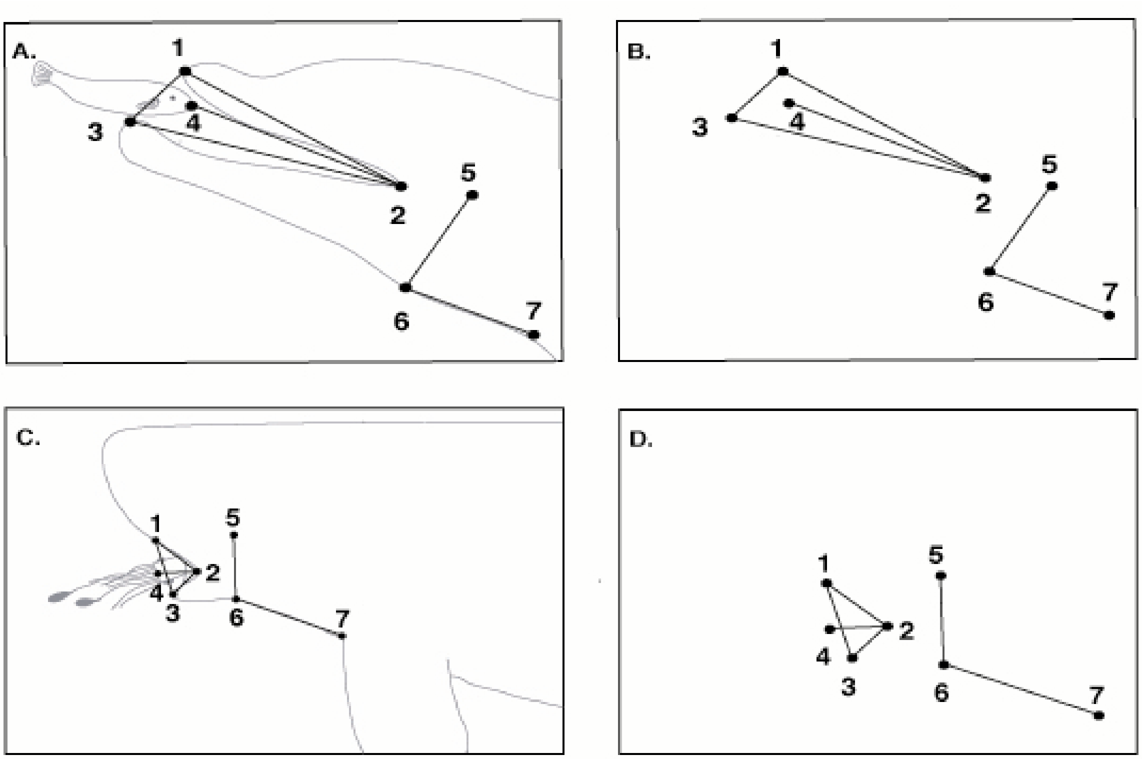

Figure 2. Kinematic landmarks. (A.) *Tursiops truncatus* digitized points identified from footage, (B.) *Tursiops truncatus* spatial model within the motion analysis software, (C.) *Kogia* digitized points from video and (D.) *Kogia* spatial model. Points include (1) maxilla tip, (2) corner of mouth, (3) mandibular tip, (4) food, (5) center of eye, (6) rostral border of externally apparent hyoid, and (7) cranial pectoral fin insertion.

2.2.4 Kinematic Variables and Analyses

A ram-suction index and 16 kinematic variables were calculated from feeding trial footage. A ram-suction index was calculated following Norton and Brainerd (1993):

$$RSI = (D_{predator} – D_{prey}) / (D_{predator} + D_{prey}),$$

where $D_{predator}$ is the subject's net distance traveled and D_{prey} is the food item's net distance traveled. Kinematics from feeding trials of *Kogia* (N = 16) and *T.*

truncatus (N = 30) were analyzed using a motion analysis software package (Peak Motus 8.1, Peak Performance Technologies, Denver, CO USA). Homologous landmarks from each field (Fig. 2) were digitized in each feeding sequence analyzed. Kinematic variables analyzed included: 1.) maximum gape, the maximum distance from maxillary tip to mandibular tip; 2.) time to maximum gape, the duration from when the jaws began to open until maximum gape; 3.) maximum gape angle, the maximum angle from the maxillary tip to mouth vertex or corner of the mouth (COM) to mandibular tip; 4.) maximum opening gape angle velocity, the greatest angular rate of jaw opening; 5.) maximum closing gape angle velocity, the greatest angular rate of jaw closure; 6.) maximum gular depression, the greatest increase in distance from the eye to external rostral border of the hyoid; 7.) time to maximum gular depression, the duration from start of gular depression to maximum gular depression; 8.) maximum gular retraction, the greatest decrease in distance from the cranial pectoral fin insertion to external rostral border of the hyoid; 9.) time to maximum gular retraction, the duration from start of gular retraction to maximum gular retraction; 10.) maximum tongue retraction, the greatest decrease in distance from tongue tip to COM; 11.) predator-food distance, the horizontal distance from the food item to maxillary tip at the start of the feeding cycle; 12.) suction distance, the horizontal distance traveled by the food item during the feeding cycle; 13.) ram distance, the horizontal distance traveled by the predator during the feeding cycle; 14.) maximum food velocity, the greatest change in distance per time of the food in a feeding event; 15) maximum hydraulic jetting, the greatest distance traveled by food when ejected from the mouth during mouth closure; and 16) maximum hydraulic jetting velocity, the greatest change in distance per time of food while exiting the mouth.

2.2.5 Statistics

Normality was calculated with the Shapiro-Wilk normality test ($Z \geq 0.05$) and variance obtained with Levene's test for equality of variance ($s^2 \leq 0.05$). When both variance and normality requirements were met, analyses of variance (ANOVA's) were performed to determine significant differences ($\alpha \leq 0.05$) of kinematic variables between feeding trials. Post-hoc analyses utilized Scheffe's test to determine which subjects and subject groups were significantly different. If variance was significant but normality was met, data were analyzed by independent sample T-tests ($\alpha \leq 0.05$). Non-parametric data were analyzed using Mann-Whitney U tests ($\alpha \leq 0.05$). Correlation analyses assessed the positive or negative relatedness of RSI, timing of feeding events and gape and gular displacements. Pearson's "r" correlation test calculated significant correlations in parametric data and Spearman's rho test was implemented for non-parametric data.

CHAPTER III

RESULTS

3.1 *Kogia* Hyolingual Osteology

The *Kogia* hyoid apparatus was composed of the same elements present in terrestrial mammals: tympanohyal, stylohyal, ceratohyal, epihyal, basihyal, and thyrohyal (Fig. 3). The first three segments, the tympanohyal, stylohyal, and ceratohyal, formed a straight rostroventral and medially directed chain. The epihyal redirected caudally to attach to the expansive basihyal located centrally along the mid-sagittal plane ventral to the proximal hyoid elements. From here, the thyrohyals branched caudolaterally and, with the basihyal, formed a broad surface area for hyal, sternal, and lingual muscle attachment. However, significant reduction of some elements was apparent. In *Kogia* specimens of shorter total body length, the tympanohyals and epihyals consisted of large, cartilaginous rods. In larger specimens, both elements were reduced to small, cartilaginous plates between the stylohyals and tympanic bones (tympanohyal) or ceratohyals (epihyal). *Kogia* basihyals and thyrohyals had a pitted appearance and seemed to have a high volume of empty space within the bone matrix relative to other bones, such as the skull and vertebrae. This apparent low bone density was apparent in all hyal bones, as illustrated by the fact that all ossified hyoid elements floated in water. Caudoventral hyoid movement was less in *K. sima* than in *K. breviceps* due to a thyrohyal-thyroid cartilage ligament that severely limited hyoid mobility. As a result of this, the basihyal and thyrohyals were incapable of movement away from the larynx, although the tympanohyal, stylohyal, and epihyal were free to rotate roughly 30˚ in the palatal plane (Fig. 4A). *Kogia* basihyal and thyrohyals were tightly connected to the stylohyal by the interhyoideus muscle located between the hyoid elements, which prevented significant separation of these elements.

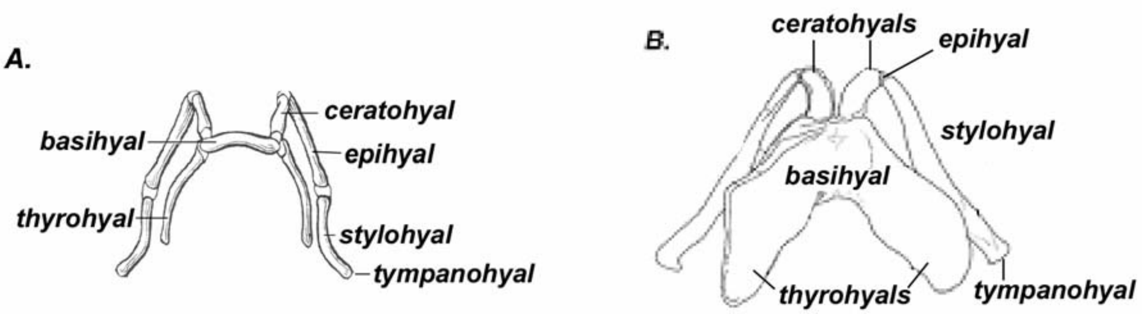

Figure 3. Hyoid apparatus of (A.) *Canis familiaris* (modified from Evans and Christensen, 1979) and (B.) *K. breviceps* (modified from Reidenberg and Laitman, 1994) in ventral view.

The dorsal-most hyoid elements, the tympanohyals, were present as cartilage rods that articulated to the tympanic bone and lacked any apparent muscular attachment. A synovial joint was evident between the tympanohyal and tympanic bone, but no such joint was identified between the tympanohyal and stylohyal. The stylohyal (Fig. 4A, 5A, and 6A) was an ossified, roughly ovoid element in cross-section located between the tympanohyal and epihyal. This stylohyal was relatively longer in specimens of greater total body length and appeared to displace the tympanohyal and epihyal with ontogenetic progression.

The interhyoideus and styloglossus muscles originated from the stylohyal. The *Kogia* epihyal was cartilaginous and had no observed muscular attachment. Stylohyal-epihyal articulation was by a loose, fibrous joint, but epihyal-ceratohyal articulation was unclear. Here, a synovial joint was not found, but may have been cryptic and simply not observed.

As with the epihyal, the *Kogia* ceratohyal was cartilaginous and lacked an apparent synovial articulation to the epihyal. The rostral interhyoideus origin constituted the only muscular attachment to the ceratohyal. The ceratohyal made a sharp ventrocaudal and medial turn to form a cryptic synovial joint to the basihyal. This element bridged the three prior long, straight hyoid chain sections to the broad, flattened basihyal and thyrohyals to which most hyolingual musculature attached.

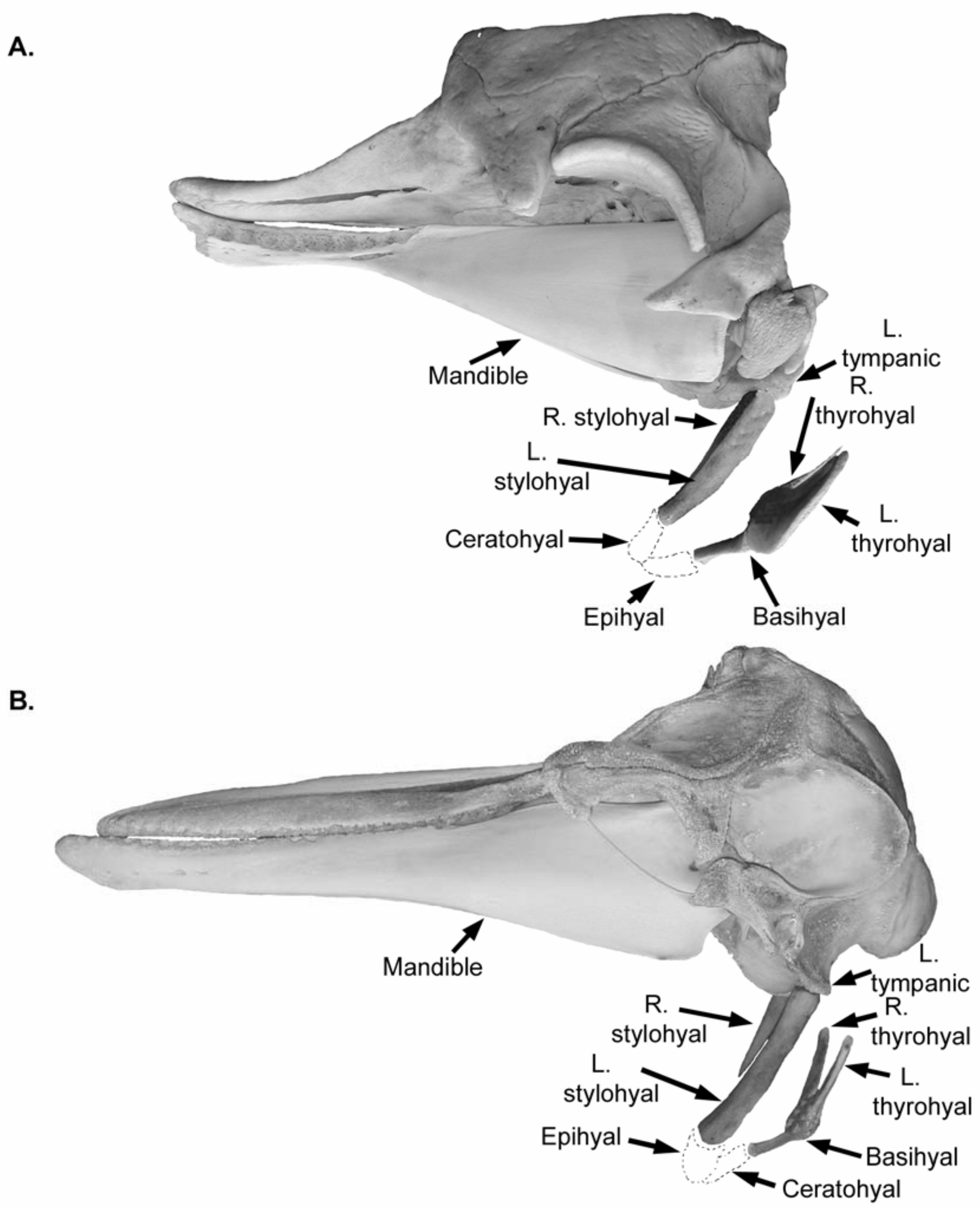

Figure 4. Lateral perspective of the hyoid in a representative retracted position for (A.) *K. breviceps* and (B.) *T. truncatus*. Both stylohyals could be manually retracted to nearly 30° relative to the basal position. The interhyoideus muscle prevented significant movement of the basihyal or thyrohyals away from the stylohyals.

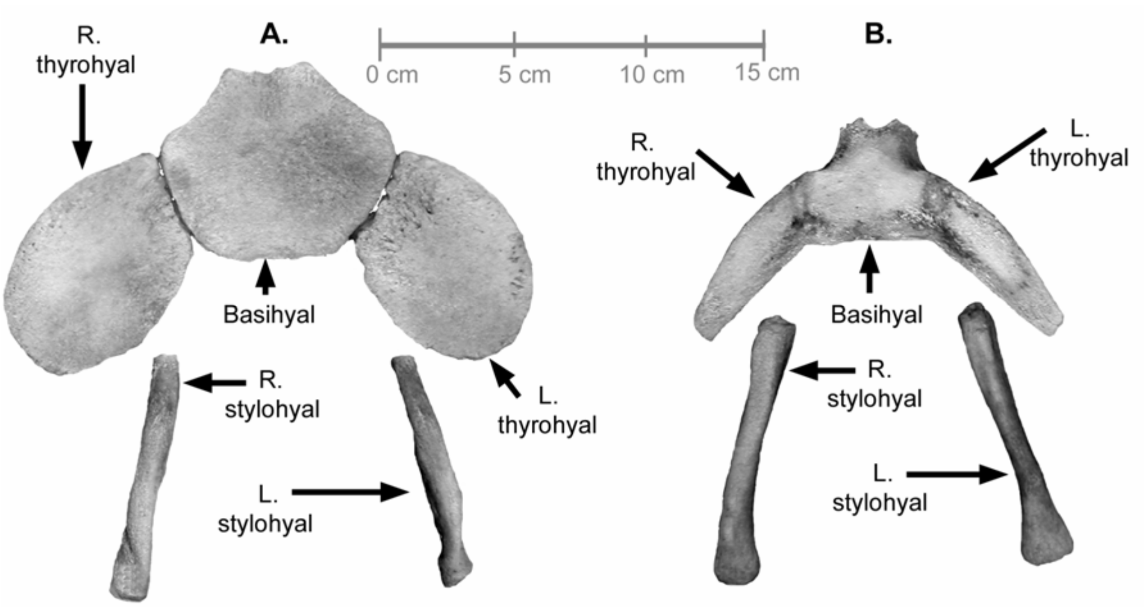

Figure 5. Ventral views of the ossified hyoid complex elements from (A.) *K. breviceps* and (B.) *T. truncatus*. Note prominences for epihyal articulations along the rostromedial basihyal surface.

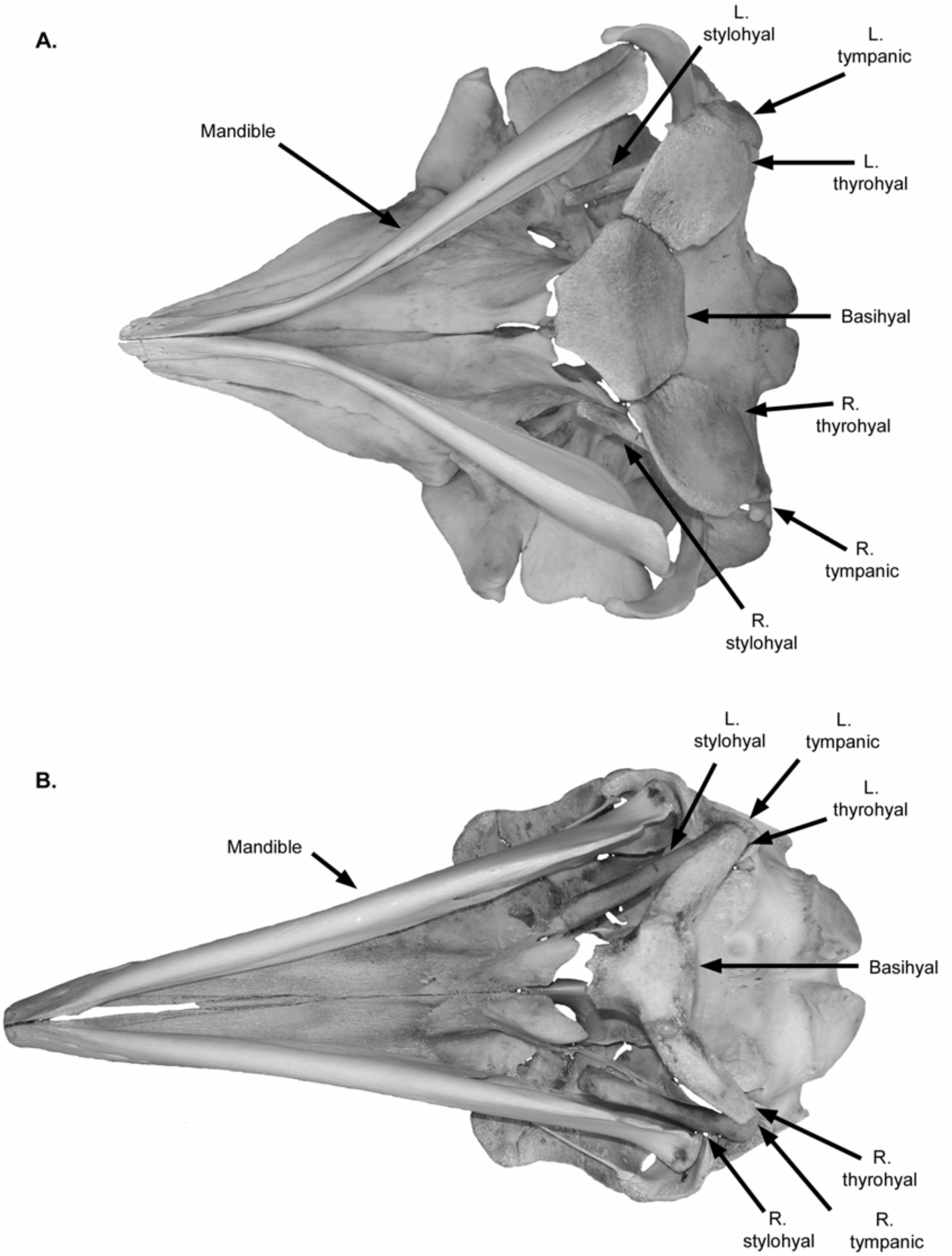

Figure 6. Skulls, mandibles, and ossified hyoid elements of (A.) *K. breviceps* and (B.) *T. truncatus* viewed from the ventral aspect.

The *Kogia* basihyal and thyrohyals (Fig. 4A, 5A, and 6A) formed a large surface area for sternal, lingual, and hyal muscle attachment. The basihyal initially articulated to the epihyals along its rostromedial aspect before expanding to form a wide, convex ventral plate. Five muscles attached to the basihyal: the mylohyoideus and hyoglossus rostrolaterally, the sternohyoideus and thyrohyoideus ventrally, and the interhyoideus dorsally. The basihyal attached caudolaterally to the ossified thyrohyals by a cartilaginous connection. Mean basihyal surface areas (as measured in Fig. 5) at a scaled total body length of 227 cm were 35.6 cm^2 for *K. sima* and 36.5 cm^2 for *K. breviceps*. As with the basihyal, the thyrohyals were broad, flattened elements that, combined with the basihyal, extended expansively between the mandible. The mylohyoideus, sternohyoideus, hyoglossus, and interhyoideus muscles had origins or insertions on the thyrohyals. In *K. sima,* a robust connection was present between the thyrohyal and thyroid cartilage of the larynx that significantly limited ventral hyoid movement away from the larynx. This ligament was similar, although much more robust, to the condition found in canids (Evans and Christensen 1979). *Kogia breviceps* lacked this connection and exhibited a greater hyoid mobility. The mean scaled thyrohyal surface areas were 32.3 cm^2 (right) and 30.6 cm^2 (left) for *K. sima* and 25.6 cm^2 (right) and 26.6 cm^2 (left) for *K. breviceps*. Overall, the mean scaled combined basi-thyrohyal surface area was 98.6 cm^2 for *K. sima* and 88.7 cm^2 for *K. breviceps* at the scaled total body length. All observed osteological data for *Kogia* are summarized in Table A-1. Five *K. sima*

Table 2. Mean hyoid osteology values for *K. sima*, *K. breviceps*, pooled *Kogia*, *and T. truncatus*.

Species	Basihyal SA (cm^2) ± SD	Right thyrohyal SA (cm^2) ± SD	Left thyrohyal SA (cm^2) ± SD	Combined basi/thyrohyal SA (cm^2) ± SD	Right stylohyal width (cm) ± SD	Left stylohyal width (cm) ± SD	Right stylohyal length (cm) ± SD	Left stylohyal length (cm) ± SD	Right stylohyal width:length ratio ± SD	Left stylohyal width:length ratio ± SD
K. sima	31.6 ± 8.33	29.7 ± 8.68	28.1 ± 7.47	89.4 ± 23.2	10.1 ± 1.96	9.87 ± 1.78	68.6 ± 9.58	69.7 ± 10.7	0.149 ± 0.029	0.143 ± 0.027
K. breviceps	39.9 ± 30.0	27.7 ± 20.9	28.8 ± 21.9	96.5 ± 72.4	9.97 ± 4.45	10.2 ± 4.40	85.0 ± 41.2	81.2 ± 37.7	0.119 ± 0.007	0.127 ± 0.006
pooled Kogia	34.7 ± 17.7	29.0 ± 13.0	28.3 ± 13.0	92.0 ± 42.6	10.1 ± 2.80	9.99 ± 2.71	74.7 ± 24.7	74.0 ± 22.5	0.138 ± 0.027	0.137 ± 0.026
T. truncatus	18.5 ± 2.43	11.3 ± 1.36	11.0 ± 1.27	40.8 ± 4.66	9.17 ± 0.67	9.19 ± 0.82	89.2 ± 9.70	88.8 ± 10.8	0.104 ± 0.015	0.105 ± 0.018

Table 3. Scaled means of hyoid osteology variables for *K. sima*, *K. breviceps*, pooled *Kogia*, and *T. truncatus* at a standardized body length of 227 cm.

Species	Basihyal SA (cm^2) ± SE	Right thyrohyal SA (cm^2) ± SE	Left thyrohyal SA (cm^2) ± SE	Combined basi/thyrohyal SA (cm^2) ± SE	Right stylohyal width (cm) ± SE	Left stylohyal width (cm) ± SE	Right stylohyal length (cm) ± SE	Left stylohyal length (cm) ± SE	Right stylohyal width:length ratio ± SE	Left stylohyal width:length ratio ± SE
K. sima	35.6 ± 2.58	32.3 ± 3.15	30.6 ± 3.19	98.6 ± 8.47	9.45 ± 0.71	10.5 ± 0.58	74.2 ± 3.91	75.0 ± 3.58	0.148 ± 0.011	0.142 ± 0.010
K. breviceps	36.5 ± 3.31	25.6 ± 4.05	26.6 ± 4.09	88.7 ± 10.9	9.45 ± 0.71	9.69 ± 0.74	80.2 ± 5.02	76.7 ± 4.59	0.120 ± 0.014	0.128 ± 0.013
pooled Kogia	36.0 ± 2.02	29.8 ± 2.47	29.1 ± 2.50	94.9 ± 6.63	10.3 ± 0.44	10.2 ± 0.45	76.5 ± 3.06	75.6 ± 2.80	0.138 ± 0.008	0.137 ± 0.008
T. truncatus	15.2 ± 2.35	9.16 ± 2.87	8.84 ± 2.90	33.2 ± 7.71	8.66 ± 0.51	8.71 ± 0.53	84.5 ± 3.56	84.5 ± 3.26	0.105 ± 0.010	0.106 ± 0.009

and four *K. breviceps* were incorporated in hyoid morphometry. Overall mean values for hyoid osteology and at the standardized total body length are summarized in Tables 2 and 3.

3.2 *Tursiops truncatus* Hyolingual Osteology

The same hyoid elements identified in *Kogia* were also found in *T. truncatus*: tympanohyal, stylohyal, epihyal, ceratohyal, basihyal, and thyrohyal. Overall, the hyoid chain was situated medially between the mandible and progressed rostroventrally until the epihyals turned caudoventrally to the basihyal. The tympanohyal, epihyal, and ceratohyal appeared reduced and lacked ossification. The thyrohyals branched caudolaterally and were fused to the basihyal in larger specimens. Basihyal and thyrohyal surface areas were reduced relative to *Kogia*, although one additional muscle was found to insert on the lateral thyrohyal. The *T. truncatus* hyoid was also of higher density than in *Kogia*. All hyoid elements sank when placed in water and the pitted appearance present in *Kogia* basihyal and thyrohyals was absent. The hyoid was capable of significant ventrocaudal movement, with the tympanohyal, stylohyal, and epihyal capable of -30˚ retraction from the basal position relative to the palatal plane (Fig. 4B). However, the basihyal and thyrohyals were generally constrained from significant extension, as the interhyoideus muscle between the stylohyal and the basihyal and thyrohyal severely limited movement between these elements.

Tursiops truncatus tympanohyal, epihyal, and ceratohyal characteristics were similar in several aspects to *Kogia*. The cartilaginous tympanohyal connected to the tympanic bone by a synovial joint and served as a partial origin for the interhyoideus. Only adult *T. truncatus* were studied and specimens of small size and young age were not available for comparisons of tympanohyal ontogeny. The tympanohyal extended rostroventrally to form a fibrous attachment to the stylohyal base. The ossified stylohyal (Fig. 4B, 5B, and 6B) was roughly ovoid in cross-section and articulated to the cartilaginous epihyal by a fibrous connection. As in *Kogia*, the *T. truncatus* stylohyal was the origin for the styloglossus and interhyoideus muscles. The epihyal continued rostroventrally and narrowed before it formed a fibrous joint with the cartilaginous ceratohyal. A muscular attachment on the epihyal was not identified. The ceratohyal turned sharply ventrocaudally and medially from its loose fibrous attachment to the epihyal to join the basihyal. The ceratohyal connected to the basihyal by means of a synovial joint on a projection from the basihyal's rostral aspect and lacked muscular attachment. The ossified basihyal (Fig. 4B, 5B, and 6B) was a wide, but short, medial plate with a convex ventral surface. Several muscles attached to the basihyal: the mylohyoideus, sternohyoideus, thyrohyoideus, hyoglossus, and interhyoideus. The mean surface area of the *T. truncatus* basihyal at a scaled total body length of 227 cm was 15.2 cm^2. In most specimens, the basihyal fused to the thyrohyals. However, smaller specimens lacked a bony basihyal-thyrohyal articulation and instead had a thin cartilaginous interface. The thyrohyals (Fig. 4B, 5B, and 6B) were ossified and branched caudolaterally from the basihyal to form "wings" that tapered to a blunt tip. The fibrous connection to the thyroid cartilage of the larynx present in *K. breviceps* was absent. The mylohyoideus, sternohyoideus, hyoglossus, and interhyoideus attached to the thyrohyals. The mean thyrohyal surface areas at a scaled total body length of 227 cm were 9.16 cm^2 (right) and 8.84 cm^2 (left). The mean scaled combined basi-thyrohyal surface area was 33.2 cm^2 at the same scaled total body length. All observed osteological data for *T. truncatus* (N = 6) are presented in Table A-1. Overall mean values for hyoid osteology and at a standardized body length are summarized in Tables 2 and 3.

3.3 Comparative Hyoid Osteology

The major osteological difference between *Kogia* and *T. truncatus* was the much greater surface areas of *Kogia* basihyal and thyrohyals after scaling for total body length (ANCOVA). For all species, thyrohyal and stylohyal data were not significantly different between right and left sides. Osteological symmetry was not assumed, since *Kogia* have the most asymmetrical skulls of all mammals (James Mead, pers. comm.). Stylohyal width:length ratios were not significantly different between any groups.

All *Kogia* groups (*K. sima*, *K. breviceps*, and pooled *Kogia*) had significantly greater combined basi-thyrohyal surface areas than *T. truncatus* ($P \leq 0.001$; adjusted $r^2 = 0.830$). All *Kogia* groups had significantly greater basihyal ($P \leq 0.001$; adjusted $r^2 = 0.892$), right thyrohyal ($P \leq 0.005$; adjusted $r^2 = 0.780$), and left thyrohyal ($P \leq 0.01$; adjusted $r^2 = 0.750$) surface areas than *T. truncatus*.

3.4 *Kogia* Hyolingual Myology

Investigations of *Kogia* hyolingual myology investigated the following muscles: mylohyoideus, geniohyoideus, sternohyoideus, thyrohyoideus, hyoglossus, interhyoideus, genioglossus, styloglossus, and sternothyroideus. Myology was characterized by bilateral strap muscles that, with the exception of lingual insertions, attached by aponeuroses to ossified and cartilaginous hyal, laryngeal, and sternal elements. Of these muscles, the sternohyoideus was the most massive and covered nearly the entire ventral basihyal and thyrohyal surfaces. Means of *Kogia* hyolingual muscle variables are summarized in Tables 4 through 6. Predicted values at a standardized total body length of 252 cm are presented in Tables 7 through 9. All observed myological data for *K. sima* and *K. breviceps* muscle dimensions, cross-sectional areas, and maximum tetanic tensions are available in Tables B-1 through B-22.

Table 4. Mean hyolingual myology length and angle values for *K. sima*, *K. breviceps*, pooled *Kogia*, and *T. truncatus*.

Muscle	Species	Length (mm) ± SD	Parasagittal angle ± SD	Transverse angle ± SD
Mylohyoideus	*K. sima*	84.9 ± 13.0	-68.0 ± 12.9	-83.3 ± 22.0
	K. breviceps	161.6 ± 37.3	-104.1 ± 5.48	-94.3 ± 13.9
	pooled *Kogia*	110.5 ± 44.1	-80.0 ± 21.3	-87.0 ± 19.0
	T. truncatus	80.2 ± 14.7	-69.7 ± 17.7	-82.3 ± 8.21
Geniohyoideus	*K. sima*	132.0 ± 36.2	-14.5 ± 3.54	7.02 ± 1.01
	K. breviceps	198.4 ± 101.5	-12.5 ± 13.4	7.14 ± 7.98
	pooled *Kogia*	156.9 ± 69.8	-13.5 ± 8.10	7.07 ± 4.33
	T. truncatus	213.6 ± 48.4	-23.6 ± 11.4	-1.27 ± 3.53
Sternohyoideus	*K. sima*	255.0 ± 43.7	156.3 ± 6.35	10.4 ± 1.93
	K. breviceps	259.8 ± 156.7	164.5 ± 4.95	6.84 ± 2.60
	pooled *Kogia*	256.9 ± 84.3	159.6 ± 6.80	9.00 ± 2.73
	T. truncatus	230.6 ± 40.4	152.6 ± 5.94	9.40 ± 3.23
Thyrohyoideus	*K. sima*	88.4 ± 22.4	-166.3 ± 9.87	-14.3 ± 3.12
	K. breviceps	113.6 ± 46.3	-157.0 ± 11.3	-6.42 ± 3.52
	pooled *Kogia*	97.9 ± 32.7	-162.6 ± 10.3	-11.3 ± 5.05
	T. truncatus	62.3 ± 14.6	-149.6 ± 20.0	-21.7 ± 20.4
Stylohyoideus	*T. truncatus*	29.0 ± 13.1	-64.1 ± 9.48	-41.4 ± 6.70
Hyoglossus	*K. sima*	114.4 ± 29.8	147.2 ± 10.5	-8.61 ± 3.14
	K. breviceps	169.7 ± 50.7	128.0 ± 5.66	-26.9 ± 9.02
	pooled *Kogia*	132.8 ± 43.2	141.7 ± 12.9	-14.7 ± 10.5
	T. truncatus	171.6 ± 58.2	151.5 ± 8.78	-9.25 ± 13.0
Interhyoideus	*K. sima*	16.8 ± 4.22	-133.2 ± 20.9	163.1 ± 11.7
	K. breviceps	12.0 ± 3.11	-142.0 ± 5.66	136.0 ± 44.3
	pooled *Kogia*	15.2 ± 4.34	-136.2 ± 17.0	154.0 ± 25.9
	T. truncatus	12.7 ± 0.53	-138.3 ± 20.0	163.2 ± 14.8
Genioglossus	*K. sima*	141.0 ± 12.4	-9.00 ± 3.61	-1.15 ± 6.13
	K. breviceps	191.8 ± 93.9	-8.00 ± 3.46	-2.22 ± 6.94
	pooled *Kogia*	160.0 ± 57.4	-8.63 ± 3.34	-1.55 ± 5.96
	T. truncatus	202.2 ± 35.4	-11.7 ± 9.03	-2.33 ± 3.43
Styloglossus	*K. sima*	139.5 ± 26.5	164.8 ± 5.72	-17.1 ± 5.16
	K. breviceps	175.1 ± 67.2	156.3 ± 3.22	-4.83 ± 0.52
	pooled *Kogia*	152.8 ± 45.1	161.6 ± 6.39	-12.5 ± 7.45
	T. truncatus	204.9 ± 23.3	170.8 ± 3.82	-10.6 ± 1.59
Sternothyroideus	*K. sima*	169.8 ± 21.4	148.5 ± 0.71	-6.34 ± 0.47
	K. breviceps	181.7 ± 86.0	153.0 ± 7.07	-10.6 ± 11.0
	pooled *Kogia*	175.8 ± 51.6	150.8 ± 4.86	-8.54 ± 6.83
	T. truncatus	157.6 ± 18.8	134.8 ± 27.8	-1.40 ± 4.21
Cricothyroideus	*T. truncatus*	58.0 ± 9.31	142.0 ± 9.78	17.9 ± 6.22

Table 5. Mean hyolingual myology height, width and mass values for *K. sima*, *K. breviceps*, pooled *Kogia*, and *T. truncatus*.

Muscle	Species	Height (mm) ± SD	Width (mm) ± SD	Mass (g) ± SD
Mylohyoideus	*K. sima*	9.59 ± 4.21	181.9 ± 15.9	58.2 ± 10.7
	K. breviceps	8.03 ± 2.96	282.5 ± 31.8	184.7 ± 0.87
	pooled *Kogia*	9.07 ± 3.61	215.5 ± 55.2	100.4 ± 65.8
	T. truncatus	7.40 ± 2.14	178.9 ± 75.7	97.1 ± 51.2
Geniohyoideus	*K. sima*	8.86 ± 3.05	30.0 ± 6.30	26.1 ± 7.96
	K. breviceps	9.64 ± 3.85	32.8 ± 9.58	34.5 ± 26.4
	pooled *Kogia*	9.15 ± 3.12	31.1 ± 7.15	29.3 ± 16.0
	T. truncatus	11.6 ± 3.40	38.7 ± 21.3	40.8 ± 10.9
Sternohyoideus	*K. sima*	30.8 ± 1.59	66.9 ± 4.72	329.2 ± 37.4
	K. breviceps	25.5 ± 9.96	63.5 ± 35.8	321.3 ± 354.6
	pooled *Kogia*	28.7 ± 5.86	65.6 ± 18.3	326.0 ± 179.3
	T. truncatus	33.3 ± 6.24	57.3 ± 8.83	266.2 ± 94.7
Thyrohyoideus	*K. sima*	5.65 ± 0.87	27.8 ± 5.67	7.61 ± 2.74
	K. breviceps	6.26 ± 1.04	25.7 ± 5.63	14.6 ± 9.00
	pooled *Kogia*	5.88 ± 0.92	27.0 ± 5.34	10.2 ± 6.37
	T. truncatus	6.18 ± 1.58	36.5 ± 3.53	8.40 ± 1.15
Stylohyoideus	*T. truncatus*	12.6 ± 2.63	3.60 ± 0.083	1.47 ± 0.65
Hyoglossus	*K. sima*	5.82 ± 2.87	15.5 ± 6.52	6.54 ± 2.41
	K. breviceps	3.87 ± 0.88	35.4 ± 6.34	22.0 ± 10.4
	pooled *Kogia*	5.17 ± 2.47	22.1 ± 11.8	11.7 ± 9.38
	T. truncatus	8.16 ± 2.41	53.8 ± 16.3	49.7 ± 13.8
Interhyoideus	*K. sima*	34.3 ± 7.72	125.2 ± 12.7	36.9 ± 9.82
	K. breviceps	25.4 ± 13.3	145.3 ± 115.5	42.2 ± 49.4
	pooled *Kogia*	31.3 ± 9.60	131.9 ± 53.6	38.6 ± 23.5
	T. truncatus	28.8 ± 16.0	93.5 ± 9.31	19.7 ± 10.1
Genioglossus	*K. sima*	10.4 ± 4.04	22.6 ± 7.52	22.5 ± 6.98
	K. breviceps	9.16 ± 1.18	24.4 ± 7.95	40.8 ± 25.5
	pooled *Kogia*	9.94 ± 3.18	23.3 ± 7.16	29.4 ± 17.4
	T. truncatus	7.14 ± 1.93	26.5 ± 9.11	31.0 ± 12.6
Styloglossus	*K. sima*	12.4 ± 3.19	5.11 ± 2.71	7.45 ± 1.29
	K. breviceps	13.5 ± 3.26	4.16 ± 0.89	16.83 ± 12.4
	pooled *Kogia*	12.8 ± 3.03	4.76 ± 2.16	11.0 ± 8.25
	T. truncatus	18.6 ± 3.59	5.58 ± 1.34	22.5 ± 4.91
Sternothyroideus	*K. sima*	36.2 ± 2.47	15.0 ± 1.78	75.3 ± 1.49
	K. breviceps	28.7 ± 12.5	8.71 ± 2.57	53.5 ± 56.1
	pooled *Kogia*	32.4 ± 8.54	11.9 ± 4.08	64.4 ± 34.7
	T. truncatus	23.2 ± 1.42	9.92 ± 2.15	28.5 ± 4.84
Cricothyroideus	*T. truncatus*	3.39 ± 1.08	38.4 ± 7.58	5.24 ± 1.54

Table 6. Mean hyolingual myology values for physiological cross-sectional area (PCSA), physiological maximum tetanic tension (PMTT), morphological cross-sectional area (MCSA), and morphological maximum tetanic tension (MMTT) for *K. sima*, *K. breviceps*, pooled *Kogia*, and *T. truncatus*.

Muscle	Species	PCSA (cm^2) ± SD	PMTT (N) ± SD	MCSA (cm^2) ± SD	MMTT (N) ± SD
Mylohyoideus	*K. sima*	6.49 ± 0.87	146.1 ± 19.5	12.3 ± 3.64	276.9 ± 81.9
	K. breviceps	11.1 ± 2.51	249.1 ± 56.4	34.9 ± 7.72	784.4 ± 173.6
	pooled *Kogia*	8.02 ± 2.70	180.4 ± 60.8	19.8 ± 12.5	446.0 ± 280.6
	T. truncatus	10.9 ± 4.17	245.8 ± 93.8	16.2 ± 5.57	264.0 ± 125.4
Geniohyoideus	*K. sima*	2.04 ± 1.09	45.8 ± 24.6	2.71 ± 1.18	60.9 ± 26.5
	K. breviceps	1.41 ± 0.75	31.8 ± 16.8	3.12 ± 1.71	70.3 ± 38.5
	pooled *Kogia*	1.80 ± 0.97	40.6 ± 21.9	2.86 ± 1.29	64.4 ± 29.1
	T. truncatus	1.93 ± 0.95	43.5 ± 21.3	3.60 ± 0.53	81.0 ± 12.0
Sternohyoideus	*K. sima*	12.3 ± 0.75	275.9 ± 16.8	17.1 ± 1.89	385.5 ± 42.6
	K. breviceps	9.51 ± 7.14	214.1 ± 160.5	17.4 ± 15.2	392.2 ± 342.1
	pooled *Kogia*	11.2 ± 3.91	251.2 ± 87.9	17.3 ± 7.72	388.2 ± 173.7
	T. truncatus	10.8 ± 2.62	243.2 ± 59.0	17.8 ± 5.47	400.3 ± 123.1
Thyrohyoideus	*K. sima*	0.81 ± 0.26	18.2 ± 5.76	1.81 ± 0.28	40.6 ± 6.38
	K. breviceps	1.13 ± 0.49	25.5 ± 11.0	2.10 ± 1.12	47.3 ± 25.1
	pooled *Kogia*	0.93 ± 0.37	20.9 ± 8.23	1.92 ± 0.65	43.1 ± 14.7
	T. truncatus	1.32 ± 0.29	29.6 ± 6.64	2.46 ± 0.42	55.4 ± 9.43
Stylohyoideus	*T. truncatus*	0.67 ± 0.63	15.0 ± 14.2	0.80 ± 0.68	17.9 ± 15.2
Hyoglossus	*K. sima*	0.53 ± 0.057	11.9 ± 1.27	0.85 ± 0.17	19.1 ± 3.89
	K. breviceps	1.19 ± 0.22	26.7 ± 4.98	3.03 ± 0.73	68.1 ± 16.4
	pooled *Kogia*	0.75 ± 0.36	16.9 ± 8.00	1.57 ± 1.18	35.4 ± 26.6
	T. truncatus	2.84 ± 0.75	63.9 ± 17.0	3.24 ± 1.99	72.9 ± 44.8
Interhyoideus	*K. sima*	1.44 ± 0.82	32.5 ± 18.5	n/a	n/a
	K. breviceps	2.23 ± 1.14	50.1 ± 25.6	n/a	n/a
	pooled *Kogia*	1.70 ± 0.91	38.4 ± 20.5	n/a	n/a
	T. truncatus	0.96 ± 0.51	21.6 ± 11.5	n/a	n/a
Genioglossus	*K. sima*	1.51 ± 0.47	33.9 ± 10.5	2.62 ± 0.75	59.0 ± 16.8
	K. breviceps	1.86 ± 0.58	41.8 ± 13.0	2.29 ± 1.23	51.5 ± 27.7
	pooled *Kogia*	1.64 ± 0.50	36.9 ± 11.3	2.50 ± 0.88	56.2 ± 19.9
	T. truncatus	1.50 ± 0.70	33.8 ± 15.8	2.11 ± 0.61	47.4 ± 13.7
Styloglossus	*K. sima*	0.51 ± 0.076	11.5 ± 1.72	0.62 ± 0.14	13.9 ± 3.23
	K. breviceps	0.82 ± 0.43	18.4 ± 9.69	1.07 ± 0.44	24.1 ± 9.90
	pooled *Kogia*	0.63 ± 0.29	14.1 ± 6.42	0.79 ± 0.35	17.8 ± 7.86
	T. truncatus	1.04 ± 0.20	23.3 ± 4.45	1.06 ± 0.54	23.8 ± 12.1
Sternothyroideus	*K. sima*	4.22 ± 0.61	94.9 ± 13.8	4.31 ± 0.46	96.9 ± 10.4
	K. breviceps	2.35 ± 1.80	52.9 ± 40.5	3.70 ± 3.43	83.2 ± 77.3
	pooled *Kogia*	3.28 ± 1.54	73.9 ± 34.6	4.00 ± 2.03	90.1 ± 45.7
	T. truncatus	1.70 ± 0.12	38.3 ± 2.59	2.66 ± 0.84	59.9 ± 19.0
Cricothyroideus	*T. truncatus*	0.85 ± 0.21	19.2 ± 4.76	1.63 ± 0.46	36.7 ± 10.3

Table 7. Scaled means of hyolingual myology length and angle variables for *K. sima*, *K. breviceps*, pooled *Kogia*, and *T. truncatus* at a standardized body length of 252 cm. Cricothyroideus and stylohyoideus values are set to 241 cm for greater accuracy in *T. truncatus* scaling.

Muscle	Species	Length (mm) ± SE	Parasagittal angle ± SE	Transverse angle ± SE
Mylohyoideus	*K. sima*	107.4 ± 12.6	-69.7 ± 9.81	-82.9 ± 9.84
	K. breviceps	117.0 ± 22.3	-67.6 ± 17.3	-82.9 ± 17.4
	pooled *Kogia*	110.6 ± 10.0	-69.0 ± 7.77	-82.9 ± 7.80
	T. truncatus	101.2 ± 10.7	-79.3 ± 8.30	-88.6 ± 8.33
Geniohyoideus	*K. sima*	137.7 ± 35.3	-14.5 ± 7.55	8.49 ± 2.91
	K. breviceps	187.0 ± 62.5	-3.13 ± 13.9	10.4 ± 5.14
	pooled *Kogia*	154.2 ± 28.0	-10.7 ± 6.19	9.12 ± 2.30
	T. truncatus	208.6 ± 29.9	-23.6± 5.05	-0.52 ± 2.46
Sternohyoideus	*K. sima*	300.1 ± 24.3	160.4 ± 4.02	7.95 ± 1.54
	K. breviceps	291.6 ± 42.9	166.2 ± 7.38	9.98 ± 2.73
	pooled *Kogia*	297.3 ± 19.2	162.3 ± 3.30	8.62 ± 1.22
	T. truncatus	245.8 ± 20.5	153.0 ± 2.69	7.75 ± 1.30
Thyrohyoideus	*K. sima*	103.6 ± 3.28	-161.4 ± 13.0	-13.9 ± 2.70
	K. breviceps	105.1 ± 5.81	-160.8 ± 23.9	-11.4 ± 4.78
	pooled *Kogia*	104.1 ± 2.60	-161.2 ± 10.7	-13.0 ± 2.14
	T. truncatus	79.6 ± 2.78	-146.9 ± 8.73	-8.12 ± 2.28
Stylohyoideus	*T. truncatus*	29.0 ± 1.78	-64.1 ± 0.96	-41.4 ± 5.06
Hyoglossus	*K. sima*	130.4 ± 36.8	148.6 ± 10.6	-13.7 ± 8.77
	K. breviceps	102.1 ± 65.2	142.9 ± 19.5	-17.6 ± 15.5
	pooled *Kogia*	121.0 ± 29.2	146.7 ± 8.71	-15.0 ± 6.94
	T. truncatus	199.4 ± 31.2	148.6 ± 7.11	-16.0 ± 7.41
Interhyoideus	*K. sima*	18.6 ± 1.00	-121.6 ± 13.7	172.4 ± 7.67
	K. breviceps	17.7 ± 1.77	-133.8 ± 24.2	162.1 ± 13.6
	pooled *Kogia*	18.3 ± 0.79	-125.6 ± 10.8	169.0 ± 6.08
	T. truncatus	11.6 ± 0.84	-142.0 ± 11.6	164.8 ± 6.49
Genioglossus	*K. sima*	156.0 ± 36.9	-7.98 ± 5.10	0.31 ± 3.148
	K. breviceps	205.2 ± 65.2	-9.08 ± 9.36	-1.31 ± 5.57
	pooled *Kogia*	172.4 ± 29.2	-8.35 ± 4.18	-0.90 ± 2.49
	T. truncatus	227.8 ± 31.2	-9.38 ± 3.41	-2.98 ± 2.66
Styloglossus	*K. sima*	169.5 ± 19.7	166.8 ± 3.54	-17.3 ± 5.00
	K. breviceps	194.6 ± 34.9	165.7 ± 6.49	-13.2 ± 8.84
	pooled *Kogia*	177.9 ± 15.6	166.4 ± 2.90	-15.9 ± 3.96
	T. truncatus	220.3 ± 16.7	169.7 ± 2.37	-8.10 ± 4.23
Sternothyroideus	*K. sima*	186.6 ± 11.3	147.6 ± 16.6	-8.71 ± 1.04
	K. breviceps	182.3 ± 20.0	152.0 ± 30.5	-9.94 ± 1.83
	pooled *Kogia*	185.1 ± 9.0	149.1 ± 13.6	-9.12 ± 0.82
	T. truncatus	177.9 ± 9.57	133.9 ± 11.1	-1.43 ± 0.88
Cricothyroideus	*T. truncatus*	60.8 ± 5.9	145.0 ± 4.93	15.2 ± 0.39

Table 8. Scaled means of hyolingual myology height, width, and mass variables for *K. sima*, *K. breviceps*, pooled *Kogia*, and *T. truncatus* at a standardized body length of 252 cm. Cricothyroideus and stylohyoideus values are set to 241 cm for greater accuracy in *T. truncatus* scaling.

Muscle	Species	Height (mm) ± SE	Width (mm) ± SE	Mass (g) ± SE
Mylohyoideus	*K. sima*	11.1 ± 3.24	193.3 ± 51.2	93.3 ± 11.1
	K. breviceps	11.7 ± 5.74	256.8 ± 90.6	82.0 ± 19.6
	pooled *Kogia*	11.3 ± 2.57	214.5 ± 40.6	89.6 ± 8.78
	T. truncatus	6.93 ± 2.74	193.1 ± 43.3	127.7 ± 9.38
Geniohyoideus	*K. sima*	11.7 ± 2.00	40.1 ± 13.8	31.3 ± 6.91
	K. breviceps	14.2 ± 3.54	22.2 ± 24.3	29.5 ± 12.2
	pooled *Kogia*	12.5 ± 1.59	34.1 ± 10.9	30.7 ± 5.47
	T. truncatus	9.91 ± 1.69	48.4 ± 11.6	49.7 ± 5.84
Sternohyoideus	*K. sima*	31.5 ± 3.84	71.8 ± 5.19	406.7 ± 36.0
	K. breviceps	26.7 ± 6.80	75.1 ± 9.18	365.0 ± 63.7
	pooled *Kogia*	29.9 ± 3.05	72.9 ± 4.11	392.8 ± 28.6
	T. truncatus	34.5 ± 3.25	65.1 ± 4.39	346.4 ± 30.5
Thyrohyoideus	*K. sima*	5.87 ± 0.52	30.0 ± 1.78	11.8 ± 1.32
	K. breviceps	6.53 ± 0.93	30.0 ± 3.14	13.5 ± 2.33
	pooled *Kogia*	6.09 ± 0.42	30.0 ± 1.41	12.4 ± 1.04
	T. truncatus	5.63 ± 0.44	34.4 ± 1.50	10.2 ± 1.11
Stylohyoideus	*T. truncatus*	12.7 ± 1.48	3.60 ± 0.056	1.47 ± 0.17
Hyoglossus	*K. sima*	7.07 ± 2.07	19.7 ± 8.08	11.0 ± 7.21
	K. breviceps	5.28 ± 3.66	26.7 ± 14.3	1.26 ± 12.8
	pooled *Kogia*	6.47 ± 1.64	22.1 ± 6.40	7.77 ± 5.71
	T. truncatus	8.59 ± 1.75	48.0 ± 6.83	55.2 ± 6.10
Interhyoideus	*K. sima*	37.2 ± 10.3	149.4 ± 17.3	50.8 ± 2.25
	K. breviceps	26.7 ± 18.3	172.0 ± 30.5	50.8 ± 3.97
	pooled *Kogia*	33.7 ± 8.18	156.9 ± 13.7	50.8 ± 1.78
	T. truncatus	31.2 ± 8.74	109.8 ± 14.6	27.4 ± 1.90
Genioglossus	*K. sima*	11.5 ± 3.21	27.3 ± 5.54	29.4 ± 4.06
	K. breviceps	11.7 ± 5.68	24.1 ± 9.80	33.8 ± 7.19
	pooled *Kogia*	11.6 ± 2.54	26.2 ± 4.39	30.9 ± 3.22
	T. truncatus	5.30 ± 2.72	22.9 ± 4.69	32.5 ± 3.44
Styloglossus	*K. sima*	15.3 ± 0.93	7.47 ± 1.61	12.5 ± 3.56
	K. breviceps	15.3 ± 1.65	5.77 ± 2.84	15.5 ± 6.30
	pooled *Kogia*	15.3 ± 0.74	6.90 ± 1.27	13.5 ± 2.82
	T. truncatus	19.7 ± 0.79	5.50 ± 1.36	28.4 ± 3.01
Sternothyroideus	*K. sima*	36.2 ± 1.62	14.2 ± 1.13	79.3 ± 1.02
	K. breviceps	37.6 ± 2.86	13.4 ± 2.00	78.7 ± 1.81
	pooled *Kogia*	36.6 ± 1.28	14.0 ± 0.90	79.1 ± 0.81
	T. truncatus	23.5 ± 1.37	8.00 ± 0.96	34.4 ± 0.86
Cricothyroideus	*T. truncatus*	3.92 ± 0.089	36.7 ± 5.08	5.23 ± 1.54

Table 9. Scaled means of hyolingual myology physiological cross-sectional area (PCSA), physiological maximum tetanic tension (PMTT), morphological cross-sectional area (MCSA), and morphological maximum tetanic tension (MMTT) for *K. sima*, *K. breviceps*, pooled *Kogia,* and *T. truncatus* at a standardized body length of 252 cm. Cricothyroideus and stylohyoideus values are set to 241cm for greater accuracy in *T. truncatus* scaling.

Muscle	Species	PCSA (cm^2) ± SE	PMTT (N) ± SE	MCSA (cm^2) ± SE	MMTT (N) ± SE
Mylohyoideus	*K. sima*	8.00 ± 1.69	179.9 ± 38.1	18.0 ± 2.33	404.0 ± 52.5
	K. breviceps	5.66 ± 3.00	127.3 ± 67.4	17.4 ± 4.12	391.9 ± 92.8
	pooled *Kogia*	7.22 ± 1.34	162.4 ± 30.2	17.8 ± 1.85	400.0 ± 41.6
	T. truncatus	12.0 ± 1.43	270.0 ± 32.2	19.7 ± 1.97	444.0 ± 44.4
Geniohyoideus	*K. sima*	2.05 ± 0.60	46.1 ± 13.6	3.89 ± 0.49	87.5 ± 11.0
	K. breviceps	1.38 ± 1.07	31.0 ± 24.0	3.66 ± 0.87	82.3 ± 19.5
	pooled *Kogia*	1.82 ± 0.48	41.0 ± 10.7	3.81 ± 0.39	85.8 ± 8.75
	T. truncatus	2.43 ± 0.51	54.6 ± 11.5	3.96 ± 0.42	89.0 ± 9.34
Sternohyoideus	*K. sima*	12.8 ± 1.16	287.5 ± 26.1	19.6 ± 2.57	440.4 ± 57.7
	K. breviceps	11.3 ± 2.05	253.4 ± 46.2	18.6 ± 4.54	418.7 ± 102.0
	pooled *Kogia*	12.3 ± 0.92	276.1 ± 20.7	19.3 ± 2.03	433.2 ± 45.7
	T. truncatus	12.8 ± 0.98	288.4 ± 22.1	22.8 ± 2.17	513.8 ± 48.8
Thyrohyoideus	*K. sima*	1.05 ± 0.18	23.5 ± 3.99	1.71 ± 0.23	38.5 ± 5.22
	K. breviceps	1.22 ± 0.31	27.4 ± 7.05	2.04 ± 0.41	45.8 ± 9.23
	pooled *Kogia*	1.10 ± 0.14	24.8 ± 3.16	1.82 ± 0.18	40.9 ± 4.14
	T. truncatus	1.24 ± 0.15	27.9 ± 3.37	2.41 ± 0.20	54.3 ± 4.42
Stylohyoideus	*T. truncatus*	0.67 ± 0.018	15.0 ± 0.40	0.80 ± 0.012	17.9 ± 0.26
Hyoglossus	*K. sima*	0.67 ± 0.31	15.2 ± 6.92	1.23 ± 1.13	27.6 ± 25.3
	K. breviceps	0.60 ± 0.54	13.5 ± 12.2	0.64 ± 1.99	14.4 ± 44.8
	pooled *Kogia*	0.65 ± 0.24	14.6 ± 5.48	1.03 ± 0.89	23.2 ± 20.1
	T. truncatus	2.69 ± 0.26	60.5 ± 5.86	3.65 ± 0.95	82.1 ± 21.4
Interhyoideus	*K. sima*	1.30 ± 0.34	29.2 ± 7.62	n/a	n/a
	K. breviceps	1.63 ± 0.60	36.6 ± 13.5	n/a	n/a
	pooled *Kogia*	1.41 ± 0.27	31.7 ± 6.04	n/a	n/a
	T. truncatus	0.90 ± 0.29	20.2 ± 6.45	n/a	n/a
Genioglossus	*K. sima*	1.68 ± 0.19	37.7 ± 4.19	2.08 ± 0.31	46.9 ± 7.05
	K. breviceps	1.54 ± 0.33	34.7 ± 7.40	1.82 ± 0.55	40.9 ± 12.5
	pooled *Kogia*	1.63 ± 0.15	36.7 ± 3.32	2.00 ± 0.25	44.9 ± 5.59
	T. truncatus	1.32 ± 0.16	29.7 ± 3.54	1.75 ± 0.27	39.4 ± 5.96
Styloglossus	*K. sima*	0.66 ± 0.10	14.9 ± 2.29	0.81 ± 0.28	18.2 ± 6.33
	K. breviceps	0.69 ± 0.18	15.6 ± 4.04	0.47 ± 0.50	10.6 ± 11.2
	pooled *Kogia*	0.67 ± 0.080	15.2 ± 1.81	0.70 ± 0.22	15.6 ± 5.01
	T. truncatus	1.25 ± 0.086	28.1 ± 1.93	1.22 ± 0.24	27.5 ± 5.35
Sternothyroideus	*K. sima*	4.12 ± 0.34	92.7 ± 7.66	4.52 ± 0.78	101.8 ± 17.5
	K. breviceps	3.98 ± 0.60	89.5 ± 13.5	5.35 ± 1.38	120.3 ± 31.0
	pooled *Kogia*	4.07 ± 0.27	91.6 ± 6.07	4.80 ± 0.62	108.0 ± 13.9
	T. truncatus	1.66 ± 0.29	37.4 ± 6.48	2.93 ± 0.66	66.0 ± 14.8
Cricothyroideus	*T. truncatus*	0.80 ± 0.17	18.0 ± 3.84	1.48 ± 0.34	33.2 ± 7.67

3.4.1 Mylohyoideus

The mylohyoideus (Fig. 7 and 8) was a broad, relatively thin muscle that originated upon the ventromedial mandibular border of both rami from the mandibular symphasis to near the mandible’s caudal extent. Right and left muscles inserted to a ventromedial raphe that formed a ventral lingual sling. The insertion extended from the mandibular symphasis, rostrally, to near the rostral basihyal border, caudally, where a “V” shaped fascial sheet joined right and left muscles. Although thin medially (2-3 mm), the mylohyoideus thickened (2-3 cm) laterally near its origin. Based on observed data, each mylohyoideus was predicted to have a PMTT (MMTT) at a total body length of 252 cm of 179.9 N (404.0 N) at an angle of 110.3° relative to the palatal plane in *K. sima*, and 127.3 N (391.9 N) at 112.4° in *K. breviceps*, and 162.4 N (400.0 N) at 111.0° in pooled *Kogia*. These values support the mylohyoideus as the second most powerful *Kogia* hyolingual muscle. The mylohyoideus likely assisted in hyoid return to its basal position. The mylohyoideus was tightly adhered to the superficial platysma and digastricus, while the deep stylohyoideus, styloglossus, hyoglossus, and genioglossus were loosely attached to the mylohyoideus by fascia.

Figure 7. Caudal musculature associated with the *Kogia* hyolingual complex. MH = mylohyoideus, GH = geniohyoideus, SteH = sternohyoideus, TH = thyrohyoideus, and SC = sternocephalicus.

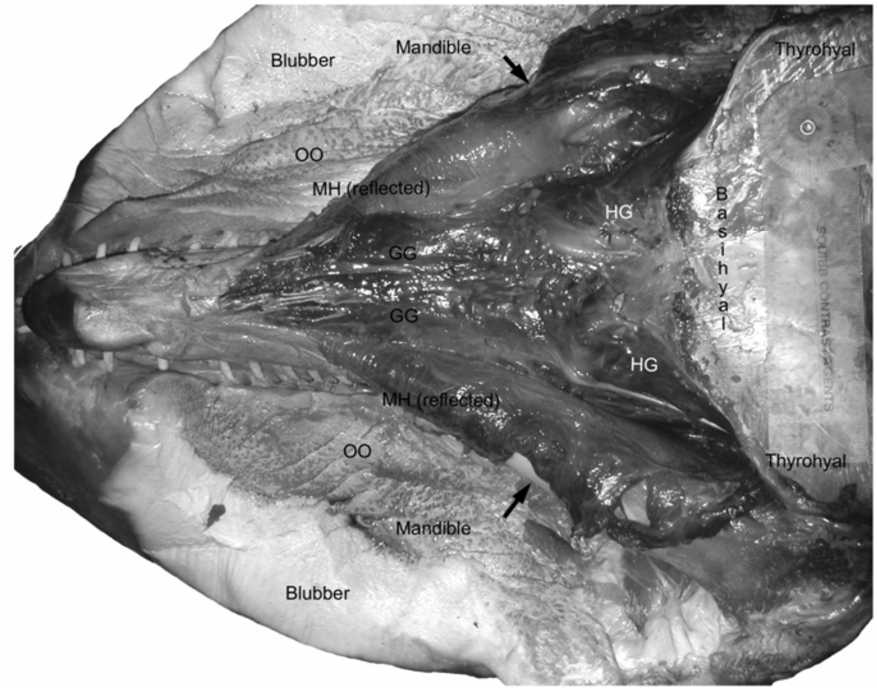

Figure 8. Ventral view of rostral *Kogia* hyolingual muscles. OO = orbicularis oris, MH = mylohyoideus, GG = genioglossus, and HG = hyoglossus.

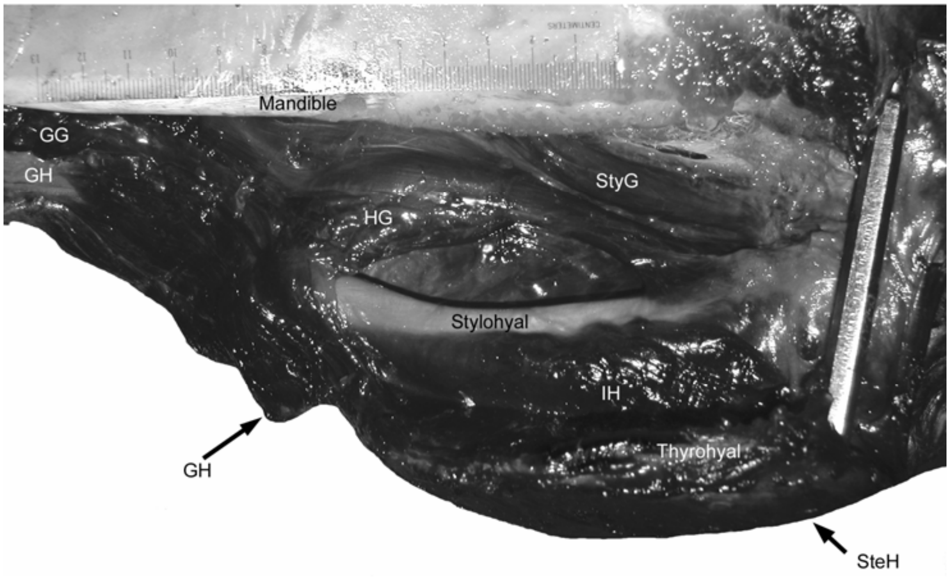

Figure 9. Lateral view of *Kogia* hyolingual musculature. Note: the geniohyoideus was cut to clarify its insertion to the sternohyoideus. The hyoglossus was also partly reflected to reveal the interhyoideus. GH = geniohyoideus, GG = genioglossus, HG = hyoglossus, StyG = styloglossus, IH = interhyoideus, and SteH = sternohyoideus.

3.4.2 Geniohyoideus

The geniohyoideus (Fig. 7 and 9) originated upon the caudoventral surface of the mandibular symphasis by a long tendon shared by right and left muscles. Although fascicles intermingled caudally, a distinct division was present between right and left muscles. A bony insertion was lacking, but an attachment directly to the rostromedial border of the sternohyoideus was present. Muscle measurements support predicted geniohyoideus PMTT (MMTT) and angles of 46.1 N (87.5 N) at 165.5° (relative to the palatal plane) in *K. sima*, 31.0 N (82.3 N) at 176.9° in *K. breviceps*, and 41.0 N (85.8 N) at 169.3° in pooled *Kogia*. The geniohyoideus likely enhanced mandibular depression when the hyoid depressed and, after mandibular elevation, assisted hyoid return to the basal position. The geniohyoideus was loosely held by fascia the superficial mylohyoideus and to the deep genioglossus along the entire genioglossal length. The geniohyoideus near its insertion was also attached loosely by fascia to the deep hyoglossus.

3.4.3 Sternohyoideus

The sternohyoideus (Fig. 7 and 9) originated upon the medial aspect of the manubrium’s cranioventral surface. This massive strap muscle extended craniodorsally to insert upon the entire ventral surface of the thyrohyals and basihyal. The broad sternohyoideus insertion left only a thin border for attachment of several hyolingual muscles to the rostral basihyal and thyrohyal borders. Along its rostromedial border, the sternohyoideus formed an aponeurosis to the geniohyoideus. Estimated PMTT (MMTT) vectors for the sternohyoideus in *K. sima* were 287.5 N (440.4 N) at -19.6°, 253.4 N (418.7 N) at -13.8° in *K. breviceps* and 276.1 N (433.2 N) at -17.7° in pooled *Kogia*. These values were the greatest PMTT values of any *Kogia* hyolingual muscle and likely functioned to draw the hyoid caudoventrally. The sternohyoideus was bordered laterally by the sternothyroideus and sternocephalicus, and the pectoralis major caudoventrally.

3.4.4 Thyrohyoideus

The thyrohyoideus (Fig. 7) originated upon the ventrolateral thyroid cartilage and rostral cornu of the arytenoid cartilage of the larynx. This strap muscle extended rostromedially to insert upon the medial basihyal and thyrohyals, caudal to the sternohyoideus insertion. Vector predictions of thyrohyoideus values were 23.5 N (38.5 N) at 18.6° in *K. sima*, 27.4 N (45.8 N) at 13.8° in *K. breviceps*, and 24.8 N (40.9 N) at 17.7° in pooled *Kogia*. The function of the thyrohyoideus was to draw the hyoid caudodorsally. The thyrohyoideus was deep to the sternohyoideus and was bordered caudodorsally by the sternothyroideus; both muscles were attached to the sternohyoideus loosely by fascia.

3.4.5 Stylohyoideus

The stylohyoideus was not identified in *Kogia*.

3.4.6 Hyoglossus

The hyoglossus (Fig. 8 and 9) originated upon the rostral basihyal border as a thin, triangular sheet on the basihyal-ceratohyal articulation laterally to the caudolateral extremity of the thyrohyals. The hyoglossus narrowed to insert diffusely in the middle one-third of the tongue body in *K. sima*, and in the caudal one-third in *K. breviceps*. Each hyoglossus was predicted to have a PMTT (MMTT) of 15.2 N (27.6 N) at an angle of -31.4° relative to the palatal plane in *K. sima*, 13.5 N (14.4 N) at -37.1° in *K. breviceps*, and 14.6 N (23.2 N) at -33.3° in pooled *Kogia*. The hyoglossus pulled the tongue caudoventrally and was the primary tongue depressor. This strap muscle was loosely connected by fascia to the deep interhyoideus.

3.4.7 Interhyoideus

The interhyoideus (Fig. 9) was a short, thick, and wide strap muscle that originated upon the ventral stylohyal and caudal ceratohyal surfaces. The muscle's origin widened laterally along the middle one-third of the stylohyal. The muscle extended caudoventrally to insert upon the entire dorsal thyrohyal and basihyal surfaces; all other hyoid muscles attached to the ventral, rostral or lateral hyoid surfaces. Vectors of predicted interhyoideus PMTT and angles were 29.2 N at 58.4° relative to the palatal plane in *K. sima*, 36.6 N at 46.2° in *K. breviceps*, and 31.7 N at 54.4° in pooled *Kogia*. The interhyoideus functioned to approximate the basihyal and thyrohyal to the stylohyal. The interhyoideus was deep to the hyoglossus rostrally and the mylohyoideus caudolaterally; both muscles attached to the interhyoideus loosely by fascia.

3.4.8 Genioglossus

The genioglossus (Fig. 8 and 9) originated upon the ventral mandibular symphasis and the adjacent medial mandibular surface. In *K. sima*, the insertion was dispersed into the tongue's entire ventral body. The *K. breviceps* genioglossal insertion was centralized into the middle one-third of the tongue's ventrolateral body. Predicted genioglossal values of PMTT (MMTT) and vector angles were 37.7 N (46.9 N) at 172.0° in *K. sima*, 34.7 N (40.9 N) at 170.9° in *K. breviceps*, and 36.7 N (44.9 N) at 171.7° in pooled *Kogia*. The genioglossus was the only studied muscle capable of tongue protraction. The genioglossus was loosely attached by fascia to the superficial geniohyoideus.

3.4.9 Styloglossus

The styloglossus (Fig. 9) was a small strap muscle that originated along the caudolateral one-third of the stylohyal's dorsocaudal border. The muscle extended rostrally to gradually diffuse along the middle one-third of the ventrolateral tongue body. Vector predictions of styloglossus values were 14.9 N (18.2 N) at -13.2° in *K. sima*, 15.6 N (10.6 N) at -14.3° in *K. breviceps*, and 15.2 N (15.6 N) at -13.6° in pooled *Kogia*. The styloglossus functioned to retract the tongue caudoventrally. The styloglossus was deep to the mylohyoideus, which was attached to the styloglossus loosely by fascia along the caudally.

3.4.10 Sternothyroideus

The sternothyroideus (Fig. 7) originated upon the craniolateral surface of the ventral manubrium and over the articulation of the manubrium with the first true rib. This muscle extended craniodorsally to insert upon the caudolateral surface of the rostrolateral portion of the thyroid cartilage and its rostral cornu. The sternothyroideus was the third most powerful muscle measured, with predicted vector values of 92.7 N (101.8 N) at -32.4° in *K. sima*, 89.5 N (120.3 N) at -28.0° in *K. breviceps*, and 91.6 N (108.0 N) at -30.9° in pooled *Kogia*. The sternothyroideus functioned to draw the larynx caudoventrally and was the primary retractor and depressor of the larynx. Adjacent structures included the ventromedially situated sternohyoideus, caudoventrally placed sternobrachialis and medially located larynx; all were attached loosely by fascia.

3.4.11 Cricothyroideus

The cricothyroideus was not identified in *Kogia*.

3.4.12 Orbicularis Oris

The orbicularis oris (Fig. 8) was a diffuse fascicular collection embedded within dense connective tissue. The muscle originated adjacent to the maxilla just deep to the blubber. These rostrocaudal fascicles turned dorsoventrally at the corner of the mouth. There, the orbicularis oris intermingled with fascicles of the buccinator before returning to a rostrocaudal orientation in the dense connective tissue along the mandible. Transverse fascicles also emanated from the orbicularis oris, but diffused into the blubber.

3.4.13 Buccinator

The buccinator was a diffuse dorsoventrally directed muscle that originated near the ventral maxillary border. The buccinator extended caudally to the corner of the mouth, where its fascicles intermingled with those of the orbicularis oris. From here, the buccinator shifted rostrally to border the mandible at the level of the caudal-most mandibular tooth, where it fused with the platysma. The orbicularis oris and buccinator partially composed a lateral mouth occlusion. Based on manual manipulation of dissection specimens, this occlusal structure was folded along the mandible when the mouth was closed or at minimal gape. However, as the mandible depressed, a tissue flap composed of dense connective tissue, skin, the orbicularis oris, and buccinator unfolded and formed a flap along the side of the mouth.

3.4.14 Biomechanical Modeling

A biomechanical model of *Kogia* feeding was developed to identify muscle function and describe mechanical advantage of hyoid retraction and depression. Figure 10 identifies muscle vectors associated with hyolingual depression and retraction. More than an order of magnitude separated PMTT values of the greatest and least powerful muscles. Muscle vectors that depressed or retracted the hyoid (sternohyoideus, thyrohyoideus, and sternothyroideus) are summarized in Figure 11. Predicted PMTTs of hyoid depression and retraction were calculated and resultant vectors determined to identify the predicted net tension exerted upon the hyoid at the moment of contraction. The same vectors were determined for tongue depressors and retractors (hyoglossus and styloglossus). Vector analysis and implications of biomechanical modeling are addressed in “Discussion”.

Aspects of the *Kogia* tongue, blubber, and lateral mouth aspects were likely significant to *Kogia* feeding strategy. The tongue formed a short triangle that was contoured to fit into a palatal elevation. A short frenulum was present, but the fang-like mandibular teeth limited lateral tongue movement. Rostral manipulation was hindered by muscular connections to the hyoid, but caudal manipulation was easily facilitated by hyoid depression or retraction. The blubber was more-fibrous and less-pliable rostral to the hyoid, where a sharp transition occurred to an apparently more elastic character caudally and ventrally. Lateral gape was partially occluded by the buccinator, orbicularis oris, and dense fibrous tissue so that only the rostral one third of the mandibular teeth were laterally visible.

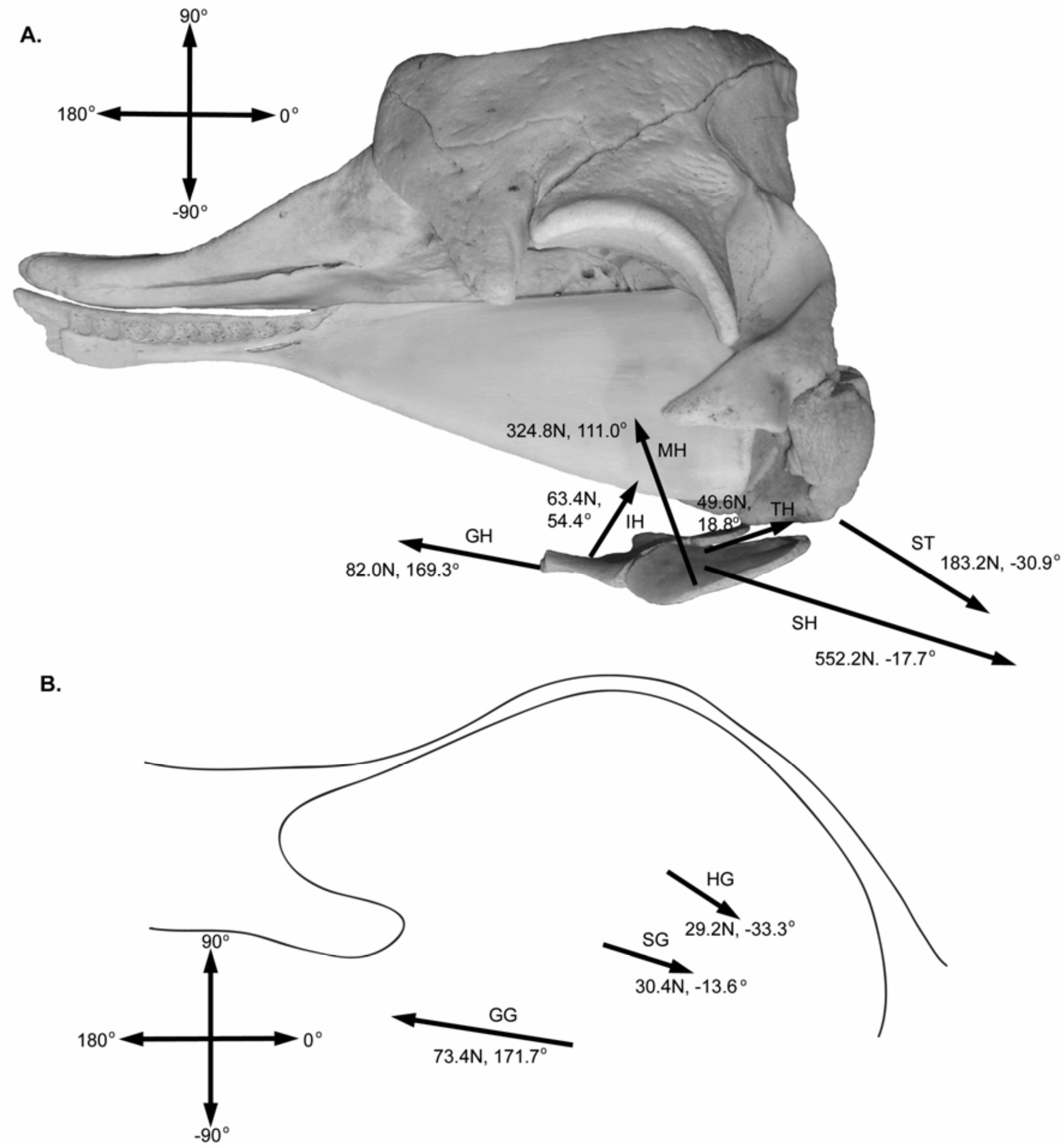

Figure 10. Kogia biomechanical model of hyolingual muscle vectors. Values reflect combined right and left muscles (A.) Muscles associated with hyoid depression, retraction, or return to the basal position. (B.) Lingual muscles associated with tongue movement.

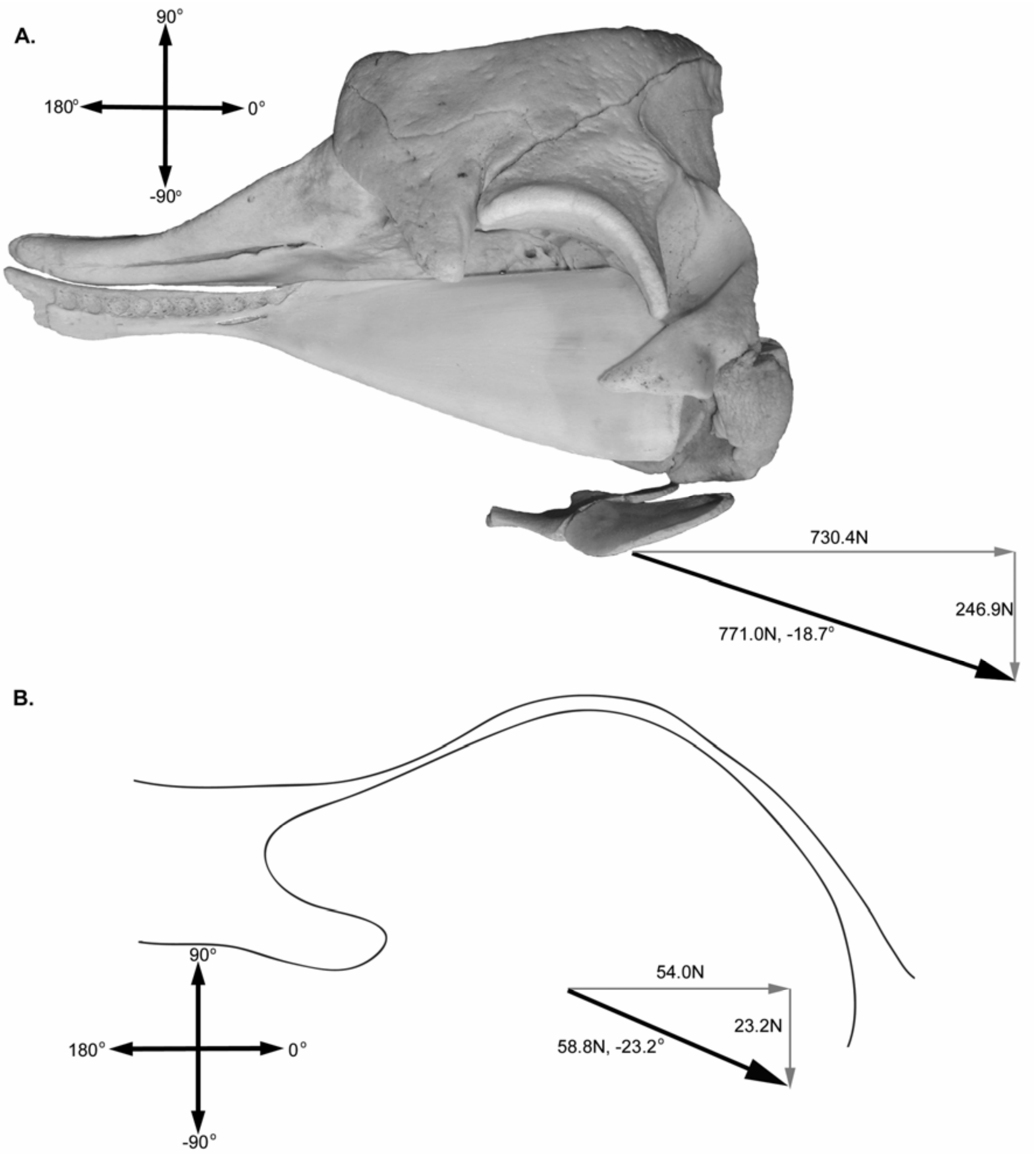

Figure 11. Net tension vectors of *Kogia* hyoid and tongue depressors and retractors. (A.) The right and left sternohyoideus, thyrohyoideus, and sternothyroideus were hyoid depressors and retractors. (B.) The hyoglossus and styloglossus were tongue depressors and retractors.

3.5 *Tursiops truncatus* Hyolingual Myology

Tursiops truncatus hyolingual myology consisted of well-developed bilateral strap muscles that, with the exception of extrinsic lingual muscles, attached by aponeuroses to ossified or cartilaginous structures. As with *Kogia*, the most robust of these was the sternohyoideus, which inserted upon most of the ventral basihyal and thyrohyal surfaces. Stylohyoideus and cricothyroideus muscles absent in *Kogia* were identified in *T. truncatus*. Mean *T. truncatus* hyolingual muscle variables are summarized in Tables 4 through 6. Predicted values at a standardized total body length of 252 cm are presented in Tables 7 through 9. All observed myological data for *K. sima* and *K. breviceps* muscle dimensions, cross-sectional areas and maximum-tetanic tensions are available in Tables B-1 through B-22. The hyolingual myology of *T. truncatus* was not expected to be as robust as *Kogia*. However, most PMTT and MMTT means between the genera were generally not significantly different ($P < 0.05$).

3.5.1 Mylohyoideus

The *T. truncatus* mylohyoideus (Fig. 12, 13, and 14) was a thin, delicate muscle throughout most of its length. However, it thickened to several centimeters near its origin along the medial aspect of each mandibular rami. This origin included the entire space from the mandibular symphasis to near the mandible’s caudal extent. Right and left mylohyoideus muscles traveled ventromedially to insert upon a medial raphe. A “V” shaped fascial sheet joined both sides at the mediocaudal aspect, but only extended approximately one-fifth of the mylohyoideus' width. The *T. truncatus* mylohyoideus was wider than in *Kogia* and reflected the species' telescoped mandible. As a whole, the mylohyoideus formed a lingual sling that enclosed deeper hyolingual muscles. The mylohyoideus was the second most-powerful muscle measured, with predicted PMTT (MMTT) vector values of 270.0 N (444.0 N) at 100.7°. As in *Kogia*, the *T. truncatus* mylohyoideus formed a lingual sling and could assist to return the hyoid to its basal position. Superficially, the platysma rostrally and the digastricus caudally were tightly adhered to the mylohyoideus. Several deeper muscles were attached loosely by fascia, including the stylohyoideus, styloglossus, hyoglossus, and genioglossus.

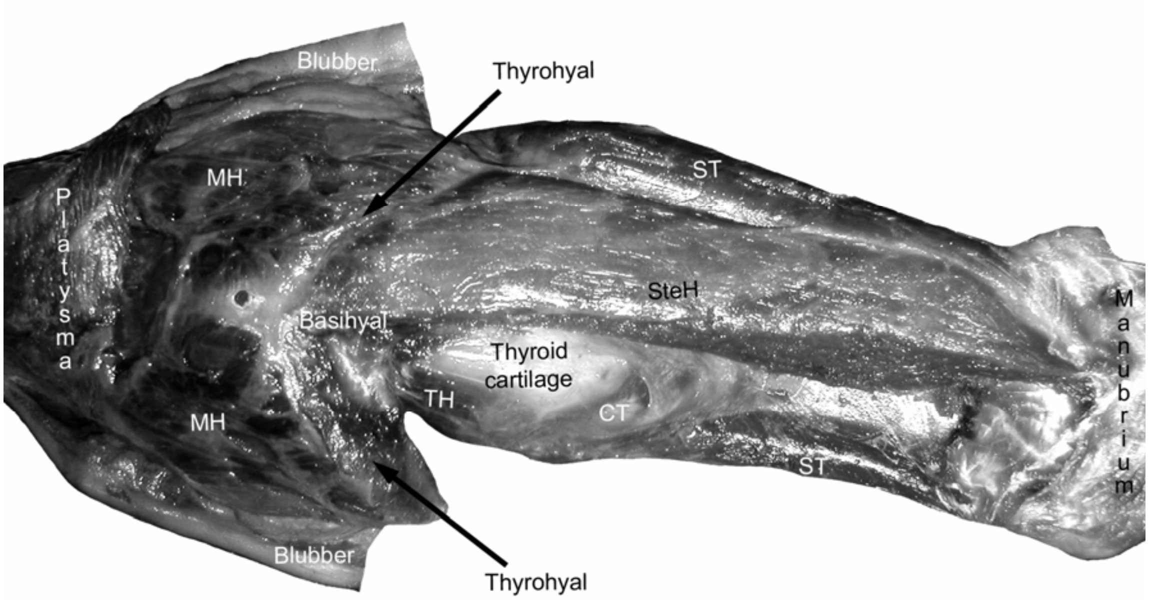

Figure 12. Ventral view of the caudal musculature associated with the *T. truncatus* hyolingual complex. MH = mylohyoideus, TH = thyrohyoideus, CT = cricothyroideus, SteH = sternohyoideus, and ST = sternothyroideus.

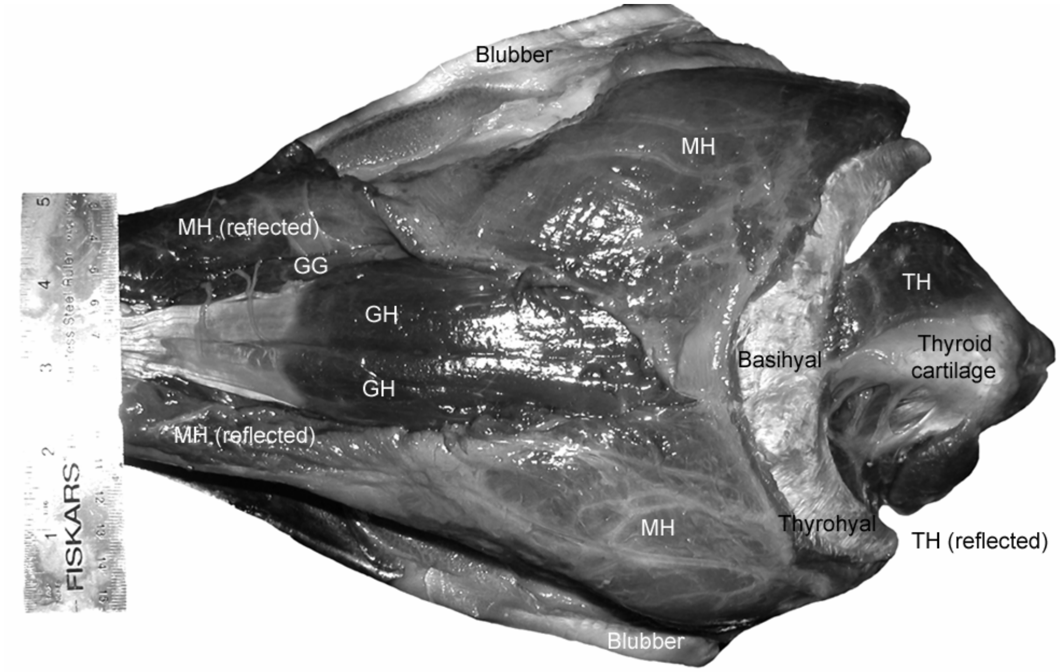

Figure 13. Rostral *T. truncatus* hyolingual myology viewed from the ventral aspect. Note the long geniohyoideus tendon of origin. MH = mylohyoideus, GG = genioglossus, GH = geniohyoideus, and TH = thyrohyoideus.

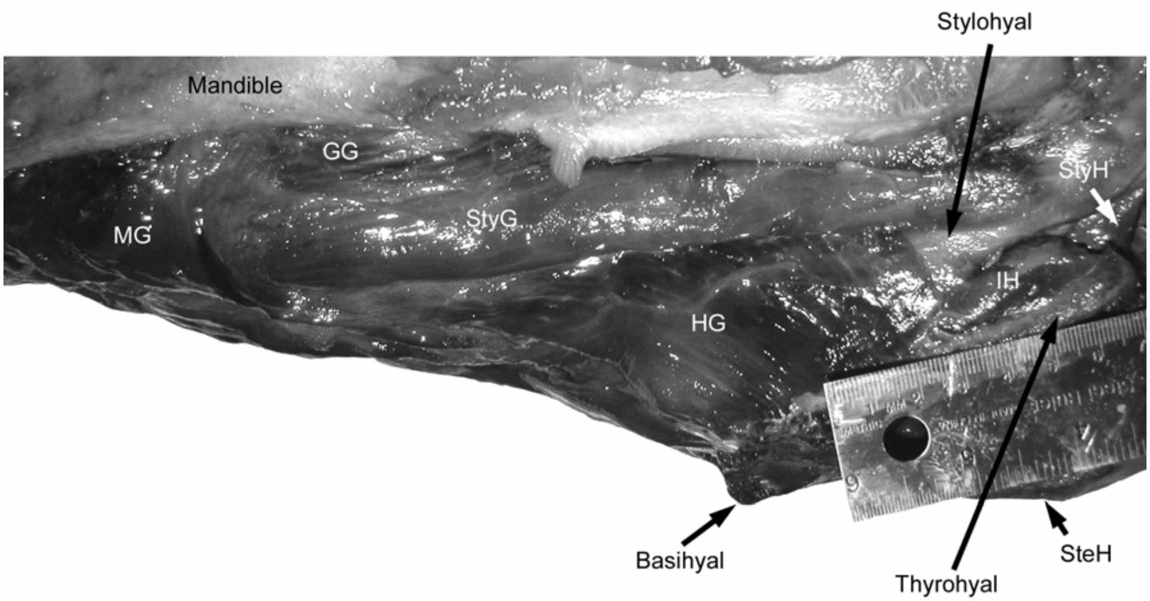

Figure 14. *Tursiops truncatus* hyolingual musculature viewed laterally. MH = mylohyoideus, GG = genioglossus, StyG = styloglossus, HG = hyoglossus, IH = interhyoideus, StyH = stylohyoideus, and SteH = sternohyoideus.

3.5.2 Geniohyoideus

The geniohyoideus (Fig. 13) of *T. truncatus* originated on the mandibular symphasis by a long, caudally-directed tendon. The tendon continued caudally approximately one-third of the distance to the insertion, where a sharp transition to fascicles occurred. Right and left muscles were tightly adhered to one another along much of the muscle's length caudal to the common tendon of origin. Unlike *Kogia*, the *T. truncatus* geniohyoideus inserted on the rostromedial basihyal edge just rostral to the sternohyoideus. Vector predictions of mean geniohyoideus PMTT (MMTT) and palatal angle were 54.6 N (89.0 N) at 156.4°. The geniohyoideus functioned to return the hyoid to its basal position following hyoid depression and retraction and may have aided in mandibular depression. The geniohyoideus was deep to the mylohyoideus and superficial to the genioglossus. These muscles attached to the geniohyoideus loosely by fascia.

3.5.3 Sternohyoideus

As in *Kogia*, the *T. truncatus* sternohyoideus (Fig. 12 and 14) originated on the manubrium at its cranioventral border and included the ventral surface of the first true rib at its articulation to the manubrium. The muscle was directed craniodorsally, with right and left muscles tightly adhered. The sternohyoideus inserted on nearly the entire ventral basihyal and thyrohyal surfaces and, with the exception of the thyrohyoideus, displaced several hyolingual muscles to attach along the rostral basihyal and thyrohyal borders. Vector values of the sternohyoideus were 288.4 N (513.8 N) at -27.0°, making the sternohyoideus the most powerful muscle of the *T. truncatus* hyolingual complex and the primary depressor and retractor of the hyoid by drawing the basihyal caudoventrally. A direct attachment to the geniohyoideus was not present as it was in *Kogia*. The sternohyoideus was bordered by three muscles that adhered to it loosely by fascia: the sternothyroideus and sternocephalicus along the sternohyoideus' lateral aspect, and the pectoralis major ventrally at the sternohyoideus' origin.

3.5.4 Thyrohyoideus

The thyrohyoideus (Fig. 12 and 13) of *T. truncatus* originated from the craniolateral surface of the rostral cornu and thyroid cartilage of the larynx. The insertion was to the ventrocaudal and medial aspects of the basihyal in the only space not occupied by the more-superficial sternohyoideus. Data support a vector of predicted thyrohyoideus PMTT (MMTT) of 27.9 N (54.3 N) at 33.1°. The thyrohyoideus functioned to draw the hyoid caudodorsally. The thyrohyoideus was bordered rostrolaterally by the sternothyroideus and was loosely attached to it by fascia.

3.5.5 Stylohyoideus

The stylohyoideus (Fig. 14) was identified only in *T. truncatus*. This muscle originated on the ventrocaudal and caudolateral stylohyal surfaces at the tympanic articulation and narrowed to an insertion tendon on the caudolateral tip of the thyrohyal. The stylohyoideus was predicted to have a PMTT (MMTT) of 15.0 N (17.9 N) in an initial palatal direction of 115.9° at a standardized total body length of 241 cm. The function of the stylohyal was to pull the lateral thyrohyal tips dorsally and anchor the thyrohyal to the stylohyal. Although small, the stylohyoideus was distinct and clearly separated from the more rostral mylohyoideus and hyoglossus, which were loosely attached to the stylohyoideus by fascia.

3.5.6 Hyoglossus

The hyoglossus (Fig. 14) in *T. truncatus* originated from the rostral basihyal and thyrohyal borders by a thin aponeurosis between the ventral mylohyoideus and the deeper interhyoideus. This muscle became wider as it extended rostrodorsally to insert diffusely into the caudal one-third to two-thirds of the ventrolateral tongue body. Vector predictions of hyoglossus values were 60.5 N (82.1 N) at -31.4° and support the hyoglossus as the third most powerful hyolingual muscle in *T. truncatus*. The hyoglossus was easily removed from the superficial mylohyoideus and the deeper interhyoideus, both of which were held the hyoglossus loosely by fascia.

3.5.7 Interhyoideus

The *T. truncatus* interhyoideus (Fig. 14) was similar to that of *Kogia*, although it did not share the broad insertion found in *Kogia*. The muscle arose from the ventral surface of the stylohyal and was directed obliquely to insert upon the entire dorsal basihyal and thyrohyal surfaces. The predicted vector values of PMTT and palatal angle were 20.2 N at 38.0°. The interhyoideus prevented significant separation of the basihyal and thyrohyal from the stylohyal and may have approximated these elements. The interhyoideus was the deepest muscle of the *T. truncatus* hyoid complex, but a loose, fascial attachment to the superficial hyoglossus and mylohyoideus (extreme caudal portion of both muscles) was present.

3.5.8 Genioglossus

The *T. truncatus* genioglossus (Fig. 13 and 14) was similar to *Kogia* in its origin on the mandibular symphasis. The insertion was variable and ranged from the caudal one-third of the ventromedial tongue body to the entire ventromedial tongue surface. The vector value of genioglossus predicted PMTT (MMTT) and measured palatal angle was 29.7 N (39.4 N) at 170.6°. The genioglossus functioned to draw the tongue rostrally. The only surrounding muscle was the superficial geniohyoideus, which was held to the genioglossus loosely by fascia.

3.5.9 Styloglossus

The *T. truncatus* styloglossus (Fig. 14) originated from the stylohyal's dorsocaudal surface and inserted rostrally along the middle one-third of the lateral tongue body. Although small, the styloglossus had a predicted vector of 28.1 N (27.5 N) at -10.3°. The styloglossus was the primary tongue retractor in *T. truncatus* and functioned to pull the tongue caudoventrally. The superficial mylohyoideus attached loosely by fascia to the styloglossus.

3.5.10 Sternothyroideus

The sternothyroideus (Fig. 12) of *T. truncatus* shared a similar origin to *Kogia* along the manubrium's craniolateral surface. This long strap muscle extended cranially to insert upon the caudolateral anterior cornu of the laryngeal thyroid cartilage. The predicted sternothyroideus PMTT (MMTT) and palatal angle values were 37.4 N (66.0 N) at -46.1°. As in *Kogia*, the sternothyroideus was the primary retractor and depressor of the larynx. Several structures bordered the sternothyroideus along its path and attached loosely to it be fascia: the sternohyoideus ventromedially, the sternobrachialis caudoventrally, and the larynx near its insertion.

3.5.11 Cricothyroideus

The cricothyroideus (Fig. 12) was identified only in *T. truncatus* as a muscle that originated upon the caudoventral and caudolateral border of the cricoid cartilage of the larynx. This small muscle extended rostrodorsally to insert upon the caudal border of the rostral cornu of the laryngeal thyroid cartilage. The predicted cricothyroideus vector was 18.0 N (33.2 N) at -35.0° at a standardized total body length of 241 cm. The cricothyroideus approximated the cricoid and thyroid cartilages. The superficial sternohyoideus was the only muscle that bordered the cricothyroideus and was loosely attached to it by fascia.

3.5.12 Orbicularis Oris

The orbicularis oris shared a similar structure in *T. truncatus* as in *Kogia*. Fascicles were embedded within the dense connective tissue lateral to the maxilla and mandible. However, this muscle did not form a lateral mouth occlusion as in *Kogia*. The orbicularis oris extended from approximately half-way along the mandible, around the corner of the mouth, and along the caudal one-third of the maxilla.

3.5.13 Buccinator

The buccinator was not identified in *T. truncatus*.

3.5.14 Biomechanical Modeling

A similar vector model of *T. truncatus* hyolingual myology was developed as for *Kogia*. Figure 15 shows vectors of hyolingual muscles presumed to be influential in *T. truncatus* feeding. The stylohyoideus and cricothyroideus were excluded from analysis, as their contraction was likely insignificant in hyolingual movement. A large disparity was identified between muscle tensions values, with the thyrohyoideus and styloglossus an order of magnitude lower than the sternohyoideus and mylohyoideus. The sternohyoideus, thyrohyoideus and sternothyroideus produced caudoventral hyoid rotation. Tension components for these muscles, as well as lingual depressors and retractors (hyoglossus and styloglossus), are summarized in Figure 16.

The tongue and ventral blubber of *T. truncatus* also displayed notable characteristics. As in *Kogia*, the tongue fit into a dorsal cleft in the soft palate. However, this palatal vault was much reduced relative to *Kogia*. The tongue was also much more elongated relative to *Kogia* and extended approximately one-third to one-half of its length beyond the frenulum. The tongue was long and ovoid in shape, with a blunt tip versus the pointed tongue tip of *Kogia*. The ventral blubber appeared to gradually shift from a pliable state found over much of the trunk to a progressively less elastic character rostrally near the hyoid's rostral border. *Tursiops truncatus* lacked any lateral gape occlusion and gape was visible along the rostral two-thirds of the mandible.

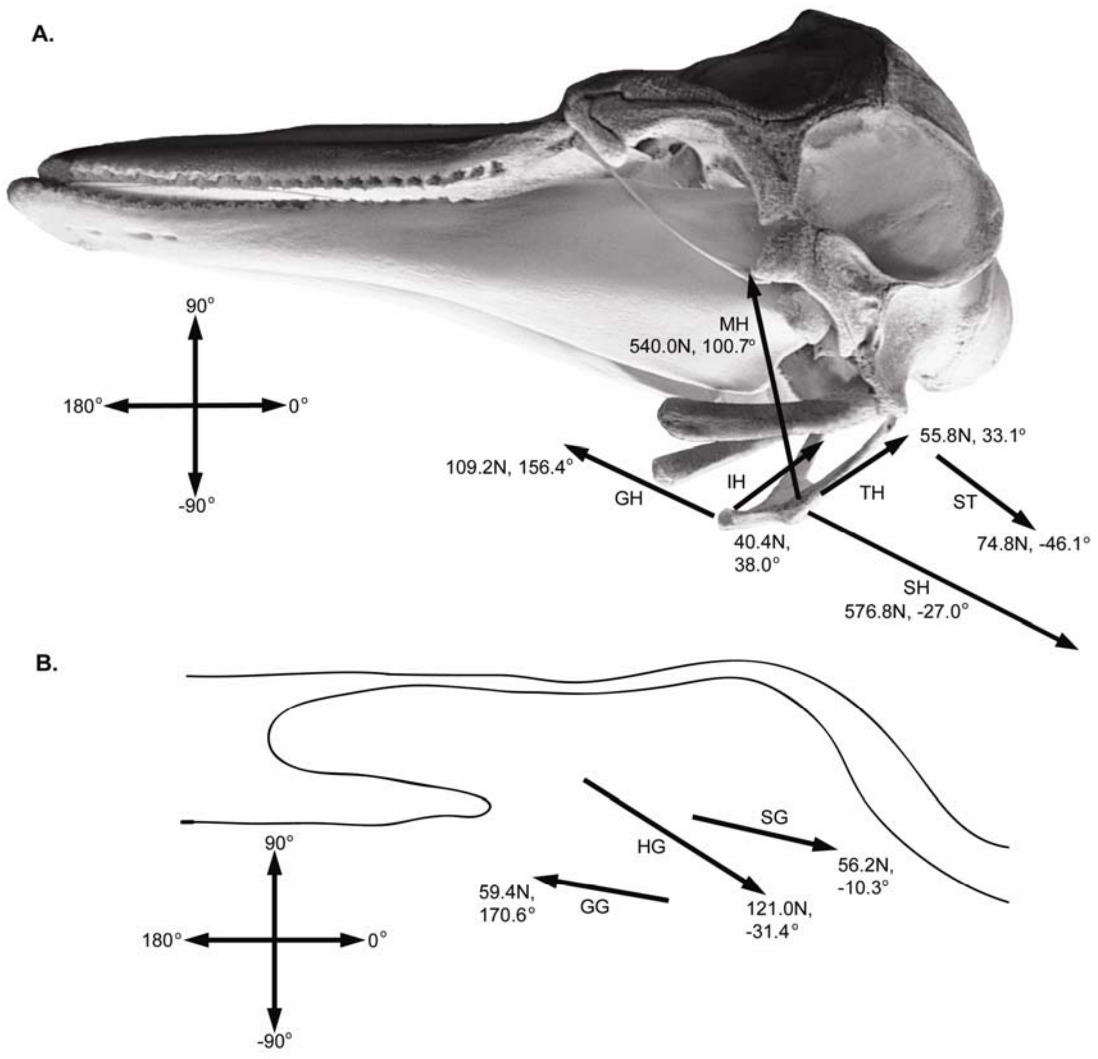

Figure 15. *Tursiops truncatus* biomechanical model of hyolingual muscle vectors. (A.) Muscles associated with hyoid depression, retraction, or return to the basal position. (B.) Lingual muscles associated with tongue movement.

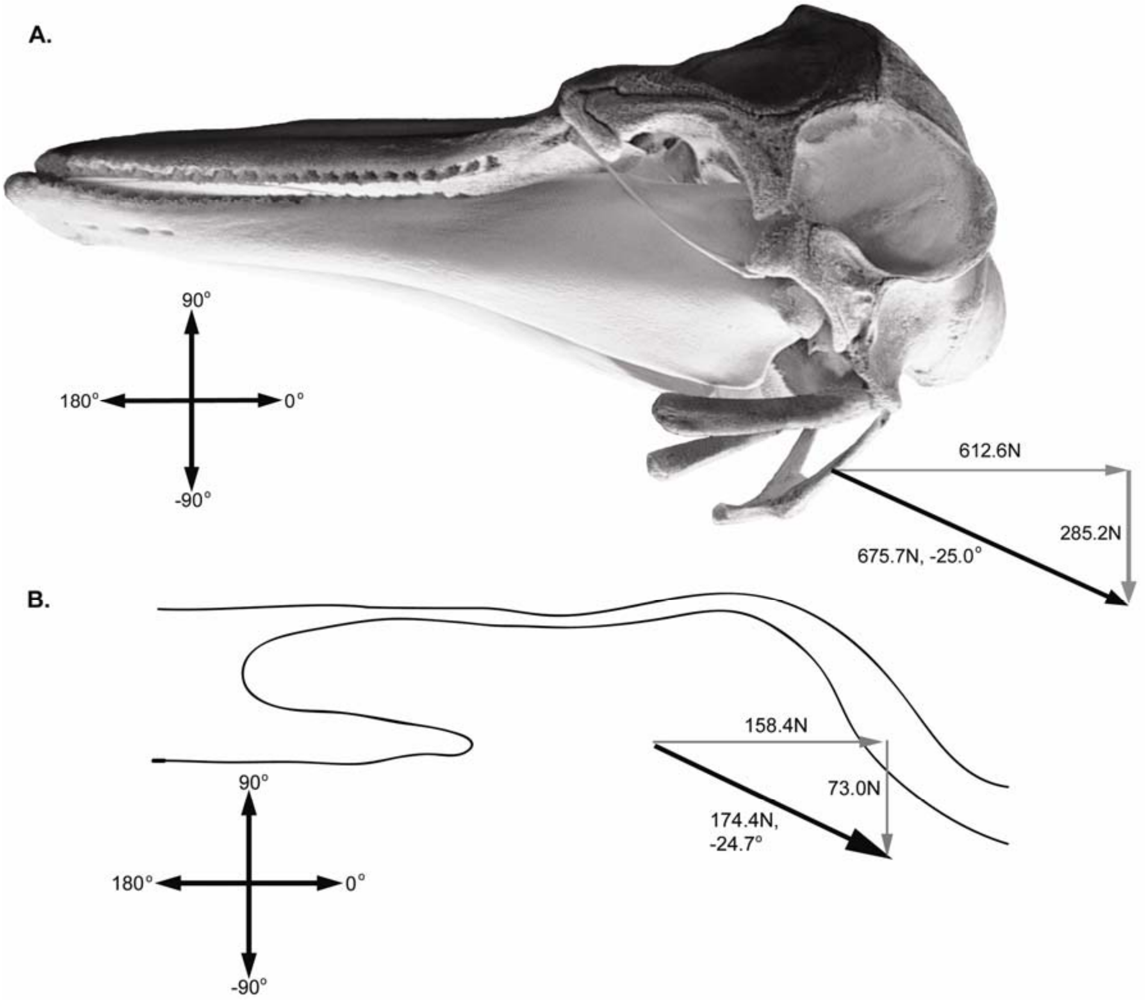

Figure 16. Tursiops truncatus net hyolingual depression and retraction vectors. (A.) Sternohyoideus, thyrohyoideus, and sternothyroideus predicted PMTT and palatal angles combined into a net vector of hyoid movement. (B.) The PMTT and palatal angles of hyoglossus and styloglossus vectors were added to produce a resultant vector of lingual movement.

3.6 Comparative Hyolingual Myology

It was hypothesized that *Kogia* muscles would be capable of significantly greater maximum tetanic tensions than *T. truncatus* to produce more powerful tongue and hyoid depression and retraction. However, ANCOVA's of PMTT and MMTT values rejected this hypothesis and identified only a few significant differences between *Kogia* and *T. truncatus* PMTT after scaling for either total body length or mass. Sidedness was not found to be significantly different between right and left muscles in any species group. Styloglossus PMTT was significantly less in *K. sima* ($P < 0.005$) and pooled *Kogia* ($P < 0.01$) than in *T. truncatus* (adjusted $r^2 = 0.732$). Hyoglossus PMTT was significantly less in all *Kogia* groups ($P < 0.05$) than in *T. truncatus* (adjusted $r^2 = 0.758$). Sternothyroideus PMTT was significantly greater in *K. sima* ($P < 0.01$) and pooled *Kogia* ($P < 0.05$) compared to *T. truncatus* (adjusted $r^2 = 0.656$).

3.7 Feeding Behavior

3.7.1 *Kogia* Feeding Behavior

Kogia behavioral observations supported anatomical measurements that hyoid depression and retraction, as well as the utility of lateral gape occlusion, are significant for effective suction feeding. *Kogia* subjects either swam freely to food items, or were stationary as food items were placed in front of their mouths (Fig. 17A and B). *Kogia* feeding involved nearly simultaneous jaw opening, gular depression and retraction. Minute fluctuations in gape and gular movement were identified immediately prior to feeding. Observations indicated food began an initial movement into the oral cavity with gape increase in response to presumed suction forces. However, food velocity did not increase rapidly until gular depression was observed. Once jaw opening began, it progressed rapidly and extensively, with maximum gape angle frequently in excess of 60º. Suction generation was likely aided by a tissue structure on each side of the mandible that occluded lateral gape and assisted in forming a circular aperture. Jaw closure was slower than opening and involved the gular region's return to its initial position.

3.7.2 *Kogia* Feeding Kinematics

Kogia kinematic variables are summarized in Table 10. The *Kogia* feeding cycle (Fig. 18A) consisted of four phases: preparatory, jaw opening, gular depression, and jaw closing. Phase I (preparatory) was observed when the maxillary tip, mandibular tip, COM, eye, and external rostral border of the hyoid were identified within a single video field, and gape was 25% greater than minimum gape (to eliminate pre-feeding gape fluctuations). Phase II (jaw opening) was initiated when gape began to increase by ≥ 0.2 cm/field. Phase III (gular depression) began at maximum gape. Gular depression and retraction were not exclusive to the gular depression phase, but also occurred in jaw opening and closing phases. Phase IV (jaw closing) began when gape started to close by ≥ 0.2 cm/field and ended when jaw closure decreased to ≤ 0.2 cm/field. Mean maximum gape angle, mean maximum opening gape angle velocity and mean maximum gape occurred during phase II, while maximum closing gape angle velocity, mean maximum gular depression, mean time to maximum gular depression, mean maximum gular retraction, and mean time to maximum gular retraction generally occurred in phase III.

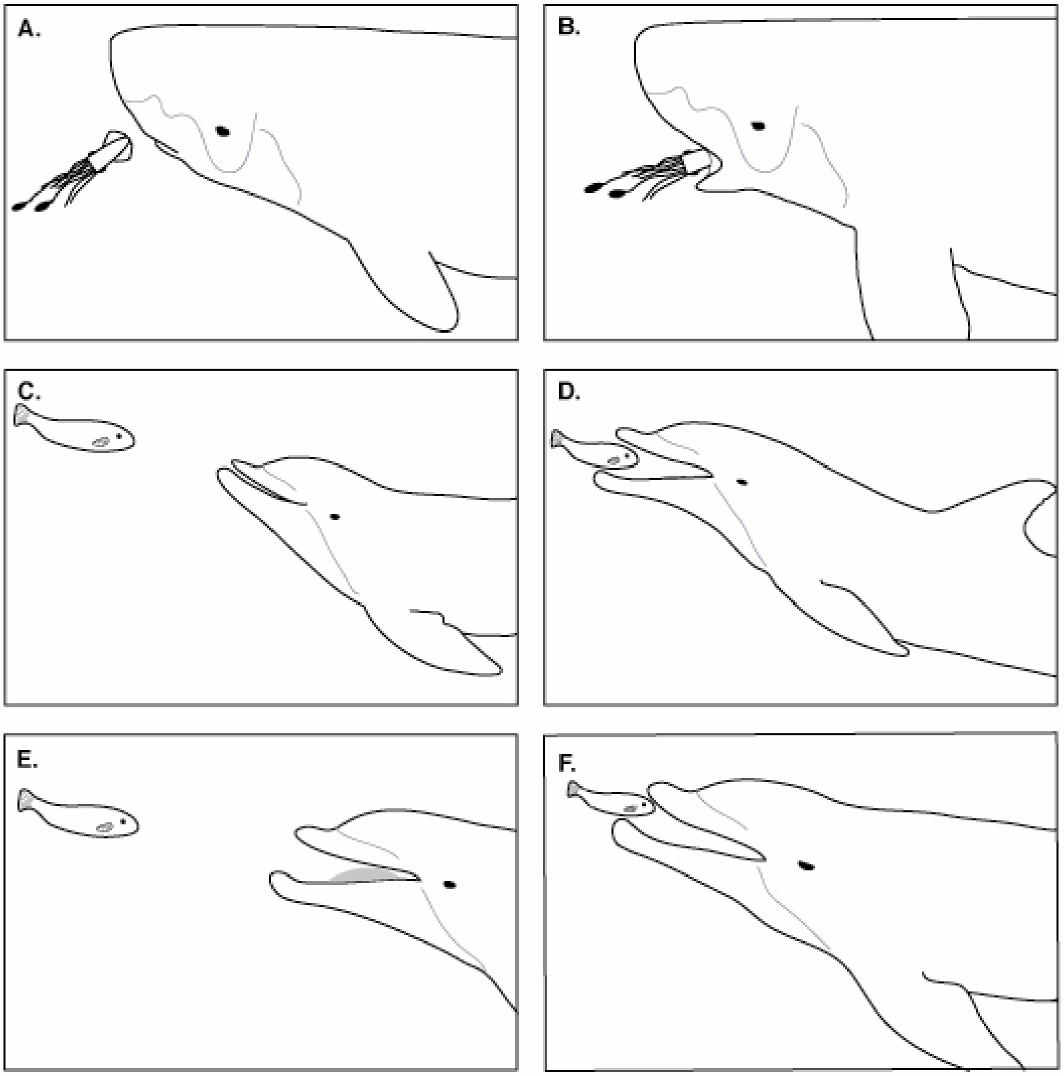

Figure 17. *Kogia* and *T. truncatus* feeding near the beginning of the observed feeding cycle and at maximum gape. (A.) *Kogia* preparatory phase with minimal gape (B.) phase II ending with maximum gape. (C.) *Tursiops truncatus* closed gape approach feeding begins with slight gape, tucked pectoral fin, and forward motion and (D.) overtakes prey at maximum gape. (E) *Tursiops truncatus* open gape approach enters the frame at or near maximum gape, continues forward motion with open gape, and (F.) closes jaws as prey is overtaken.

Table 10. Summary of feeding kinematic variable means and standard deviations for *Kogia*, pooled *T. truncatus*, *T. truncatus* open gape approach, and *T. truncatus* closed gape approach.

	Kogia	*T. truncatus* pooled	*T. truncatus* Open	*T. truncatus* Closed
Kinematic Variable	Mean ± SD	Mean ± SD	Mean ± SD	Mean ± SD
Mean RSI	-0.67 ± 0.29	0.94 ± 0.11	0.95 ± 0.076	0.93 ± 0.12
Mean feeding cycle dur. (ms)	470.4 ± 139.2	863.3 ± 337.0	1210.6 ± 207.0	662.3 ± 206.8
Mean phase I dur. (ms)	38.9 ± 65.4	59.4 ± 109.7	20.0 ± 60.3	83.3 ± 125.3
Mean phase II dur. (ms)	195.4 ± 114.9	492.8 ± 276.1	756.1 ± 277.2	340.4 ± 115.0
Mean phase III dur. (ms)	36.1 ± 75.5	45.0 ± 88.1	77.3 ± 126.6	26.3 ± 51.0
Mean phase IV dur. (ms)	200.0 ± 85.2	266.1 ± 176.0	359.1 ± 248.1	212.3 ± 85.9
Mean maximum gape angle (º)	39.8 ± 18.9	24.8 ± 6.60	24.5 ± 7.33	24.9 ± 6.34
Mean max. opening gape angle vel. (º/s)	293.5 ± 261.1	83.7 ± 55.6	40.5 ± 17.7	108.8 ± 54.7
Mean max. gape (cm)	7.73 ± 3.09	11.6 ± 3.29	11.2 ± 3.51	11.8 ± 3.24
Mean time to max. gape (s)	282.5 ± 147.1	563.9 ± 251.0	781.8 ± 252.9	437.7 ± 141.9
Mean max. closing gape angle vel. (º/s)	223.2 ± 120.9	120.4 ± 53.9	108.5 ± 48.6	127.4 ± 56.8
Mean max. gular depress. (cm)	2.25 ± 1.81	4.75 ± 2.57	4.88 ± 2.32	4.61 ± 2.91
Mean time to max. gular depress. (ms)	283.3 ± 153.2	623.3 ± 208.1	695.0 ± 217.3	551.7 ± 181.1
Mean max. gular retract. (cm)	2.67 ± 2.35	5.57 ± 3.07	1.79 ± 0.11	4.11 ± 3.35
Mean time to max. gular retract. (ms)	343.3 ± 137.2	397.4 ± 197.2	261.1 ± 154.0	438.3 ± 196.2
Mean max. food vel. (cm/s)	40.6 ± 22.7	n/a	n/a	n/a
Mean max. hydraulic jetting dist. (cm)	2.59 ± 1.13	n/a	n/a	n/a
Mean max. hydraulic jetting vel. (cm/s)	22.0 ± 5.90	n/a	n/a	n/a
Mean max. tongue retract. (cm)	n/a	4.65 ± 3.73	n/a	5.13 ± 3.76
Mean time to max. tongue retract. (ms)	n/a	167.0 ± 57.0	n/a	148.0 ± 20.0

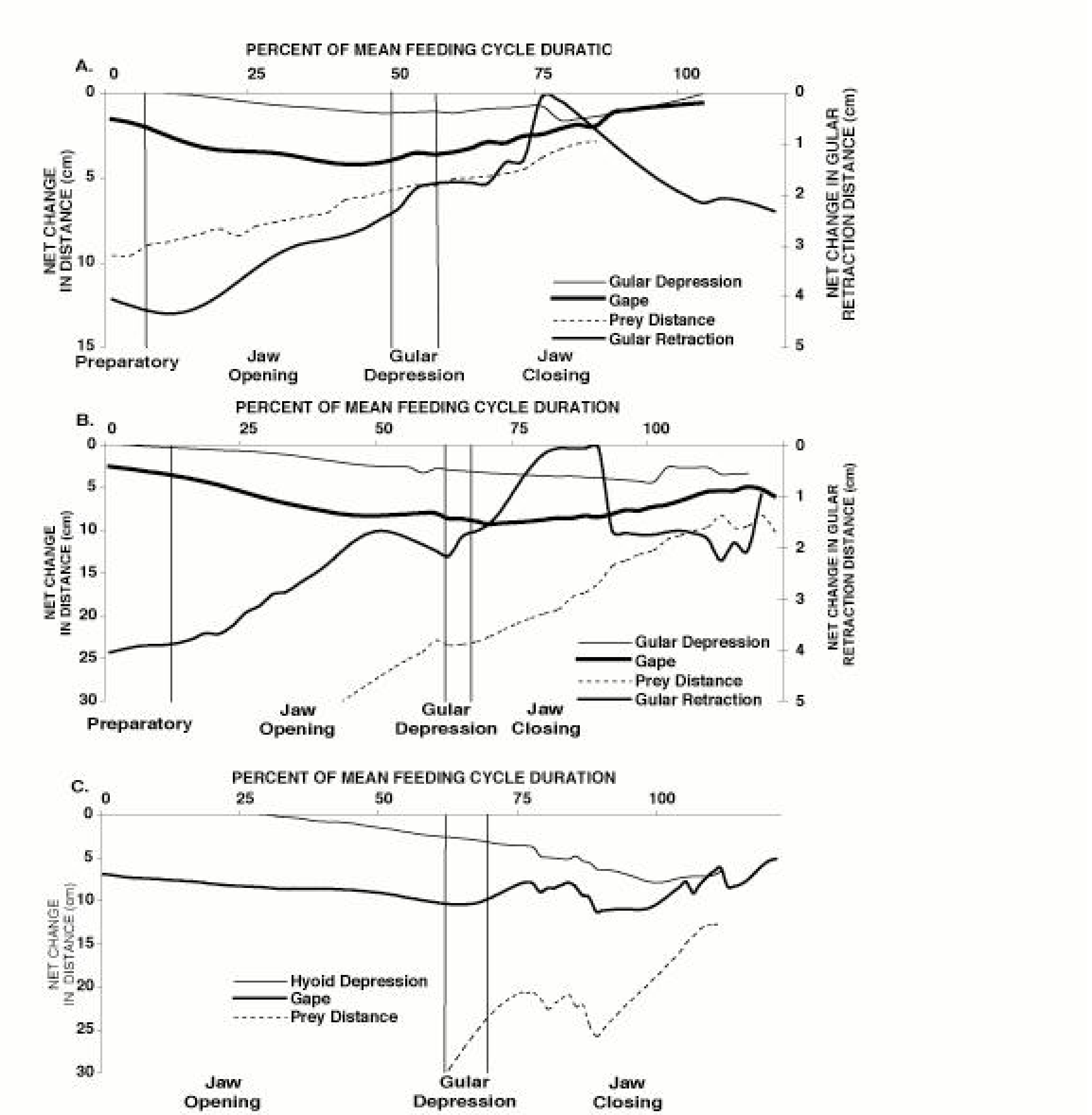

Figure 18. Profiles of key kinematic variables in *Kogia* and *T. truncatus* as a percentage of total feeding cycle duration: gape, gular depression, gular retraction, and prey distance. Gular retraction scaled along the right Y-axis and all other variables on the left Y-axis. (A.) Kinematic profile of *Kogia*. (B.) Kinematic profile of *T. truncatus* closed gape approach. (C.) Kinematic profile of *T. truncatus* open gape approach (gular retraction is not depicted). Feeding phases I-IV (preparatory, jaw opening, gular depression, and jaw closing) are denoted below each graph. *Tursiops truncatus* open gape approach included a notably delayed gular depression phase onset as a result of slow gape increase. Note gular return to baseline following completion of the feeding cycle.

Kogia correlation analysis supports a more negative RSI with decreased time to maximum gape (Spearman’s rho; α ≤ 0.05) and slower maximum closing gape angle velocity (Spearman’s rho; α ≤ 0.05). RSI values decreased in association with increased time to maximum gular depression (Pearson’s ‘r’; α ≤ 0.05) and increased maximum gular depression (Pearson’s ‘r’; α ≤ 0.05). RSI also decreased with increased time to maximum gular retraction (Pearson’s ‘r’; α ≤ 0.01) and increased maximum gular retraction (Pearson’s ‘r’; α ≤ 0.01). Maximum gular depression increased with maximum gular retraction (Spearman’s rho; α ≤ 0.01). Time to maximum gape increased with larger maximum gape and faster maximum food velocity (Pearson’s ‘r’; α ≤ 0.05).

3.7.3 *Tursiops truncatus* Feeding Behavior

Tursiops truncatus subjects exhibited distinct feeding behaviors from *Kogia*. Feeding was more locomotory and subjects approached frozen herring from at least three to four meters away. Some fluctuations in gape and gular movement were noted immediately prior to feeding. Pectoral fins were frequently flared or rotated outward with the lateral surface of the flipper faced forward (pronation), presumably as an effort to slow forward progress within centimeters of food items. Mandibular depression was slow and gular depression was extensive relative to *Kogia*. Gular depression and retraction were not limited to the gular depression phase and were observed in jaw opening and jaw closing phases (Fig. 18B and C). Two distinct ram-based feeding patterns were identified, *T. truncatus* open gape approach, and *T. truncatus* closed gape approach (Fig.

17C-F). Subjects performing *T. truncatus* open gape approach feeding behavior entered the camera’s view with 50% of maximum gape or more. Gape increased slowly to maximum gape while the subject swam to and captured the food item, at which time the jaws closed. *Tursiops truncatus* closed gape approach was utilized by both subjects, but *T. truncatus* open gape approach was utilized only by “Clicker.” Subjects performing *T. truncatus* closed gape approach feeding behavior entered the first video field at or near closed gape (< 3 cm gape); a preparatory phase was observed before the jaws rapidly opened to maximum gape within centimeters of food. Gular depression and retraction and tongue retraction were visible in most sequences.

3.7.4 *Tursiops truncatus* Feeding Kinematics

Pooled *T. truncatus*, open gape approach, and closed gape approach feeding variables are summarized in Table 10. Four feeding phases (preparatory, jaw opening, gular depression and jaw closing) were identified (Fig. 18B and C). Phase I began when maxillary and mandibular tips were identified and gape was 25% greater than minimum gape. The mean maximum gape angle, mean maximum opening gape angle velocity, mean maximum gape and mean time to maximum gape occurred in phase II. Mean maximum closing gape angle velocity occurred in phase IV. *Tursiops truncatus* closed gape approach feeding behavior was more representative of the pooled data while *T. truncatus* open gape approach feeding behavior was more divergent. Phase I was observed in only one of 11 *T. truncatus* open gape approach feeding sequences, and the only trial in which tongue retraction was observed measured 1.31 cm and occurred in a time to maximum tongue retraction was 300 ms.

Pooled *T. truncatus* correlation analysis showed an increased maximum gape angle with both increased maximum opening and closing gape angle velocities (Pearson's "r"; $\alpha \leq 0.01$). *Tursiops truncatus* open gape approach correlations included increased maximum closing gape angle velocity with increased maximum opening gape angle velocities (Spearman's rho; $\alpha \leq 0.05$). Maximum gape angle increased with both maximum opening and closing gape angle velocity (Pearson's "r"; $\alpha \leq 0.01$). Maximum gular depression increased with increased maximum gular retraction (Spearman's rho; $\alpha \leq 0.01$). Within *T. truncatus* closed gape approach feeding mode, increased RSI correlated with decreased feeding cycle duration (Spearman's rho; $\alpha \leq 0.01$), and decreased time to maximum gular depression (Spearman's rho; $\alpha \leq 0.05$). Maximum closing gape angle velocity increased with maximum opening gape angle velocity (Pearson's "r"; $\alpha \leq 0.01$). Maximum gape angle increased with both increased maximum opening and increased closing gape angle velocity (Pearson's "r"; $\alpha \leq 0.01$).

3.7.5 Comparative Odontocete Kinematics

3.7.5.1 *Kogia* and Pooled *T. truncatus*

Numerous significant differences were demonstrated between genera. Mean *Kogia* RSI values were significantly less than any *T. truncatus* group (pooled, open gape, or closed gape trials) ($P < 0.001$). *Kogia* suction distances were greater than any *T. truncatus* group ($P < 0.05$) (Table 11) and *Kogia* ram distances were less than any *T. truncatus* group ($P < 0.001$). The mean total feeding cycle and jaw opening durations (phase II) were significantly shorter in *Kogia* than any *T. truncatus* group ($P \leq 0.002$). Mean gular depression (phase III) duration was significantly longer in *Kogia* than *T. truncatus* open gape approach ($P < 0.01$). Mean maximum gape angle was greater in *Kogia* than any *T. truncatus* group ($P \leq 0.005$). Mean maximum opening and closing gape angle velocities were significantly faster in *Kogia* compared to any *T. truncatus* group ($P < 0.01$). Mean maximum gape was significantly smaller in *Kogia* than any *T. truncatus* group ($P < 0.01$). Mean time to maximum gape was shorter in *Kogia* compared to any *T. truncatus* group ($P \leq 0.002$). Mean maximum gular depression was less in *Kogia* compared to pooled *T. truncatus* and *T. truncatus* open gape approach ($P < 0.05$). Mean time to maximum gular depression was significantly faster in *Kogia* than any *T. truncatus* group ($P < 0.05$).

Table 11. Capture distances and durations from onset of feeding cycle for two *Kogia* species and *Kogia* pooled data, pooled *T. truncatus*, open gape approach (OGA), and *T. truncatus* closed gape approach (CGA). $t_{capture}$ represents feeding cycle duration.

Predator	$t_{capture}$ (ms) ± SD	Predator-prey distance (cm) ± SD	Suction distance (cm) ± SD	Ram distance (cm) ± SD	RSI ± SD
Kogia sima	481.9 ± 145.4	8.80 ± 5.24	4.45 ± 3.00	0.54 ± 1.68	-0.71 ± 0.34
Kogia breviceps	447.2 ± 135.6	14.5 ± 6.24	5.93 ± 2.73	1.78 ± 0.55	-0.60 ± 0.17
Pooled *Kogia*	470.4 ± 139.2	10.5 ± 5.88	4.89 ± 2.86	0.90 ± 1.52	-0.67 ± 0.29
T. truncatus (pooled)	863.3 ± 337.0	41.6 ± 21.0	-2.45 ± 6.87	46.1 ± 21.0	0.94 ± 0.11
T. truncatus (OGA)	1210.6 ± 207.0	66.4 ± 8.21	-1.81 ± 7.51	71.4 ± 8.49	0.95 ± 0.076
T. truncatus (CGA)	662.3 ± 206.8	28.5 ± 11.6	-2.79 ± 6.69	32.8 ± 10.2	0.93 ± 0.12

3.7.5.2 *Tursiops truncatus Open and Closed Gape Approach Feeding*

Numerous significant differences were also demonstrated between *T. truncatus* feeding modes. The mean ram distance of *T. truncatus* open gape approach was significantly greater than pooled *T. truncatus* and *T. truncatus* closed gape approach ($P \leq 0.005$). *Tursiops truncatus* open gape approach mean feeding cycle duration was longer than pooled *T. truncatus* or *T. truncatus* closed gape approach ($P < 0.02$). The mean jaw opening duration was also longer for *T. truncatus* open gape approach than for pooled *T. truncatus* ($P < 0.02$) and *T. truncatus* closed gape approach ($P < 0.001$). The mean gular depression (phase III) duration was significantly longer in *T. truncatus* open gape approach than *T. truncatus* closed gape approach ($P < 0.01$). Mean maximum opening gape angle velocity was significantly slower in *T. truncatus* open gape approach compared to pooled *T. truncatus* ($P = 0.012$) and *T. truncatus* closed gape approach ($P < 0.001$). Mean time to maximum gape was also significantly longer in *T. truncatus* open gape approach than pooled *T. truncatus* or *T. truncatus* closed gape approach ($P < 0.05$). Mean maximum gular retraction was significantly greater in *T. truncatus* open gape approach compared to *Tursiops* closed gape approach ($P < 0.05$).

CHAPTER IV

DISCUSSION

4.1 Biomechanics of Hyolingual Anatomy

Although significant differences in maximum tetanic tension were not identified between most *Kogia* and *T. truncatus* hyolingual muscles, biomechanical modeling illustrated the importance of mechanical advantage and leverage to feeding in *Kogia*. As in *G. melas*, the sternohyoideus was the primary depressor and retractor of the hyoid (Werth 1992, 2000*a*). Initially, the *Kogia* sternohyoideus orientation was roughly 19° relative to the palatal plane. The basihyals and thyrohyals likely remained closely-spaced to the stylohyal by the firm interhyoideus attachment. Therefore, most hyoid movement occurred at the tympanohyal-tympanic bone articulation. As the *Kogia* sternohyoideus contracted, initial hyoid movement was almost exclusively in the ventral direction. The degree of depression decreased relative to retraction as the hyoid swung ventrocaudally. During caudoventral hyoid retraction, the angular difference (relative to the palatal plane) between the sternohyoideus insertion and origin was reduced, effectively increasing the mechanical advantage for retraction of the muscle. When the hyoid was fully retracted, the sternohyoideus' palatal angle was likely reduced to near 0°, making it a pure hyoid retractor.

Although the sternohyoideus' palatal angle relative was different between *Kogia* and *T. truncatus* the difference was only 8° in scaled muscle angles. It is doubtful that this minor difference can account for the divergent feeding behavior observed between *Kogia* and *Tursiops*. Mechanical advantage might have been greater in either *Kogia* or *T. truncatus* if the mean scaled stylohyal lengths (lever arms) were longer in either genus. However, this was not the case. The lack of greater PMTT or mechanical advantage in *Kogia* is surprising, as one or both of these factors could increase the force transmitted for oral volume increase. However, it is apparent that available tension is not the primary factor in suction feeding ability. Additional factors, such as hyoid, orofacial, tongue, and skull morphology, are dissimilar between *Kogia* and *T. truncatus*, and likely responsible for their divergent feeding behavior.

Hyoid depression was somewhat of a retraction by-product, as basihyal and thyrohyal retraction required ventral stylohyal rotation, which facilitated caudoventral tongue movement due to hyolingual, hyoglossal, and styloglossal attachments. In beaked and pilot whales, the genioglossus and hyoglossus were also the primary tongue retractors (Heyning and Mead 1996, Werth 2000*a*). This is of evolutionary interest, as the tympanohyal-stylohyal-epihyal chain facilitated both ventral and caudal tongue movement where no other means appeared available. In theory, lingual muscle attachment to the nasal bones could produce a purely caudal tongue motion. However, nasal bones proximity to the caudal oral cavity would likely limit such motion. No ossified structure is present ventral of the tongue for lingual depression. Although a thick blubber layer is present, the elastic character of the blubber would likely reduce the effectiveness of any strong lingual depressor originating from it. Although a mobile hyoid is present in all vertebrates, *Kogia* hyoid size suggests that its original function as a facilitator of caudoventral lingual movement has been strongly conserved, possibly more so than any other cetacean.

The order and rapidity in which hyolingual muscles contracted was likely influential in *Kogia* suction generation. Behavioral observations demonstrated that gular depression and retraction coincided with mandibular depression (Fig. 15). To maximize intraoral pressure development, the sternohyoideus, sternothyroideus, and thyrohyoideus almost certainly depressed and retracted the hyoid, which in itself depressed the mandible by geniohyoideus insertion to the sternohyoideus. Although cetaceans do not masticate (Werth 2000*b*), a small digastricus was present to aid mandibular depression (Schulte and Smith 1918, Chaine 1914, Reidenberg and Laitman 1994, Heyning and Mead 1996). Hyoid rotation alone likely pulled the tongue caudoventrally, but simultaneous hyoglossal and styloglossal contraction at, or slightly after, initial hyoid rotation likely enhanced the rapidity of oral volume increase. During hyoid depression and retraction, the interhyoideus restrained basihyal and thyrohyal movement away from the rest of the hyoid chain. Once these muscles reached or approached maximum contraction, oral volume was likely maximized and oral pressure peaked. Kinematic data showed that gape began to decrease before maximum hyoid depression and retraction. This was likely critical to prey capture. When the hyoid began returning to basal position before gape closure, food was forced out of the mouth in hydraulic jetting events. However, when gape closed before hyoid return and the long, fang-like teeth blocked food escape, rostrodorsal hyoid rotation could not force food from the mouth. Jaw closure was likely facilitated by the pterygoideus medialis, pterygoideus lateralis, masseter, and temporalis (Schulte and Smith 1918, Reidenberg and Laitman 1994). The hyoid's rostrodorsal return was likely a result of mylohyoideus contraction, which also assisted lingual return. Rostral lingual movement could be further assisted by genioglossal contraction. Mylohyoideus and genioglossus contraction likely aided to increase positive oral pressures and produced the observed hydraulic jetting. The interhyoideus may also have approximated the basihyal and thyrohyals to the stylohyal and enhanced hydraulic jetting capability.

4.2 Implications of Hyolingual Anatomy to Suction Feeding

The current understanding of vertebrate feeding supports the hyoid chain as a primary facilitator of suction feeding (Lauder 1985, Thexton et al. 1998, Werth 2000*b*, Edmonds et al. 2001, Sanford and Wainwright 2002). *Kogia*'s suction feeding ability and kinematic profile was established through behavioral performance trials of free-swimming subjects. A normal aspect of this feeding pattern was hyoid depression and retraction. It was hypothesized that *Kogia* hyolingual musculature would be capable of larger maximum tensions than *Tursiops* as an adaptation for better developed for suction feeding to produce a more forceful hyoid rotation. Although *Kogia* hyoid muscles are known to be large (Reidenberg and Laitman 1994) and were shown to be capable of high maximum tetanic tensions, predicted muscle tensions were generally similar to *T. truncatus*. The primary finding of hyolingual investigations was that a combination of morphological features was likely responsible for the generation of negative intraoral pressures during *Kogia* suction feeding

A significant morphological finding was that *Kogia* had combined basihyal and thyrohyal surfaces areas that were several times larger than those of *T. truncatus*. Heyning and Mead (1996) considered hyoid size and surface area between cetacean suction and raptorial feeders and identified hyoid enlargement as an adaptation for more robust sternohyoideus muscles in suction-feeding beaked whales. Although *Kogia* also appeared to have larger muscles relative to *T. truncatus*, this apparent difference may have stemmed from the larger basihyal and thyrohyal surface areas for sternohyoideus insertion. Although maximum tetanic tensions were not found to be significantly different in this study, basihyal and thyrohyal size likely played a key role in the development of presumably larger negative intraoral pressure in *Kogia*. By having a larger oral surface area caudally, a greater intraoral volume was likely displaced by caudoventral tongue and soft tissue movement than if a smaller hyoid surface were retracted, such as in *T. truncatus*. It is probable that not only the tongue, but also the pharyngeal region was distended by the broad hyoid's depression and retraction. As greater oral volume increase allows for more negative oral pressure development, suction feeding ability was likely strongly enhanced by hyoid enlargement. The ability of *Kogia* to depress and retract the hyoid more rapidly than *T. truncatus* corresponded to a greater suction component and likely enhanced an already significant suction feeding ability. However, *Kogia* hyoid enlargement relative to *T. truncatus* was likely the primary facilitator for effective *Kogia* suction feeding.

Hyoid enlargement raises the question of how can *Kogia* and *T. truncatus* sternohyoideus muscles of comparable CSA attach to disparately sized insertions. This discrepancy can be resolved by the more oblique sternohyoideus insertion angle in *Kogia* relative to *T. truncatus*. As the angle of a cross-section increases with departure from the perpendicular, the cross-sectional area must also increase. This is relevant to the sternohyoideus' insertion because, the more oblique the insertion angle, the greater the surface area on the basihyal and thyrohyal required for insertion. The roughly 8° difference in the palatal plane between *Kogia* and *T. truncatus* meant that the *Kogia* sternohyoideus required a greater insertion area. Further, the basihyal and thyrohyals of *Kogia* were generally situated at a palatal angle more rostrocaudal than in *T. truncatus*. This made the *Kogia* sternohyoideus insertion angle more oblique, which further necessitated a broader sternohyoideus insertion area.

Although terrestrial mammals, such as canids, maintain most hyoid elements as individual, ossified bones (except the tympanohyals), odontocetes may lose ossification or develop fused elements. For example, *T. truncatus* ceratohyals and epihyals are as cartilaginous elements and the thyrohyals can be fused to the basihyal (Reidenberg and Laitman 1994). A similar condition exists in *Kogia*, although the thyrohyals are retained as individual elements (Benham 1902, Hale 1962, Reidenberg and Laitman 1994). This brings into doubt the robustness of the cetacean hyoid to withstand hyolingual muscle tensions. However, cartilaginous elements identified in *Kogia* and *T. truncatus* generally lacked attachments for hyolingual muscles and were likely not directly exposed to their developed tensions. Tensions were likely transferred to these elements through hyoid rotation, but their elastic properties likely accommodated these forces through flexation. Even when whole heads were manually swung by the basihyal, the hyoid chain remained in tact. Furthermore, the presence of cartilaginous elements may aid significantly to hyoid motion. Cartilagenous surfaces are a standard component of highly mobile vertebrate joints and support fluid movement between bones. Cartilagenous elements likely have similar importance in cetacean hyoid biomechanics. Future investigations of hyoid cartilage composition may reveal how cartilaginous hyoid elements accommodate rapid and forceful motion and their specific contributions to hyoid biomechanics.

Cranial morphology was likely highly-influential in intraoral pressure development. *Kogia* have the bluntest rostra of all odontocetes (Miller 1923) and a relatively wider skull and mandible; adaptations that may in part be to enhance suction feeding. To maximize a change in oral cavity volume, starting volume should be minimized and volume displaced maximized. The short and wide *Kogia* rostrum and mandible could effectively result in a greater change in intraoral volume. This would permit *Kogia* to rapidly lower intraoral pressures relative to a longer, narrower mouth, such as in *T. truncatus*. However, this may not apply to all suction feeding cetaceans. Beaked whales have significantly elongated rostra and are known to produce suction (Heyning and Mead 1996). Further morphological, biomechanical, and kinematic investigation is necessary to adequately describe cetacean suction feeding strategies.

Tongue morphology is critical for suction feeding in some marine mammals (Gordon 1984) and is likely also significant for *Kogia*. Based on kinematic data, the short, triangular tongue acted as a piston that rapidly and forcefully traveled caudoventrally (via the hyoid apparatus) during a suction event. This action was much more rapid in *Kogia* than *T. truncatus* and was likely more effective by the tight fit of the *Kogia* tongue against a palatal elevation. The match between tongue and palate was so similar that individual ridges in the tongue and palate matched one another exactly. By pressing the tongue against the palate prior to feeding, suction was likely enhanced by this seal displacing a larger volume during tongue depression and retraction. Additionally, the presence of throat grooves in the blubber ventral to the hyoid in some suspected suction feeders, such as beaked whales, sperm whales, and *K. sima* may allow for additional gular distension when the hyoid is retracted (Clarke et al. 1968, Heyning and Mead 1991, 1996, Werth 2000*b*, 2005). Although the *T. truncatus* tongue also fit into a palatal elevation, the match was not as close. Presumably, a ram-based feeder would not require such an exact tongue-to-palate condition. The large basihyal-thyrohyal and short, wide tongue in *Kogia* versus the small basi-thyrohyal and large tongue in *T. truncatus* is likely significant in each genera's relative abilities to effectively increase oral volume while feeding.

Once developed, negative intraoral pressures must be directed for effective suction feeding. In *T. truncatus*, any negative pressure generated likely dissipated immediately along the lateral gape. However, the lateral mouth occlusions of *Kogia* would have prevented pressure dissipation laterally. The combination of a lateral occlusion and a short rostrum probably maintained a negative pressure gradient that was directed to the rostral mouth opening. This circular orifice presumably formed an efficient mechanism to draw water and prey into the mouth. Walruses are known to purse their lips during suction feeding potentially to restrict water flow away from prey items (Kastelein et al. 1994). The combination of oral and hyolingual morphology makes *Kogia* one of, if not the best, morphologically-suited cetacean for the production of large, directed, negative oral pressures necessary for suction feeding.

In summary, osteological and morphological features of *Kogia* and *T. truncatus* hyolingual and oral regions support *Kogia* as effective suction feeders and *T. truncatus* as ram feeders. Enlarged basihyals and thyrohyals relative to *T. truncatus* were likely key in oral volume increase and validate the functional hypothesis that enlarged hyoids are associated with suction feeding. A lateral gape occlusion, vaulted palate with matching, short, tongue, short mouth, and throat grooves are likely morphological adaptations for suction feeding in *Kogia*.

4.3 Kinematics of Suction-Based Feeding

The current functional hypothesis for negative intraoral pressure generation by feeding marine mammals is the rapid depression and retraction of the tongue by the hyoid apparatus. Much anatomical data exist to support this hypothesis (e.g., Gordon 1984, Reidenberg and Laitman 1994, Heyning and Mead 1996, this study). However, few cetacean investigations have examined the mechanics of suction production. The major finding of this study is that the kinematic profile of presumed suction feeders, *K. breviceps* and *K. sima*, validates that these odontocetes use suction and supports the functional hypothesis that suction is produced by rapid depression and retraction of the tongue and associated gular structures, such as the hyoid apparatus.

Negative *Kogia* RSI values were likely generated by the simultaneous depression and retraction of the hyoid apparatus, which in turn would have depressed and retracted the tongue. The rapidity of this movement, relative to *T. truncatus*, would likely have produced negative intraoral pressures and analysis of feeding trial footage verifies that suction is produced (food moved into the mouth), and is integral in the suction producing mechanism. In addition, suction production was also likely influenced by the rapid increase in gape and gape angle relative to *T. truncatus*. The fact that *Kogia* hyoid depression and retraction were not as extensive as *T. truncatus* is likely a scaling factor and not related to the relative magnitude of suction produced. *Kogia* subjects possessed a mandible that was largely recessed within the confines of the head, and only the distal one-third of the mandible was externally apparent compared to two-thirds for *T. truncatus*. This resulted in a larger gape in *T. truncatus* compared to *Kogia*. However, gape angle was greater in *Kogia* versus *T. truncatus*, and this wide gape angle is likely one of the greatest of any odontocete, with the possible exception of *Physeter* (Werth 2005). The short external mandible in conjunction with the specialized tissue ridges on the lateral perimeter of the mandible served to occlude the lateral gape of the jaw and helped produce a circular mouth opening; a surprising adaptation in an odontocete. Other marine mammals, such as walruses (*Odobenus rosmarus*; Kastelein et al. 1991) and belugas (*Delphinapterus leucas*; Brodie 1989), use elaborate orofacial musculature to occlude this region. Several throat grooves present in the gular region of *K. sima* may have assisted in allowing greater depression and retraction of the hyoid apparatus.

Kogia feeding must allow for the expulsion of water following food capture. *Kogia* subjects generally maintained a partial gape subsequent to phase IV, probably to allow water to exit. When *Kogia* subjects retained food after a feeding event, squid were restrained by the mandibular teeth, but partial gape was maintained. It appeared that only a light pressure was applied to food and it was doubtful that a soft-bodied cephalopod could significantly encumber gape closure. Furthermore, more forceful jaw closure could hinder squid removal from the teeth. The opposite behavior to suction is the forceful ejection of water out of the mouth, or hydraulic jetting. Hydraulic jetting was observed in 25% of *Kogia* feeding trials and could be influential in the capture of benthic prey or in manipulation of prey.

Two major caveats of the *Kogia* data were that subjects were young and that feeding trials ended prematurely due to the death of both subjects. This event was not unexpected since kogiids have a poor success rate in captivity (Sylvestre 1983). The situation in this study was unique in that these subjects survived for more than one year (Manire 2004). At the time of study, *Kogia* subjects were less than one year old, at least partially dependent upon formula diets, and did not swallow food in any recorded session. It is possible that sucking behavior could have been derived from suckling as in other mammals (Gordon and Herring 1987, German et al. 1992), and not completely representative of feeding in adult *Kogia*. However, the *K. breviceps* subject had consumed whole squid for the last 15 of 21 months of captivity. Food was routinely manipulated and introduced into the mouth by both subjects. Only events that mimicked feeding were analyzed; manipulatory behaviors were eliminated from analyses. Due to their young age and inexperience, feeding behavior by *Kogia* subjects was likely uncoordinated. However, significant suction events were still recorded despite the subjects' inexperience. Further study of older kogiids may show an even stronger suction capability than reported in this study.

The rapid feeding cycle of *Kogia* is consistent with kinematic data from pilot whales (*G. melas*), another demonstrated suction feeder. Werth (2000) also found a four-phase feeding cycle in *G. melas* that is unlike the feeding cycle of terrestrial mammals (Hiiemae and Crompton 1985), but likely derived from it. The mean *Kogia* feeding cycle duration was approximately 100 ms shorter than *G. melas* and 10 – 179 ms shorter in all phases except jaw closing (phase IV), where *G. melas* was 120 ms shorter. The more rapid *Kogia* feeding cycle suggests a greater suction capability than *G. melas* and this is supported by hyolingual anatomical data for both species (Reidenberg and Laitman 1994). Once food entered the oral cavity, greater water expulsion may have slowed *Kogia* jaw closure. A longer *Kogia* jaw closing duration than *G. melas* may also have resulted from an ability of *Kogia* to retain food with elongated teeth and not have required the more rapid gape closure of *G. melas*.

4.4 Kinematics of Ram-Based Feeding

Tursiops truncatus RSI values were distinctly ram-based, with little, if any suction component to feeding. Effective suction occurs over a limited distance and changes in RSI values result primarily from modulation of ram distance (Wainwright 2001). The greater ram distances of *T. truncatus* relative to *Kogia* are responsible for the greater RSI values of *T. truncatus* and support a more locomotory feeding strategy in this study. Suction distance means likewise support a lesser degree of suction feeding in *T. truncatus*, as food items frequently moved away from subjects, potentially due to bow waves formed at the rostral maxillae and mandibular tips of subjects. A small *T. truncatus* suction component may have been present to help reduce the affect of this positive pressure wave. Although a significant suction feeding component was not observed here, *T. truncatus* is known to participate in a variety of feeding modes under different conditions and a significant suction component may be present under different conditions.

Tursiops truncatus gape kinematics were distinct from *Kogia*. The relatively slower gape velocities, time to maximum gape, and jaw opening (phase II) durations of *T. truncatus* likely resulted in more positive RSI values. The observation that maximum closing gape angle velocity was generally faster than maximum opening gape angle velocity in *T. truncatus* was likely due to the need to capture food items once within reach and would be expected for a ram-based feeder.

As in *Kogia*, *T. truncatus* hyoid movement occurred over most of the feeding cycle and was not limited to the gular depression phase. Forward motion of *T. truncatus* was essential in food capture. In several cases, numerous capelin (*Mallotus villosus*) were simultaneously offered to *T. truncatus* subjects. Gape and gular movements alone were insufficient to draw food items into the mouth and in several trials successful food capture did not involve any hyoid depression or retraction. This was a key behavioral difference between *Kogia* and *T. truncatus*. Flaring of the pectoral fins appeared to slow forward motion in *T. truncatus* subjects when in close proximity to food. Pectoral pronation was similarly observed in a kinematic analysis of pilot whales (Werth 2000) to slow forward motion in the final stages of food approach.

Tursiops truncatus closed and open gape approaches were different from each other, but were both strongly ram-based. The slowly increasing gape of *T. truncatus* open gape approach resulted in all significant differences of gape and feeding duration variables between *T. truncatus* closed and open gape approaches. Gular depression and retraction were observed even when a large partial gape was present. A preparatory phase was observed in only one of 11 trials of *T. truncatus* open gape approach behavior and was not included in the kinematic profile of *T. truncatus* open gape approach feeding (Fig. 4C). However, it is likely that a preparatory phase was always present in *T. truncatus* open gape approach, but occurred before the subject entered the video camera’s field of view. Early gape may have served to slow forward motion by increasing drag.

CHAPTER V

CONCLUSION

In summary, broad morphological differences between *Kogia* and *T. truncatus* are reflected in their different feeding performances. *Kogia* was observed to feed primarily using suction, which likely relied upon rapid gape and gular kinematics to produce negative intraoral pressures and draw food into the mouth. *Tursiops truncatus* was primarily ram-based, exhibited slower gape and gular kinematics, and always overtook food by locomotion. The *T. truncatus* feeding repertoire in this study included two distinct feeding patterns that were dissimilar in the timing of gape increase. Kinematic data support the functional hypothesis that odontocetes produce suction by the rapid depression and retraction of the hyolingual apparatus but also demonstrate that rapid jaw opening and wide gape may serve to increase suction capability. Furthermore, these data serve to provide a foundation for future kinematic studies that can place odontocete feeding biomechanics within an evolutionary perspective.

Results of morphological and kinematic investigations have significant implications for *Kogia* and *T. truncatus* evolutionary and ecological understanding. *Kogia* are particularly poorly-known and their characterization as suction feeders is essential to establishing predatory strategies. *Kogia* share the base of Odontodeti phylogeny with the Physeteridae and Ziphiidae, all of whom are suspected or reported suction feeders. Also shared are a deep-diving ability, teuthophagous diet, deep-water distribution, and the greatest degree of mammalian cranium asymmetry. It seems likely that some or all of these characteristics are linked to suction feeding, either as morphological and behavior facilitators. These attributes may enable predation in physiologically challenging niches. Kinematic results suggest that *Kogia* subjects voluntarily remained nearly stationary while feeding. This aspect may be exploited by free-ranging *Kogia* during deep dives for cephalopod prey. *Kogia* likely dive to a depth where cephalopod prey are abundant and may remain stationary in or move slowly through a prey school while employing suction to draw cephalopods and myctophids into the mouth. This strategy would allow *Kogia* to avoid active locomotion while at depth and maximize feeding duration.

Tursiops truncatus are well-known to actively locomote in pursuit of prey, but biomechanical and kinematic aspects of *T. truncatus* feeding have not been previously addressed. Surprisingly, hyolingual musculature in these raptorial feeders was potentially as powerful as a suction feeder, demonstrating that force alone is not a measure of suction feeding ability. Kinematic investigations verified that *T. truncatus* is capable of more than one feeding pattern. This suggests that *T. truncatus* motor patterns are flexible and subjects can modulate feeding. This allows *T. truncatus* to be more effective predator by adapting to variable conditions, such as prey type, size, location, and evasiveness. Further investigation under a variety of conditions would likely show additional modulation of feeding patterns than those observed in this study.

LITERATURE CITED

ABOLLO, E., A. Lopez, C. Gestal, P. Benavente and S. Pascual. 1998. Macroparasites in cetaceans stranded on the northwestern Spanish Atlantic coast. Diseases of Aquatic Organisms 32(3):227-231.

AERTS, P. 1990. Variability of the fast suction feeding process in *Astatotilapia elegans* (Teleostei, Cichlidae): a hypothesis of peripheral feedback control. Journal of Zoology (London) 220:653-678.

ARNASON, U. A., A. Gullberg and B. Widegren.1993. Cetacean mitochondrial DNA control region: sequences of all extant baleen whales and two sperm whale species. Molecular Biology and Evolution 10(5):960-970.

BACCETTI, N., F. Cancelli and T. Renieri. 1991. First record of *Kogia simus* (Cetacea, Physeteridae) from the Mediterranean Sea. Mammalia 55(1):152-154.

BAIRD, R. W., D. Nelson, J. Lein, and D. W. Nagorsen. 1993. Status of the pygmy sperm whale, *Kogia breviceps* in Canada. Canadian Field Naturalist 110:525-532.

BALANCE, L. T. and R. L. Pitman. 1998. Cetaceans of the western tropical Indian Ocean: distribution, relative abundance, and comparisons with cetacean communities of two other tropical ecosystems. Marine Mammal Science 14(3):429-459.

BARROS, N. B. and D. K. Odell. 1990. Food habits of bottlenose dolphins in the southeastern United States. Pages 309-328 *in* S. Leatherwood and R. R. Reeves, eds. The Bottlenose Dolphin. Academic Press, San Diego, CA.

BAUMGARTNER, M., K. Mullin, L. May, and T. Leming. 2001. Cetacean habitats in the northern Gulf of Mexico. Fisheries Bulletin 99:219-239.

BEL'KOVICH, V. M. 1991. Herd structure, hunting and play: bottlenose dolphins in the Black Sea. Pages 17-78 *in* K. Pryor and K. S. Norris, eds. Dolphin Societies: Discoveries and Puzzles. University of California Press, Berkley, CA.

BENHAM, W. B. 1901. On the anatomy of *Cogia breviceps*. Proceedings of the Zoological Society of London 1:107-134, plates 8-11, fig.s 7-8.

BENHAM, W. B. 1902. Notes on the osteology of the short nosed sperm whale. Proceedings of the Zoological Society of London 1:54-62.

BERTA, A. and J. L. Sumich. 1999. Cetacean evolution and systematics. Pages 49-85 *in* A. Berta and J. L. Sumich, eds. Marine Mammals: Evolutionary Biology. Academic Press, San Diego, CA.

BIANUCCI, G. and W. Landini. 1999. *Kogia pusilla* from the middle Pliocene of Tuscany (Italy) and a phylogenetic analysis of the family Kogiidae (Odontoceti, Cetacea) Rivista Italiana di Paleontologiae Stratigrafia 105(3):445-453.

BRODIE, P. F. 1989. The white whale *Delphinapterus leucas* (Pallas, 1776). Pages 119-144 *in* S. H. Ridgeway and R. Harrison, eds. Handbook of Marine Mammals Volume 3. River Dolphins and the Larger Toothed Whales. Plenum Press, New York, NY.

BROWN, D. H. 1962. Further observations on the pilot whale in captivity. Zoologica New York 47:59-64.

CALDWELL, D. K. and M. C. Caldwell. 1989. Pygmy sperm whale *Kogia breviceps* (de Blainville, 1838), dwarf sperm whale *Kogia simus* (Owen, 1866). Pages 235-260 *in* S. H. Ridgeway and R. Harrison, eds. Handbook of Marine Mammals Volume 4. Academic Press, London.

CALDWELL, D. K., M. C. Caldwell and G. Arrindell. 1973. Dwarf sperm whale, *Kogia simus*, from the Lesser Antillean island of St. Vincent. Journal of Mammalogy 54:515-517.

CALDWELL, D. K., M. C. Caldwell and S. Zam. 1971*a*. A preliminary report on some ectoparasites and nasal sac- parasites from small odontocete cetaceans from Florida and Georgia. Marineland of Florida Research Laboratory Technical Report 5:1-7.

CALDWELL, D. K. and F. B. Golley. 1965. Marine mammals from the coast of Georgia to Cape Hatteras. Journal of the Elisha Mitchell Scientific Society 81(1):24-32.

CALDWELL, D. K., H. Neuhauser, M. C. Caldwell and H. Coolridge. 1971*b*. Recent records of marine mammals from the coasts of Georgia and South Carolina. Cetology 5:1-12.

CALDWELL, D. K., J. H. Prescott and M. C. Caldwell. 1966. Production of pulsed sounds by the pygmy sperm whale, *Kogia breviceps*. Bulletin of the Southern California Academy of Science 65(4):245-248.

CARROLL, A. M., P. C. Wainwright, S. H. Kuskey, D. C. Collar and R. G. Turingan. 2004. Morphology predicts suction feeding performance in centrarchid fishes. Journal of Experimental Biology 207:3873-3881.

CHAINE, J. 1914. Le digastrique abaisseur de la mandibule des mammifères. Journal of Anatomy and Physiology 50:248-319.

CLARKE, M. R. 1978. Buoyancy control as a function of the spermaceti organ in the sperm whale. Journal of the Marine Biological Association of the United Kingdom 58:27-71.

CLARKE, M. R. 2003. Production and control of sound by the small sperm whale, *Kogia breviceps* and *K. sima* and their implications for other Cetacea. Journal of the Marine Biological Association of the United Kingdom 83:241-263.

CLARKE, M. R., A. Aguayo and O. Paliza. 1968. Sperm whales of the southeast Pacific. Scientific Results of Marine Biological Research 51:1-80.

COCKCROFT, V. G. and G. J. B. Ross. 1990*a*. Food and feeding of the Indian Ocean bottlenose dolphin off southern Natal, South Africa. Pages 295-308 *in* S. Leatherwood and R. R. Reeves, eds. The Bottlenose Dolphin. Academic Press, San Diego, CA.

COCKCROFT, V. G. and G. J. B. Ross. 1990*b*. Age, growth and reproduction of bottlenose dolphins *Tursiops truncatus* from the east coast of South Africa. Fisheries Bulletin 88(2):289-302.

CONNOR, R. C., R. S. Wells, J. Mann and A. J. Read. 2000. The bottlenose dolphin, *Tursiops spp*: social relationships in a fission-fusion society. Pages 91-126 *in* J. Mann, R. C. Connor, P. L. Tyack and H. Whitehead, eds. Cetacean Societies: Field Studies of Dolphins and Whales. University of Chicago Press, Chicago, IL.

DAVIS, R. W., G. Fargion, N. May, T. Leming, M. Baumgartner, W. Evans, L. Hansen and K. Mullin. 1998. Physical habitat of cetaceans along the continental slope in the north-central and western Gulf of Mexico. Marine Mammal Science 14(3):490-507.

DOS SANTOS, R. A. and M. Haimovici. 2001. Cephalopods in the diet of marine mammals stranded or incidentally caught along southeastern and southern Brazil (21 - 34°S). Fisheries Research 52:99-112.

EDMONDS, M. A., P. J. Motta and R. E. Hueter. 2001. Food capture kinematics of the suction feeding horn shark, *Heterodontus francisci*. Environmental Biology of Fishes 62:415-427.

EVANS, H. and G. Christensen. 1979. Muscles: muscles of the head. Pages 289-300 *in* H. Evans and G. Christensen, eds. Miller's Anatomy of the Dog. W. B. Saunders Company, Philadelphia, PA.

FERTL, D. and S. Leatherwood. 1997. Cetacean interactions with trawls: a preliminary review. Journal of Northwest Atlantic Fisheries Science 22:219-248.

FITCH, J. and Brownell. 1968. Fish otoliths in cetacean stomachs and their importance in interpreting feeding habits. Journal of the Fisheries Research Board of Canada 25(12):2561-2574.

FORCADA, J. 2002. Distribution. Pages 327-333 *in* W. F. Perrin, B. Würsig and J. G. M. Thewissen, eds. Encyclopedia of Maine Mammals. Academic Press, San Diego, CA.

FRASER, F. C. 1974. Report on Cetacea stranded on the British coasts from 1948 to 1966. British Museum of Natural History 14:65 pp., iii, 9 maps.

GALLAGHER, M. and P. van Bree. 1980. On a dwarf sperm whale, *Kogia simus* (Owen, 1866), from the sultanate of Oman. Zeitschrift fur Saugetierkunde 45:53-57.

GANNON, D. P., N. B. Barros, D. P. Nowacek, A. J. Read, D. M. Waples and R. S. Wells. 2005. Prey detection by bottlenose dolphins (*Tursiops truncatus*): an experimental test of the passive listening hypothesis. Animal Behaviour 69:709-720.

GASKIN, D. E. 1967. Luminescence in a squid *Moroteuthis* sp. (probably *ingens* Smith), and a possible feeding mechanism in the sperm whale *Physeter catadon* L. Tuatara 15(2):86-88.

GASKIN, D. E. 1976. The evolution, zoogeography and ecology of Cetacea. Oceanography and Marine Biology Annual Review 14:247-346.

GEISLER, J. and A. Sanders. 2003. Morphological evidence for the phylogeny of Cetacea. Journal of Mammalian Evolution 10:23-129.

GERMAN, R. Z. and A. W. Crompton. 1996. Ontogeny of suckling mechanisms in opossums. Brain, Behavior and Evolution 48:157-164.

GERMAN, R. Z., A. W. Crompton, L. C. Levitch and A. J. Thexton. 1992. The mechanism of suckling in two species of infant mammal: miniature pigs and long-tailed macaques. Journal of Experimental Zoology 261:322-330.

GILL, T. 1871. The sperm whales, giant and pygmy. American Naturalist 4:723-743, fig.s 164-176.

GORDON, K. R. 1984. Models of tongue movement in the walrus (*Odobenus rosmarus*). Journal of Morphology 182:179-196.

GORDON, K. R. and S. W. Herring. 1987. Activity patterns within the genioglossus during suckling in domestic dogs and pigs: interspecific and intraspecific plasticity. Brain, Behavior and Evolution 30:249-262.

HALE, H. 1962. The pigmy sperm whale (*Kogia breviceps*) on South Australian coasts. Part III. Records of the South Australian Museum 14:197-230.

HALE, H. 1963. Young female pigmy sperm whale (*Kogia breviceps*) from Western and South Australia. Records of the South Australia Museum 14(3):561-577.

HAMILTON, P. V. and R. T. Nishimoto. 1977. Dolphin predation on mullet. Florida Science 40(3):251-252.

HANDLEY Jr., C. 1966. A synopsis of the genus *Kogia* (pygmy sperm whale). Pages 62-69 *in* K. S. Norris, ed. Whales, Dolphins and Porpoises. University of California Press, Berkley, CA.

HERMAN, L. M. 1980. Cetacean Behavior: Mechanisms and Functions. Krieger Publishing Company, Malabar, FL. 463 P.

HEYNING, J. 1989. Comparative facial anatomy of beaked whales (Ziphiidae) and a systematic revision among the families of extant Odontoceti. Contributions in Science 405:1-64.

HEYNING, J. E. and J. G. Mead. 1991. Feeding mechanisms of ziphiids: do beaked whales suck? Ninth Biennial Conference on the Biology of Marine Mammals. December 5-9, 1991. Chicago, IL. Page. 33.

HEYNING, J. E. and J. G. Mead. 1996. Suction feeding in beaked whales: morphological and observational evidence. Contributions in Science 464:1-12.

HIIEMAE, K. M. and A. Crompton. 1985. Mastication, food transport, and swallowing. Pages 262-290, 404-406 *in* M. Hildebrand, D. Bramble, K. Liem and D. Wake, eds. Functional Vertebrate Morphology. Belkamp Press of Harvard University Press, Harvard, MA

HOESE, H. D. 1971. Dolphin feeding out of water in a salt marsh. Journal of Mammalogy 52(1):222-223.

HOWELL, A. B., ed. 1930. Aquatic Mammals. Charles C. Thomas, Springfield, IL.

HUBBS, C. 1951. Eastern Pacific records and general distribution of the pygmy sperm whale. Journal of Mammalogy 32:403-410.

HUBER, D. R. and P. J. Motta. 2004. Comparative analysis of methods for determining bite force in the spiny dogfish *Squalus acanthias*. Journal of Experimental Biology 301A:26-37.

HUCKSTADT, L. and T. Antezana. 2001. An observation of parturition in a stranded *Kogia breviceps*. Marine Mammal Science 17(2):362-365.

KAMI, H. and R. Lujan. 1976. Records of the dwarf sperm whale *Kogia simus* from Guam. Micronesica 12:327-332.

KASTELEIN, R. A., J. L. Dubbeldam and M. A. G. DeBakker. 1997. The anatomy of the walrus head (*Odobenus rosmarus*). Part 5. The tongue and its function in walrus ecology. Aquatic Mammals 23:29-47.

KASTELEIN, R. A., N. M. Gerrits, and J. L. Dubbeldam. 1991. The anatomy of the walrus head (*Odobenus rosmarus*). Part 2. Description of the muscles and of their role in feeding and haul-out behavior. Aquatic Mammals 17(3):156-180.

KASTELEIN, R. A., Muller, M. and Terlouw, A. 1994. Oral suction of a Pacific walrus (*Odobenus rosmarus divergens*) in air and under water. Zeitschrift fur Saugetierkunde 59:105-115.

KENNEY, R. D. 1990. Bottlenose dolphins off the northeastern United States. Pages 369-386 *in* S. Leatherwood and R. R. Reeves, eds. The Bottlenose Dolphin. Academic Press, San Diego, CA.

KLAGES, N., V. Cockcroft and P. Best. 1989. Stomach contents of pygmy *Kogia breviceps* and dwarf *Kogia simus* sperm whales stranded on South African beaches. Abstracts of the Eighth Biennial Conference on the Biology of Marine Mammals. December 7-11, 1989. Pacific Grove, CA. Page 35.

LAMBERTSEN, R. H. 1983. Internal mechanisms of rorqual feeding. Journal of Mammalogy 64:76-88.

LAMBERTSEN, R. H. and R. J. Hintz. 2004. Maxillomandibular cam articulation discovered in north Atlantic minke whale. Journal of Mammalogy 85(3):446-452.

LAMBERTSEN, R. H., N. Ulrich and J. Straley. 1995. Frontomandibular stay of Balaenopteridae: a mechanism for momentum recapture during feeding. Journal of Mammalogy 76:877-899.

LAUDER, G. V. 1985. Aquatic feeding in lower vertebrates. Pages 210-229 *in* M. Hildebrand, D. Bramble, K. Liem and D. Wake, eds. Functional Vertebrate Morphology. Belknap Press, Cambridge, MA.

LEATHERWOOD, S. H. 1975. Some observations of feeding behavior of bottlenose dolphins (*Tursiops truncatus*) in the northern Gulf of Mexico and (*Tursiops* cd *T. gilli*) off southern California, Baja California, and Nayarit, Mexico. Marine Fisheries Research 37(9):10-16.

LEATHERWOOD, S. H. and R. R. Reeves. 1983. Pygmy sperm whale *Kogia breviceps*, Dwarf sperm whale *Kogia sima*. Pages 90-96 *in* S. H. Leatherwood and R. R. Reeves, eds. The Sierra Club Handbook of Whales and Dolphins. Sierra Club Books, San Francisco, CA.

LEATHERWOOD, S. H., R. R. Reeves, W. Perrin and W. Evans. 1988. Bottlenose dolphin, Pygmy sperm whale, Dwarf sperm whale. Pages 173-177, 193-200 *in* S. H. Leatherwood, R. R. Reeves, W. Perrin and W. Evans, eds. Whales, Dolphins and Porpoises of the Eastern North Pacific and Adjacent Arctic Waters. Dover Publications, New York, NY.

LENFANT, C. 1969. Physiological properties of blood of marine mammals. Pages 95-116 *in* H. T. Anderson, ed. The Biology of Marine Mammals. Academic Press, San Diego, CA.

LOEB, G. E. and C. Gans. 1986. Anatomical techniques. Pages 319-322 *in* G. E. Loeb and C. Gans, eds. Electromyography for Experimentalists. University of Chicago Press, Chicago, IL.

MAIGRET, J. and D. Robineau. 1981. Le genre *Kogia* (Cetacea, Physeteridae) sur les cotes du Senegal. Mammalia 45(2):199-204.

MANIRE, C. A., H. L. Rheinhardt, N. B. Barros, L. Byrd and P. Cunningham-Smith. 2004. An approach to the rehabilitation of *Kogia sp*. Aquatic Mammals 30(2):209-219.

MARTINS, H., M. Clarke, F. Reiner and R. Santos. 1985. A pygmy sperm whale, *Kogia breviceps* (Blainville, 1838) (Cetacea: Odontoceti) stranded on Fail Island, Azores, with notes on cephalopod beaks in stomach. Arquipelago, Serie Ciencia da Natureza 6:63-70.

McALPINE, D., L. Murison and E. Hoberg. 1997. New records for the pygmy sperm whale *Kogia breviceps* (Physeteridae) from Atlantic Canada with notes on diet and parasites. Marine Mammal Science 13(4):701-704.

McMAHON, T. 1984. Muscles, Reflexes, and Locomotion. Princeton Univ. Press, Princeton, NJ.

MEAD, J. G. and C. W. Potter. 1990. Natural history of bottlenose dolphins along the central Atlantic coast. Pages 165-195 *in* S. Leatherwood and R. R. Reeves, eds. The Bottlenose Dolphin. Academic Press, San Diego, CA.

MENDEZ, J. and A. Key. 1960. Density and composition of mammalian muscle. Metabolism, Clinical and Experimental 9:184-188.

MILLER, G. S. Jr. 1923. The telescoping of the cetacean skull. Smithsonian Miscellaneous Collections 76(5):1-71.

MILINKOVITCH, M. C., A. Meyer and J. R. Powell. 1994. Phylogeny of all major groups of cetaceans based on DNA sequences from three mitochondrial genes. Molecular Biology and Evolution 11(6):939-948.

MOTTA, P. J. and C. D. Wilga. 2001. Advances in the study of feeding behaviors, mechanisms, and mechanics of sharks. Environmental Biology of Fishes 60:131-156.

MULLIN, K. D. and G. L. Fulling. 2004. Abundance of cetaceans in the oceanic northern Gulf of Mexico. Marine Mammal Science 20(4):787-807.

MULLIN, K., W. Hoggard, C. Roden, R. Lohoefer, C. Rogers and B. Taggert. 1994. Cetaceans of the upper continental slope in the north-central Gulf of Mexico. Fisheries Bulletin 92:773-786.

MURPHY, R. A. and A. C. Beardsley. 1974. Mechanical properties of the cat soleus muscle in situ. American Journal of Physiology 227:1008-1013.

NAGORSEN, D. 1985. *Kogia simus*. Mammalian Species 239:1-6.

NITTA, E. 1991. The marine mammal stranding network for Hawaii, an overview. Pages 55-62 *in* J. Reynolds and D. Odell, eds. Marine Mammal Strandings in the United States. NOAA Technical Report NMFS 98.

NORRIS, K. S. and B. Møhl. 1983. Can odontocetes debilitate prey with sound? American Naturalist 122:85-104.

NORTON, S. and E. Brainerd. 1993. Convergence in the feeding mechanics of ecomorphologically similar species in the Centrarchidae and Cichlidae. Journal of Experimental Biology 176:11-29.

ORTON, L. S. and P. F. Brodie. 1987. Engulfing mechanisms of fin whales. Canadian Journal of Zoology 65:2898-2907.

OWEN, R. 1867. Note to memoir on the Indian Cetacea collected by Sir Walter Elliot. Transaction of the Zoological Society of London 6:171-174.

PABST, D. A., S. A. Rommel and W. A. McLellan. 1999. The functional morphology of marine mammals. Pages 15-72 *in* J. E. Reynolds III and S. A. Rommel, eds. Biology of Marine Mammals. Smithsonian Institution Press, Washington, DC.

PINEDO, M. 1987. First record of a dwarf sperm whale from the southwest Atlantic, with reference to osteology, food habits and reproduction. Scientific Reports of the Whales Research Institute 38:171-186.

PITTMAN, R. Personal communication via oral presentation at Biology of *Kogia* Workshop at 15th Biennial Conference on the Biology of Marine Mammals. National Marine Fisheries Service, Southwest Fisheries Science Center, La Jolla, CA.

PIVORUNAS, A. 1977. The fibrocartilage skeleton and related structures of the ventral pouch of balaenopterid whales. Journal of Morphology 151:299-314.

POWELL, P. L., R. R. Roy, P. Kanim, M. A. Bello and V. R. Edgerton 1984. Predictability of skeletal muscle tension from architectural determinations in guinea pig hindlimbs. Journal of Applied Physiology: Respiratory, Environmental and Exercise Physiology 57:1715-1721.

REIDENBERG, J. and J. Laitman. 1994. Anatomy of the hyoid apparatus in Odontoceti (toothed whales): specializations of their skeleton and musculature compared with those of terrestrial mammals. Anatomical Record 240:598-624.

RICE, D. 1998. Family Kogiidae. Pygmy sperm whale. Pages 83-85 *in* D. Wartzok, ed. Marine Mammals of the World: Systematics and Distribution. Society for Marine Mammalogy Special Publication Number 4. Allen Press, Lawrence, KS.

RIGLEY, L. 1983. Dolphins feeding in a South Carolina salt marsh. Whalewatcher 17(2):3-5.

ROMMEL, S. A. 1990. Osteology of the bottlenose dolphin. Pages 29-49 *in* S. Leatherwood and R. R. Reeves, eds. The Bottlenose Dolphin. Academic Press, San Diego, CA.

ROSS, G. J. B. 1978. Records of pygmy and dwarf sperm whales, genus *Kogia*, from southern Africa, with biological notes and some comparisons. Annals of the Cape Provincial Museum of Natural History 11:259-327.

ROSS, G. J. B. 1984. The smaller Cetacea of the south east coast of southern Africa. Annals of the Cape Provincial Museum of Natural History 15:173-411.

ROSS, G. J. B. and V. G. Cockcroft. 1990. Comments on Australian bottlenose dolphins and the taxonomic status of *Tursiops aduncus* (Ehrenberg, 1832). Pages 101-128 *in* S. Leatherwood and R. R. Reeves, eds. The Bottlenose Dolphin. Academic Press, San Diego, CA.

ROSS, G. J. B., G. Lento, M. Dalebout, M. Goode, G. Ewing, P. McLaren, A. Rodrigo, S. Laverty and C. Baker. 2003. DNA surveillance: web-based molecular identification of whales, dolphins and porpoises. Journal of Heredity 94(2):111-114.

ROSSBACH, K. A. and D. L. Herzing. 1997. Underwater observations of benthic feeding bottlenose dolphins (*Tursiops truncatus*) near Grand Bahamas Island, Bahamas. Marine Mammal Science 11(2):498-503.

ROY, R. R., I. D. Meadows, K. M. Baldwin and V. R. Edgerton. 1982. Functional significance of compensatory overloaded rat fast muscle. Journal of Applied Physiology: Respiratory, Environmental and Exercise Physiology 52:473-478.

SANFORD, C. P. J. and P. C. Wainwright. 2002. Use of sonomicrometry demonstrates the link between prey capture kinematics and suction pressure in largemouth bass. Journal of Experimental Biology 205:3445-3457.

SANINO, G. and Yaňez. 1996. Estudio del cachalote pigmeo *Kogia breviceps* (Blainville, 1838), varado en la costa de Chile. Resúmenes, VII Reunión de Trabajo de Especialistas en Mamiferos Acuáticos de América del Sur and I Congreso de la Sociedad Latinoamericana de Especialistas en Mamiferos Acuáticos. 22-25 October 1996. Viňa del Mar, Chile. Page 93.

SCHULTE, H. 1917. The skull of *Kogia breviceps* Blainville. Bulletin of the American Museum of Natural History 37(17):361-404.

SCHULTE, H von W. and M. F. Smith. 1918. The external characters, skeletal muscles, and peripheral nerves of *Kogia breviceps* (Blainville). Bulletin of the American Museum of Natural History 38:7-72.

SCOTT, M. and J. Cordaro. 1987. Behavioral observations of the dwarf sperm whale, *Kogia simus*. Marine Mammal Science 3(4):353-354.

SCOTT, M. D., A. A. Hohn, A. J. Westgate, J. R. Nicolas, B. R. Whitaker and W. B. Campbell. 2001. A note on the release and tracking of a rehabilitated pygmy sperm whale (*Kogia breviceps*). Journal of Cetacean Research and Management 3(1):87-94.

SCOTT, M. D., R. S. Wells and A. B. Irvine. 1990. A long-term study of bottlenose dolphins on the west coast of Florida. Pages 235-244 *in* S. Leatherwood and R. R. Reeves, eds. The Bottlenose Dolphin. Academic Press, San Diego, CA.

SLIJPER, E. 1962. Feeding. Pages 253-293 *in* E. Slijper, ed. Whales. Basic Books, Inc, New York, NY.

SPECTOR, S. A., P. F. Gardiner, R. F. Zernicke, R. R. Roy and V. R. Edgerton. 1980. Muscle architecture and force-velocity characteristics of cat soleus and medial gastrocnemius: implications for motor control. Journal of Neurophysiology 44:951-960.

STEWART, B. S. 2002. Diving behavior. Pages 333-344 *in* W. F. Perrin, B. Würsig and J.G.M. Thewissen, eds. Encyclopedia of Marine Mammals. Academic Press, San Diego, CA.

SYLVESTRE, J. 1983. Review of *Kogia* specimens (Physeteridae, Kogiinae) kept alive in captivity. Investigations on Cetacea 15:201-219.

SYLVESTRE, J. 1988. Note on three dwarf sperm whales *Kogia simus* (Owen, 1866) and comments on kogiids of Japanese coasts. Aquatic Mammals 14:120-122.

THEXTON, A. J., A. W. Crompton and R. Z. German. 1998. Transition from suckling to drinking at weaning: a kinematic and electromyographic study in miniature pigs. Journal of Experimental Zoology 280:327-343.

THEXTON, A. J., A. W. Crompton, T. Owerkowicz and R. Z. German. 2004. Correlation between intraoral pressures and tongue movements in the suckling pig. Archives of Oral Biology 49:567-575.

TOMILIN, A. G. 1957. Cetacea. V. G. Heptner, ed. Translation from Russian original by Israel Program for Scientific Translations, Jerusalem, 1967. 717 p.

VIDAL, O., L. Findley, P. Turk and R. Boyer. 1987. Recent records of pygmy sperm whales in the Gulf of California, Mexico. Marine Mammal Science 3(4):354-356.

WAINWRIGHT, P. C., L. A. Ferry-Graham, T. B. Waltzek, A. M. Carroll, C. D. Husley and J. R. Grubich. 2001. Evaluating the use of ram and suction during prey capture by cichlid fishes. Journal of Experimental Biology 204:3039-3051.

WANG, M., W. Walker, K. Shao and L. Chou. 2002. Comparative analysis of the diets of pygmy sperm whales and dwarf sperm whales in Taiwanese waters. Acta Zoologica Taiwanica 13(2):53-62.

WELLS, R. S., D. J. Boness and G. B. Rathbun. 1999. Behavior. Pages 324-422 *in* J. E. Reynolds III and S. A. Rommel, eds. Biology of Marine Mammals. Smithsonian Institution Press, Washington, DC.

WELLS, R. S. and M. D. Scott. 1999. Bottlenose dolphin *Tursiops truncatus* (Montagu 1821). Pages 137-182 *in* S. H. Ridgway and R. R. Harrison, eds. Handbook of Marine Mammals Volume 6. Academic Press, San Diego, CA.

WELLS, R. S. and M. D. Scott. 2002. Bottlenose dolphins. Pages 122-128 *in* W. F. Perrin, B. Würsig and J. G. M. Thewissen, eds. Encyclopedia of Marine Mammals. Academic Press, San Diego, CA.

WERTH, A. J. 1992. Anatomy and Evolution of Odontocete Suction Feeding. Ph.D. dissertation, Harvard University, Cambridge, MA.

WERTH, A. J. 2000*a*. A kinematic study of suction feeding and associated behavior in the long-finned pilot whale, *Globicephala melas* (Traill). Marine Mammal Science 16(2):299-314.

WERTH, A. J. 2000*b*. Feeding in marine mammals. Pages 487-526 *in* K. Schwenk, ed. Feeding: Form, Function and Evolution in Tetrapod Vertebrates. Academic Press, San Diego, CA.

WERTH, A. J. 2005. Functional morphology of the sperm whale (*Physeter macrocephalus*) tongue, with reference to suction feeding. Aquatic Mammals 30(3):405-418.

WINGE, H. 1921. A review of the interrelationships of Cetacea. Smithsonian Miscellaneous Collections 72:1-97.

WYNNE, K. and M. Schartz. 1999. Pygmy sperm whale, Dwarf sperm whale. Pages 28-31 *in* K. Wynne and M. Schwartz, eds. Guide to Marine Mammals and Turtles of the U.S. Atlantic and Gulf of Mexico. Rhode Island Sea Grant, Narragansett, RI.

YAMADA, M. 1954. Some remarks on the pygmy sperm whale, *Kogia*. Scientific Reports of the Whales Research Institute 9:37-61.

APPENDIX A

Table A-1 Raw data for hyoid osteology dimensions.

Stranding identification	Species	Side	Basihyal CSA (cm^2)	Thyrohyal CSA (cm^2)	Combined basi-thyrohyal CSA (cm^2)	Stylohyal width (cm)	Stylohyal length (cm)	Stylohyal width: length ratio
GA1120	*K. sima*	L	37.4	39.2	119.3	9.47	53.4	0.177
GA1120		R	n/a	42.7	n/a	9.52	53.9	0.177
MML-0232	*K. sima*	L	19.4	18.2	56.0	8.15	64.0	0.127
MML-0232		R	n/a	18.3	n/a	7.79	64.6	0.121
MML-0233	*K. sima*	L	27.9	27.2	83.3	12.9	76.4	0.169
MML-0233		R	n/a	28.1	n/a	12.8	73.7	0.174
PA636	*K. sima*	L	32.6	27.1	88.9	9.65	75.8	0.127
PA636		R	n/a	29.3	n/a	11.3	72.4	0.156
PA716	*K. sima*	L	40.6	28.5	99.4	9.19	78.7	0.117
PA716		R	n/a	30.2	n/a	9.16	78.3	0.117
CMA-01-04B	*K. breviceps*	L	5.27	4.22	13.3	5.20	38.7	0.134
CMA-01-04B		R	n/a	3.81	n/a	4.96	39.2	0.127
PI159	*K. breviceps*	L	57.6	36.1	130.6	13.5	110.6	0.122
PI159		R	n/a	36.9	n/a	13.5	119.2	0.113
SP371	*K. breviceps*	L	81.5	70.2	213.1	12.3	134.7	0.092
SP371		R	n/a	61.4	n/a	n/a	n/a	n/a
SP378	*K. breviceps*	L	56.8	46.1	145.4	11.8	94.3	0.126
SP378		R	n/a	42.5	n/a	11.5	96.5	0.119
GA1214	*T. truncatus*	L	17.5	9.00	37.7	8.78	95.5	0.092
GA1214		R	n/a	11.2	n/a	8.81	91.1	0.097
GA1248	*T. truncatus*	L	17.7	11.5	40.3	8.74	90.3	0.097
GA1248		R	n/a	11.2	n/a	9.26	90.7	0.102
GA1289	*T. truncatus*	L	16.3	10.6	37.0	9.79	76.8	0.127
GA1289		R	n/a	10.1	n/a	9.79	76.9	0.127
PA680	*T. truncatus*	L	19.1	12.1	43.5	8.03	93.1	0.086
PA680		R	n/a	12.2	n/a	8.14	94.6	0.086
PA692	*T. truncatus*	L	23.1	12.4	48.9	10.3	102.3	0.100
PA692		R	n/a	13.4	n/a	9.96	102.7	0.097
PO432	*T. truncatus*	L	17.5	10.2	37.4	9.53	75.0	0.127
PO432		R	n/a	9.73	n/a	9.06	79.1	0.115

APPENDIX B

Table B-1 Measured mylohyoideus data points for *K. sima*, *K. breviceps* and *T. truncatus* specimens.

Table B-2 Calculated mylohyoideus data points of physiological cross-sectional area (PCSA), physiological maximum tetanic force (PMTT), morphological cross-sectional area (MCSA), and morphological maximum tetanic force (MMTT) for *K. sima*, *K. breviceps*, pooled *Kogia*, and *T. truncatus*.

Table B-3 Measured geniohyoideus data points for *K. sima*, *K. breviceps*, and *T. truncatus* specimens.

Table B-4 Calculated geniohyoideus data points of physiological cross-sectional area (PCSA), physiological maximum tetanic force (PMTT), morphological cross-sectional area (MCSA), and morphological maximum tetanic force (MMTT) for *K. sima*, *K. breviceps*, pooled *Kogia*, and *T. truncatus*.

Table B-5 Measured sternohyoideus data points for *K. sima*, *K. breviceps*, and *T. truncatus* specimens.

Table B-6 Calculated sternohyoideus data points of physiological cross-sectional area (PCSA), physiological maximum tetanic force (PMTT), morphological cross-sectional area (MCSA)- and morphological maximum tetanic force (MMTT) for *K. sima*, *K. breviceps*, pooled *Kogia*, and *T. truncatus*.

Table B-7 Measured thyrohyoideus data points for *K. sima*, *K. breviceps*, and *T. truncatus* specimens.

Table B-8 Calculated thyrohyoideus data points of physiological cross-sectional area (PCSA), physiological maximum tetanic force (PMTT), morphological cross-sectional area (MCSA), and morphological maximum tetanic force (MMTT) for *K. sima*, *K. breviceps*, pooled *Kogia*, and *T. truncatus*.

Table B-9 Measured stylohyoideus data points for *K. sima*, *K. breviceps*, and *T. truncatus* specimens.

Table B-10 Calculated stylohyoideus data points of physiological cross-sectional area (PCSA), physiological maximum tetanic force (PMTT), morphological cross-sectional area (MCSA), and morphological maximum tetanic force (MMTT) for *K. sima*, *K. breviceps*, pooled *Kogia*, and *T. truncatus*.

Table B-11 Measured hyoglossus data points for *K. sima*, *K. breviceps*, and *T. truncatus* specimens.

Table B-12 Calculated hyoglossus data points of physiological cross-sectional area (PCSA), physiological maximum tetanic force (PMTT), morphological cross-sectional area (MCSA), and morphological maximum tetanic force (MMTT) for *K. sima*, *K. breviceps*, pooled *Kogia*, and *T. truncatus*.

Table B-13 Measured interhyoideus data points for *K. sima*, *K. breviceps*, and *T. truncatus* specimens.

Table B-14 Calculated interhyoideus data points of physiological cross-sectional area (PCSA), physiological maximum tetanic force (PMTT), morphological cross-sectional area (MCSA), and morphological maximum tetanic force (MMTT) for *K. sima*, *K. breviceps*, pooled *Kogia*, and *T. truncatus*.

Table B-15 Measured genioglossus data points for *K. sima*, *K. breviceps*, and *T. truncatus* specimens.

Table B-16 Calculated genioglossus data points of physiological cross-sectional area (PCSA), physiological maximum tetanic force (PMTT), morphological cross-sectional area (MCSA), and morphological maximum tetanic force (MMTT) for *K. sima*, *K. breviceps*, pooled *Kogia*, and *T. truncatus*.

Table B-17 Measured styloglossus data points for *K. sima*, *K. breviceps*, and *T. truncatus* specimens.

Table B-18 Calculated styloglossus data points of physiological cross-sectional area (PCSA), physiological maximum tetanic force (PMTT), morphological cross-sectional area (MCSA), and morphological maximum tetanic force (MMTT) for *K. sima*, *K. breviceps*, pooled *Kogia*, and *T. truncatus*.

Table B-19 Measured sternothyroideus data points for *K. sima*, *K. breviceps*, and *T. truncatus* specimens.

Table B-20 Calculated sternothyroideus data points of physiological cross-sectional area (PCSA), physiological maximum tetanic force (PMTT), morphological cross-sectional area (MCSA) and morphological maximum tetanic force (MMTT) for *K. sima*, *K. breviceps*, pooled *Kogia***,** and *T. truncatus*.

Table B-21 Measured cricothyroideus data points for *K. sima*, *K. breviceps*, and *T. truncatus* specimens.

Table B-22 Calculated cricothyroideus data points of physiological cross-sectional area (PCSA), physiological maximum tetanic force (PMTT), morphological cross-sectional area (MCSA), and morphological maximum tetanic force (MMTT) for *K. sima*, *K. breviceps*, pooled *Kogia*, and *T. truncatus*.

Table B-1

Stranding identification	Species	Side	Length (mm)	Parasagittal angle	Transverse angle	Height (mm)	Width (mm)	Mass (g)
GA1120	*K. sima*	L	n/a	-66.0	-77.3	n/a	n/a	71.3
GA1120		R	n/a	-61.0	-86.3	n/a	n/a	n/a
MML-0232	*K. sima*	L	75.6	-98.0	-107.6	9.08	202.8	54.4
MML-0232		R	n/a	-80.8	-111.5	n/a	n/a	n/a
MML-0233	*K. sima*	L	129.0	-70.8	-68.6	8.48	186.0	83.4
MML-0233		R	88.9	n/a	n/a	6.24	165.0	49.1
PA636	*K. sima*	L	73.6	-50.0	-64.0	7.39	184.1	55.7
PA636		R	71.3	-65.0	-75.0	8.97	204.2	70.1
PA716	*K. sima*	L	101.7	-71.3	-90.0	15.7	175.9	73.6
PA716		R	94.5	-70.7	-91.3	10.6	163.4	58.4
CMA-01-04B	*K. breviceps*	L	n/a	-69.3	-90.0	n/a	n/a	n/a
CMA-01-04B		R	n/a	-85.7	-88.7	n/a	n/a	n/a
SP371	*K. breviceps*	L	208.0	-77.3	-95.4	6.65	363.7	185.3
SP371		R	188.0	-100.3	-104.1	10.1	305.0	185.3
SP378	*K. breviceps*	L	135.2	-108.0	-84.5	5.94	260.0	184.1
SP378		R	138.4	-88.7	-92.3	8.45	398.0	163.1
GA1214	*T. truncatus*	L	n/a	n/a	n/a	n/a	n/a	n/a
GA1214		R	n/a	n/a	n/a	n/a	n/a	n/a
GA1248	*T. truncatus*	L	95.9	-41.7	-46.0	n/a	233.9	n/a
GA1248		R	95.8	-34.0	-45.3	n/a	238.7	n/a
GA1289	*T. truncatus*	L	65.7	-61.0	-73.7	7.41	207.4	44.3
GA1289		R	n/a	n/a	-82.0	n/a	n/a	n/a
PA680	*T. truncatus*	L	70.3	-90.0	-69.0	2.75	272.6	87.5
PA680		R	85.4	n/a	-74.0	2.65	n/a	111.6
PA692	*T. truncatus*	L	95.0	-90.0	-90.0	5.25	93.0	146.4
PA692		R	n/a	n/a	n/a	n/a	n/a	n/a
PO432	*T. truncatus*	L	79.3	-59.0	-85.3	4.35	230.9	76.3
PO432		R	79.8	-58.0	-83.3	9.53	236.2	100.5

Table B-2

Stranding identification	Species	Side	PCSA (cm^2)	PMTT (N)	MCSA (cm^2)	MMTT (N)
GA1120	*K. sima*	L	n/a	n/a	n/a	n/a
GA1120		R	n/a	n/a	n/a	n/a
MML-0232	*K. sima*	L	6.79	152.7	11.7	262.4
MML-0232		R	6.79	152.7	n/a	n/a
MML-0233	*K. sima*	L	6.10	137.3	15.9	357.5
MML-0233		R	5.21	117.3	8.30	186.8
PA636	*K. sima*	L	7.13	160.5	12.1	272.9
PA636		R	9.28	208.8	15.6	351.8
PA716	*K. sima*	L	6.83	153.8	17.1	385.4
PA716		R	5.83	131.1	15.9	358.7
CMA-01-04B	*K. breviceps*	L	n/a	n/a	n/a	n/a
CMA-01-04B		R	n/a	n/a	n/a	n/a
SP371	*K. breviceps*	L	8.40	189.1	31.5	709.1
SP371		R	9.30	209.2	29.4	661.6
SP378	*K. breviceps*	L	12.8	289.0	40.3	907.1
SP378		R	11.1	250.1	30.3	682.7
GA1214	*T. truncatus*	L	n/a	n/a	n/a	n/a
GA1214		R	n/a	n/a	n/a	n/a
GA1248	*T. truncatus*	L	n/a	n/a	6.04	135.9
GA1248		R	n/a	n/a	7.08	159.3
GA1289	*T. truncatus*	L	6.36	143.1	12.6	282.4
GA1289		R	6.36	143.1	15.7	352.6
PA680	*T. truncatus*	L	11.7	264.3	n/a	n/a
PA680		R	12.3	277.6	n/a	n/a
PA692	*T. truncatus*	L	14.5	327.0	22.6	508.3
PA692		R	14.5	327.0	n/a	n/a
PO432	*T. truncatus*	L	9.07	204.1	13.6	306.9
PO432		R	11.9	267.2	13.4	301.3

Table B-3

Stranding identification	Species	Side	Length (mm)	Parasagittal angle	Transverse angle	Height (mm)	Width (mm)	Mass (g)
GA1120	*K. sima*	L	89.8	-10.0	6.67	4.94	22.4	37.0
GA1120		R	n/a	-10.0	6.00	n/a	n/a	42.2
MML-0232	*K. sima*	L	149.6	-26.0	6.25	7.32	27.6	19.3
MML-0232		R	138.5	-26.0	5.25	7.46	27.9	16.5
MML-0233	*K. sima*	L	182.2	-14.8	8.2	8.15	27.9	26.9
MML-0233		R	n/a	-14.8	8.2	8.34	27.3	24.5
PA636	*K. sima*	L	103.6	-13.3	4.67	13.3	35.1	15.2
PA636		R	106.9	-12.3	6.00	11.9	39.1	17.5
PA716	*K. sima*	L	131.4	-16.7	8.00	12.0	33.0	29.8
PA716		R	127.6	-16.7	9.33	13.0	35.4	29.3
CMA-01-04B	*K. breviceps*	L	n/a	-22.0	5.67	7.3	21.3	5.11
CMA-01-04B		R	81.2	-22.0	5.67	5.75	21.9	5.38
SP371	*K. breviceps*	L	246.0	-3.25	9.75	9.97	38.7	61.1
SP371		R	254.0	-3.25	15.8	13.5	36.9	56.9
SP378	*K. breviceps*	L	255.0	n/a	n/a	9.49	32.7	44.1
SP378		R	260.0	-22.0	0.00	9.73	39.7	41.3
GA1214	*T. truncatus*	L	262.1	-29.0	0.00	9.99	29.0	49.5
GA1214		R	309.2	n/a	n/a	9.83	26.9	53.1
GA1248	*T. truncatus*	L	215.7	-24.0	0.00	13.3	30.4	39.9
GA1248		R	160.4	n/a	n/a	13.0	31.9	39.8
GA1289	*T. truncatus*	L	222.3	-16.3	-4.67	12.0	24.2	34.9
GA1289		R	246.1	-16.3	-1.00	12.3	22.7	28.2
PA680	*T. truncatus*	L	285.9	-15.0	0.00	14.6	31.0	39.4
PA680		R	n/a	n/a	n/a	15.2	28.5	42.4
PA692	*T. truncatus*	L	154.7	-43.0	-5.00	5.82	76.5	59.1
PA692		R	120.3	-38.3	-2.33	4.25	102.7	46.8
PO432	*T. truncatus*	L	189.3	-20.0	3.33	12.6	31.3	30.8
PO432		R	213.5	-20.0	3.67	9.99	35.1	35.1

Table B-4

Stranding identification	Species	Side	PCSA (cm^2)	PMTT (N)	MCSA (cm^2)	MMTT (N)
GA1120	*K. sima*	L	3.89	87.5	1.09	24.5
GA1120		R	4.43	99.6	n/a	n/a
MML-0232	*K. sima*	L	1.22	27.4	2.27	51.1
MML-0232		R	1.13	25.3	2.31	52.0
MML-0233	*K. sima*	L	1.39	31.3	2.69	60.5
MML-0233		R	1.27	28.6	2.99	67.3
PA636	*K. sima*	L	1.38	31.1	3.71	83.5
PA636		R	1.55	34.8	4.28	96.3
PA716	*K. sima*	L	2.14	48.2	3.21	72.2
PA716		R	2.17	48.8	3.48	78.3
CMA-01-04B	*K. breviceps*	L	0.59	13.4	1.21	27.2
CMA-01-04B		R	0.62	14.1	1.15	25.9
SP371	*K. breviceps*	L	2.34	52.7	7.10	159.8
SP371		R	2.11	47.6	4.18	94.1
SP378	*K. breviceps*	L	1.63	36.7	6.44	145.0
SP378		R	1.50	33.7	4.04	90.8
GA1214	*T. truncatus*	L	1.78	40.0	n/a	n/a
GA1214		R	1.62	36.5	n/a	n/a
GA1248	*T. truncatus*	L	1.74	39.2	3.38	76.1
GA1248		R	2.34	52.6	3.93	88.4
GA1289	*T. truncatus*	L	1.48	33.3	3.64	81.9
GA1289		R	1.08	24.3	4.00	90.0
PA680	*T. truncatus*	L	1.30	29.3	3.23	72.7
PA680		R	1.40	31.5	3.23	72.7
PA692	*T. truncatus*	L	3.60	81.1	4.51	101.4
PA692		R	3.67	82.6	4.49	101.0
PO432	*T. truncatus*	L	1.53	34.5	3.25	73.1
PO432		R	1.55	34.9	2.26	50.9

Table B-5

Stranding identification	Species	Side	Length (mm)	Parasagittal angle	Transverse angle	Height (mm)	Width (mm)	Mass (g)
GA1120	*K. sima*	L	208.7	149.3	12.7	32.5	64.8	289.1
GA1120		R	n/a	149.3	11.0	n/a	n/a	n/a
MML-0232	*K. sima*	L	n/a	n/a	n/a	20.9	56.8	n/a
MML-0232		R	n/a	n/a	n/a	19.0	58.0	n/a
MML-0233	*K. sima*	L	n/a	n/a	n/a	20.4	68.2	n/a
MML-0233		R	n/a	n/a	n/a	20.4	67.2	n/a
PA636	*K. sima*	L	289.0	160.3	11.7	28.9	69.4	n/a
PA636		R	295.6	160.3	9.33	30.3	72.3	363.2
PA716	*K. sima*	L	258.1	159.7	7.00	31.1	67.3	306.3
PA716		R	260.8	159.7	9.33	29.5	63.6	335.3
CMA-01-04B	*K. breviceps*	L	169.1	161.3	9.33	18.3	37.1	74.1
CMA-01-04B		R	149.0	161.3	8.67	18.5	38.2	70.6
SP371	*K. breviceps*	L	370.6	168.3	5.00	32.6	88.9	572.0
SP371		R	346.0	164.5	5.00	32.7	87.0	534.0
SP378	*K. breviceps*	L	n/a	n/a	n/a	28.4	81.7	n/a
SP378		R	n/a	n/a	n/a	25.1	101.1	n/a
GA1214	*T. truncatus*	L	n/a	n/a	n/a	11.6	114.1	n/a
GA1214		R	n/a	n/a	n/a	13.8	94.2	n/a
GA1248	*T. truncatus*	L	230.6	149.7	8.33	32.2	59.6	235.9
GA1248		R	235.5	149.7	6.00	32.7	42.0	250.6
GA1289	*T. truncatus*	L	207.7	157.3	12.7	27.3	56.3	184.9
GA1289		R	206.8	157.3	10.7	28.4	55.9	191.4
PA680	*T. truncatus*	L	255.0	n/a	n/a	37.7	44.2	248.8
PA680		R	255.0	29.0	11.0	36.0	43.8	239.9
PA692	*T. truncatus*	L	n/a	145.3	4.33	42.6	58.3	430.4
PA692		R	281.8	145.3	4.33	29.6	80.0	478.6
PO432	*T. truncatus*	L	177.8	160.3	10.7	28.4	68.4	239.6
PO432		R	209.1	160.3	5.67	27.9	61.0	240.3

Table B-6

Stranding identification	Species	Side	PCSA (cm^2)	PMTT (N)	MCSA (cm^2)	MMTT (N)
GA1120	*K. sima*	L	13.1	294.1	17.6	395.3
GA1120		R	13.1	294.1	n/a	n/a
MML-0232	*K. sima*	L	n/a	n/a	15.1	340.4
MML-0232		R	n/a	n/a	14.3	322.0
MML-0233	*K. sima*	L	n/a	n/a	15.9	357.5
MML-0233		R	n/a	n/a	18.2	408.4
PA636	*K. sima*	L	n/a	n/a	19.7	443.7
PA636		R	11.6	260.8	18.8	422.4
PA716	*K. sima*	L	11.2	251.9	17.9	401.6
PA716		R	12.1	272.9	15.1	338.9
CMA-01-04B	*K. breviceps*	L	4.13	93.0	6.30	141.8
CMA-01-04B		R	4.47	100.6	6.68	150.3
SP371	*K. breviceps*	L	14.6	327.6	28.2	634.1
SP371		R	14.6	327.6	34.0	765.5
SP378	*K. breviceps*	L	n/a	n/a	32.4	728.8
SP378		R	n/a	n/a	39.3	885.3
GA1214	*T. truncatus*	L	n/a	n/a	n/a	n/a
GA1214		R	n/a	n/a	n/a	n/a
GA1248	*T. truncatus*	L	9.65	217.2	12.2	273.4
GA1248		R	10.0	225.8	13.9	311.9
GA1289	*T. truncatus*	L	8.40	189.0	17.9	402.8
GA1289		R	8.73	196.5	17.7	397.6
PA680	*T. truncatus*	L	9.20	207.1	18.5	415.4
PA680		R	8.88	199.7	16.8	378.2
PA692	*T. truncatus*	L	14.4	324.2	26.8	602.5
PA692		R	16.0	360.5	25.0	562.7
PO432	*T. truncatus*	L	12.7	286.1	15.3	344.7
PO432		R	10.8	244.0	16.1	361.4

Table B-7

Stranding identification	Species	Side	Length (mm)	Parasagittal angle	Transverse angle	Height (mm)	Width (mm)	Mass (g)
GA1120	*K. sima*	L	n/a	-170.7	-9.67	n/a	n/a	8.07
GA1120		R	86.5	-170.7	-8.67	6.22	34.2	9.59
MML-0232	*K. sima*	L	69.0	-175.3	-9.00	4.92	23.8	4.27
MML-0232		R	58.2	-173.8	-15.0	5.33	22.1	3.07
MML-0233	*K. sima*	L	121.3	-174.0	-18.3	4.31	21.8	7.48
MML-0233		R	112.2	-174.3	-11.5	4.53	23.0	7.21
PA636	*K. sima*	L	78.9	-172.7	-12.3	9.68	30.6	9.42
PA636		R	89.7	-173.0	-13.3	6.52	32.1	10.1
PA716	*K. sima*	L	84.4	-158.0	-26.0	5.58	24.6	7.24
PA716		R	86.4	-155.0	-15.0	5.87	28.7	9.30
CMA-01-04B	*K. breviceps*	L	66.4	-168.0	-5.00	6.34	15.7	2.80
CMA-01-04B		R	68.4	-165.0	-5.67	6.00	19.2	4.34
SP371	*K. breviceps*	L	161.0	-148.8	-10.3	5.37	28.5	21.1
SP371		R	168.9	-161.8	-5.00	6.03	34.8	23.0
SP378	*K. breviceps*	L	111.4	-158.5	-3.33	7.40	29.4	18.4
SP378		R	106.1	-158.5	-4.67	9.20	28.0	19.5
GA1214	*T. truncatus*	L	61.3	-170.0	-6.00	4.63	39.1	8.79
GA1214		R	69.6	-170.0	-11.0	4.41	40.8	10.2
GA1248	*T. truncatus*	L	56.6	n/a	n/a	6.51	35.9	6.61
GA1248		R	53.8	-114.0	-54.0	8.32	42.0	9.48
GA1289	*T. truncatus*	L	48.3	-161.0	-3.67	7.13	34.2	6.56
GA1289		R	47.0	-152.0	-6.33	6.64	29.1	5.72
PA680	*T. truncatus*	L	68.6	-158.0	-22.0	3.48	36.7	7.05
PA680		R	68.8	-158.0	-29.0	4.65	36.0	8.84
PA692	*T. truncatus*	L	74.9	-157.3	-10.0	3.94	38.7	9.47
PA692		R	84.7	n/a	n/a	4.73	32.9	8.07
PO432	*T. truncatus*	L	63.9	-162.3	-11.3	4.74	37.5	8.39
PO432		R	56.2	-157.0	-12.7	6.06	37.6	9.06

Table B-8

Stranding identification	Species	Side	PCSA (cm^2)	PMTT (N)	MCSA (cm^2)	MMTT (N)
GA1120	*K. sima*	L	0.88	19.8	n/a	n/a
GA1120		R	1.05	23.5	2.09	47.0
MML-0232	*K. sima*	L	0.58	13.1	1.68	37.8
MML-0232		R	0.50	11.2	1.93	43.4
MML-0233	*K. sima*	L	0.58	13.1	2.00	45.1
MML-0233		R	0.61	13.6	1.99	44.8
PA636	*K. sima*	L	1.13	25.3	2.52	56.7
PA636		R	1.07	24.0	1.56	35.1
PA716	*K. sima*	L	0.81	18.2	1.06	23.9
PA716		R	1.01	22.8	1.45	32.6
CMA-01-04B	*K. breviceps*	L	0.40	8.9	0.813	18.3
CMA-01-04B		R	0.60	13.5	n/a	n/a
SP371	*K. breviceps*	L	1.24	27.8	2.78	62.5
SP371		R	1.28	28.9	2.48	55.9
SP378	*K. breviceps*	L	1.56	35.1	2.72	61.1
SP378		R	1.74	39.0	3.80	85.6
GA1214	*T. truncatus*	L	1.35	30.4	n/a	n/a
GA1214		R	1.38	31.0	n/a	n/a
GA1248	*T. truncatus*	L	1.10	24.8	1.87	42.1
GA1248		R	1.66	37.4	2.61	58.7
GA1289	*T. truncatus*	L	1.28	28.9	2.34	52.7
GA1289		R	1.15	25.8	1.37	30.8
PA680	*T. truncatus*	L	0.97	21.8	3.12	70.2
PA680		R	1.21	27.3	3.12	70.2
PA692	*T. truncatus*	L	1.19	26.8	1.88	42.4
PA692		R	0.90	20.2	2.09	47.1
PO432	*T. truncatus*	L	1.24	27.9	1.78	40.1
PO432		R	1.52	34.2	2.15	48.4

Table B-9

Stranding identification	Species	Side	Length (mm)	Parasagittal angle	Transverse angle	Height (mm)	Width (mm)	Mass (g)
GA1214	*T. truncatus*	L	n/a	n/a	n/a	n/a	n/a	n/a
GA1214		R	44.9	-83.0	-37.0	14.7	2.68	1.72
GA1248	*T. truncatus*	L	32.2	-61.3	-47.0	13.8	3.65	1.43
GA1248		R	41.8	-47.3	-37.7	13.4	4.76	1.68
GA1289	*T. truncatus*	L	34.9	-111.3	-110.7	13.5	6.61	1.83
GA1289		R	31.8	-79.7	-82.0	12.2	5.90	1.38
PA680	*T. truncatus*	L	50.6	-68.0	-56.0	7.10	2.80	0.840
PA680		R	59.5	-90.0	-86.0	4.46	3.61	1.28
PA692	*T. truncatus*	L	15.7	-73.7	-54.0	15.7	4.92	2.82
PA692		R	14.5	-74.7	-43.3	14.5	3.64	2.13
PO432	*T. truncatus*	L	35.2	-63.3	-38.3	9.63	4.90	1.15
PO432		R	40.2	-56.3	-34.0	9.64	3.50	0.840

Table B-10

Stranding identification	Species	Side	PCSA (cm^2)	PMTT (N)	MCSA (cm^2)	MMTT (N)
GA1214	*T. truncatus*	L	0.36	8.13	n/a	n/a
GA1214		R	0.36	8.13	n/a	n/a
GA1248	*T. truncatus*	L	0.42	9.43	0.520	11.7
GA1248		R	0.38	8.54	0.710	16.0
GA1289	*T. truncatus*	L	0.50	11.1	n/a	n/a
GA1289		R	0.41	9.21	n/a	n/a
PA680	*T. truncatus*	L	0.16	3.53	n/a	n/a
PA680		R	0.20	4.57	n/a	n/a
PA692	*T. truncatus*	L	1.70	38.2	1.64	36.9
PA692		R	1.38	31.1	1.57	35.3
PO432	*T. truncatus*	L	0.31	6.93	0.390	8.8
PO432		R	0.20	4.44	0.300	6.8

Table B-11

Stranding identification	Species	Side	Length (mm)	Parasagittal angle	Transverse angle	Height (mm)	Width (mm)	Mass (g)
GA1120	*K. sima*	L	n/a	143.0	-14.3	n/a	n/a	8.92
GA1120		R	n/a	121.0	-11.3	n/a	n/a	10.1
MML-0232	*K. sima*	L	n/a	155.3	-5.00	4.46	12.3	n/a
MML-0232		R	107.3	145.5	-6.25	2.97	12.5	6.16
MML-0233	*K. sima*	L	106.8	145.0	-9.50	5.05	12.4	5.35
MML-0233		R	125.2	144.0	-4.50	3.42	13.4	9.37
PA636	*K. sima*	L	93.0	146.3	-8.00	3.78	12.9	4.49
PA636		R	86.6	136.7	-6.00	5.45	11.9	4.62
PA716	*K. sima*	L	156.7	164.7	-12.7	9.81	25.3	10.0
PA716		R	155.1	162.7	-10.3	8.80	28.6	9.25
CMA-01-04B	*K. breviceps*	L	n/a	n/a	n/a	n/a	n/a	n/a
CMA-01-04B		R	n/a	n/a	n/a	n/a	n/a	n/a
SP371	*K. breviceps*	L	113.8	128.5	-34.0	3.97	35.2	12.3
SP371		R	133.8	131.5	-33.3	3.25	30.9	14.6
SP378	*K. breviceps*	L	93.5	125.0	-21.5	3.18	57.8	12.2
SP378		R	205.5	n/a	n/a	4.49	39.9	29.3
GA1214	*T. truncatus*	L	174.8	154.0	-6.00	8.79	63.7	31.6
GA1214		R	129.8	143.0	-6.00	4.89	70.9	26.5
GA1248	*T. truncatus*	L	126.1	147.7	-2.00	3.16	74.8	47.6
GA1248		R	116.3	142.3	-3.00	5.05	74.8	45.4
GA1289	*T. truncatus*	L	161.8	154.7	-1.33	7.87	48.4	33.9
GA1289		R	165.0	150.3	-3.00	7.83	50.9	37.4
PA680	*T. truncatus*	L	124.6	155.0	0.00	6.36	79.0	35.5
PA680		R	138.9	n/a	n/a	4.05	73.4	38.6
PA692	*T. truncatus*	L	253.5	163.3	-4.00	10.8	35.8	67.0
PA692		R	246.8	162.3	-3.00	9.33	33.6	53.5
PO432	*T. truncatus*	L	188.6	143.3	-30.3	8.89	56.2	48.2
PO432		R	154.7	140.3	-28.7	n/a	n/a	52.7

Table B-12

Stranding identification	Species	Side	PCSA (cm^2)	PMTT (N)	MCSA (cm^2)	MMTT (N)
GA1120	*K. sima*	L	n/a	n/a	n/a	n/a
GA1120		R	n/a	n/a	n/a	n/a
MML-0232	*K. sima*	L	0.54	12.2	1.15	25.8
MML-0232		R	0.54	12.2	0.920	20.7
MML-0233	*K. sima*	L	0.47	10.6	1.06	23.8
MML-0233		R	0.71	15.9	n/a	n/a
PA636	*K. sima*	L	0.46	10.3	0.710	16.0
PA636		R	0.50	11.3	n/a	n/a
PA716	*K. sima*	L	0.60	13.6	0.700	15.8
PA716		R	0.56	12.7	0.810	18.2
CMA-01-04B	*K. breviceps*	L	n/a	n/a	n/a	n/a
CMA-01-04B		R	n/a	n/a	n/a	n/a
SP371	*K. breviceps*	L	1.02	22.9	2.16	48.6
SP371		R	1.03	23.2	2.51	56.5
SP378	*K. breviceps*	L	1.23	27.6	2.42	54.4
SP378		R	1.34	30.2	3.54	79.7
GA1214	*T. truncatus*	L	1.70	38.3	n/a	n/a
GA1214		R	1.93	43.3	n/a	n/a
GA1248	*T. truncatus*	L	3.56	80.1	3.79	85.3
GA1248		R	3.68	82.8	3.68	82.8
GA1289	*T. truncatus*	L	1.98	44.5	0.560	12.6
GA1289		R	2.14	48.1	n/a	n/a
PA680	*T. truncatus*	L	2.69	60.4	n/a	n/a
PA680		R	2.62	59.0	n/a	n/a
PA692	*T. truncatus*	L	2.49	56.1	3.36	75.5
PA692		R	2.05	46.0	3.85	86.6
PO432	*T. truncatus*	L	2.41	54.3	n/a	n/a
PO432		R	3.21	72.3	5.36	120.6

Table B-13

Stranding identification	Species	Side	Length (mm)	Parasagittal angle	Transverse angle	Height (mm)	Width (mm)	Mass (g)
GA1120	*K. sima*	L	n/a	-160.3	146.3	n/a	n/a	37.8
GA1120		R	17.3	-157.7	159.3	35.2	113.0	37.4
MML-0232	*K. sima*	L	11.6	-143.0	149.3	23.3	135.6	26.1
MML-0232		R	10.8	-136.3	164.0	32.0	119.7	22.8
MML-0233	*K. sima*	L	12.6	n/a	n/a	35.2	137.2	36.6
MML-0233		R	12.7	n/a	n/a	37.6	140.5	32.2
PA636	*K. sima*	L	18.7	-110.7	172.7	25.7	142.7	42.1
PA636		R	11.7	-130.0	172.0	25.1	139.0	38.5
PA716	*K. sima*	L	20.5	-125.7	169.3	44.2	125.6	44.9
PA716		R	26.3	-123.3	170.7	38.3	136.0	50.1
CMA-01-04B	*K. breviceps*	L	8.03	-139.3	95.3	23.3	69.3	7.72
CMA-01-04B		R	9.80	-138.0	104.7	16.0	63.7	7.24
SP371	*K. breviceps*	L	14.2	-146.0	167.3	34.8	227.0	77.1
SP371		R	9.42	-146.3	114.5	18.9	165.0	25.6
SP378	*K. breviceps*	L	n/a	n/a	n/a	n/a	n/a	n/a
SP378		R	n/a	n/a	n/a	n/a	n/a	n/a
GA1214	*T. truncatus*	L	n/a	n/a	n/a	n/a	n/a	n/a
GA1214		R	n/a	n/a	n/a	n/a	n/a	n/a
GA1248	*T. truncatus*	L	13.1	-120.0	n/a	19.7	103.6	20.1
GA1248		R	16.0	-129.7	n/a	25.5	91.4	22.7
GA1289	*T. truncatus*	L	11.1	-159.7	155.7	15.8	98.3	13.6
GA1289		R	12.4	-158.3	152.0	14.5	97.4	12.5
PA680	*T. truncatus*	L	n/a	n/a	n/a	n/a	n/a	n/a
PA680		R	n/a	n/a	n/a	n/a	n/a	n/a
PA692	*T. truncatus*	L	7.61	-131.0	180.0	48.1	91.4	30.6
PA692		R	12.3	-138.3	180.0	46.1	82.9	31.2
PO432	*T. truncatus*	L	9.81	-135.7	152.3	22.8	100.2	14.0
PO432		R	13.3	-118.3	157.7	25.7	100.3	15.3

Table B-14

Stranding identification	Species	Side	PCSA (cm^2)	PMTT (N)
GA1120	*K. sima*	L	20.6	464.0
GA1120		R	20.4	459.8
MML0232	*K. sima*	L	21.1	475.6
MML0232		R	19.9	448.3
MML0233	*K. sima*	L	27.4	617.1
MML0233		R	24.0	540.6
PA636	*K. sima*	L	21.2	477.4
PA636		R	31.1	699.7
PA716	*K. sima*	L	20.6	464.5
PA716		R	18.0	404.4
CMA0104B	*K. breviceps*	L	9.07	204.1
CMA0104B		R	6.97	156.8
SP371	*K. breviceps*	L	51.2	1152.5
SP371		R	25.6	576.9
SP378	*K. breviceps*	L	n/a	n/a
SP378		R	n/a	n/a
GA1214	*T. truncatus*	L	n/a	n/a
GA1214		R	n/a	n/a
GA1248	*T. truncatus*	L	14.5	325.9
GA1248		R	13.4	301.5
GA1289	*T. truncatus*	L	11.5	259.6
GA1289		R	9.47	213.1
PA680	*T. truncatus*	L	n/a	n/a
PA680		R	n/a	n/a
PA692	*T. truncatus*	L	37.9	852.1
PA692		R	23.9	537.2
PO432	*T. truncatus*	L	13.5	302.9
PO432		R	10.9	245.0

Table B-15

Stranding identification	Species	Side	Length (mm)	Parasagittal angle	Transverse angle	Height (mm)	Width (mm)	Mass (g)
GA1120	*K. sima*	L	n/a	-8.67	3.00	n/a	n/a	27.3
GA1120		R	140.4	-6.67	3.67	11.9	25.8	32.7
MML-0232	*K. sima*	L	130.0	-13.8	-3.00	7.29	20.5	14.4
MML-0232		R	139.7	-19.8	-3.75	6.50	24.6	12.4
MML-0233	*K. sima*	L	162.0	-7.75	-10.8	7.76	12.1	20.6
MML-0233		R	152.2	-7.75	-4.00	6.60	22.2	21.1
PA636	*K. sima*	L	134.0	-11.3	0.00	8.27	22.1	19.0
PA636		R	131.0	-11.7	n/a	9.87	25.7	19.6
PA716	*K. sima*	L	138.6	-5.33	4.33	16.9	32.6	25.7
PA716		R	126.2	-5.33	9.00	15.6	37.5	27.3
CMA-01-04B	*K. breviceps*	L	90.5	-11.0	3.33	10.4	16.8	11.7
CMA-01-04B		R	88.3	-11.0	5.33	9.44	19.2	11.4
SP371	*K. breviceps*	L	245.0	-4.75	-4.75	8.75	19.8	42.4
SP371		R	276.0	-9.25	-10	8.00	23.7	59.1
SP378	*K. breviceps*	L	201.0	-5.00	0.00	9.51	29.8	53.3
SP378		R	208.8	-4.33	0.00	9.12	32.7	51.7
GA1214	*T. truncatus*	L	n/a	-13.0	-14	n/a	n/a	n/a
GA1214		R	265.1	-23.0	-9.00	3.65	29.7	30.3
GA1248	*T. truncatus*	L	140.1	n/a	-6.33	10.6	31.3	30.8
GA1248		R	188.0	n/a	-6.33	9.34	37.1	49.2
GA1289	*T. truncatus*	L	254.7	-9.33	-4.00	7.44	15.7	21.7
GA1289		R	198.4	-11.7	-6.00	9.61	27.5	34.3
PA680	*T. truncatus*	L	198.4	-22.0	0.00	11.2	23.8	45.9
PA680		R	277.6	-22.0	n/a	8.66	17.4	52.0
PA692	*T. truncatus*	L	188.3	-6.67	0.00	4.63	23.5	29.5
PA692		R	185.9	-6.67	0.00	4.42	23.8	28.0
PO432	*T. truncatus*	L	207.7	-9.00	1.00	7.70	35.5	32.4
PO432		R	177.6	-9.00	n/a	7.15	29.8	23.7

Table B-16

Stranding identification	Species	Side	PCSA (cm^2)	PMTT (N)	MCSA (cm^2)	MMTT (N)
GA1120	*K. sima*	L	1.34	30.1	n/a	n/a
GA1120		R	1.41	31.7	2.68	60.3
MML-0232	*K. sima*	L	1.75	39.3	3.83	86.1
MML-0232		R	2.04	45.8	2.47	55.6
MML-0233	*K. sima*	L	1.22	27.4	2.32	52.2
MML-0233		R	1.22	27.5	2.45	55.1
PA636	*K. sima*	L	1.63	36.7	1.81	40.8
PA636		R	2.02	45.5	2.25	50.6
PA716	*K. sima*	L	2.50	56.3	2.48	55.8
PA716		R	2.34	52.6	3.20	72.0
CMA-01-04B	*K. breviceps*	L	1.84	41.3	1.57	35.3
CMA-01-04B		R	2.20	49.5	1.60	36.0
SP371	*K. breviceps*	L	1.05	23.6	3.42	76.9
SP371		R	0.84	18.9	1.59	35.8
SP378	*K. breviceps*	L	1.20	26.9	3.57	80.3
SP378		R	1.31	29.5	3.71	83.4
GA1214	*T. truncatus*	L	n/a	n/a	n/a	n/a
GA1214		R	1.08	24.2	n/a	n/a
GA1248	*T. truncatus*	L	2.07	46.7	3.07	69.1
GA1248		R	2.47	55.6	2.97	66.8
GA1289	*T. truncatus*	L	0.80	18.1	1.56	35.1
GA1289		R	1.63	36.7	1.98	44.6
PA680	*T. truncatus*	L	2.19	49.2	n/a	n/a
PA680		R	1.77	39.7	n/a	n/a
PA692	*T. truncatus*	L	1.48	33.3	2.06	46.2
PA692		R	1.42	32.0	1.93	43.4
PO432	*T. truncatus*	L	1.47	33.1	2.04	45.9
PO432		R	1.26	28.3	1.84	41.4

Table B-17

Stranding identification	Species	Side	Length (mm)	Parasagittal angle	Transverse angle	Height (mm)	Width (mm)	Mass (g)
GA1120	*K. sima*	L	107.2	-8.67	-15.7	13.1	3.73	6.99
GA1120		R	n/a	-6.67	-21.7	n/a	n/a	5.40
MML-0232	*K. sima*	L	145.5	-13.8	-11.8	8.27	2.86	6.75
MML-0232		R	140.5	-19.8	-16.8	9.37	3.94	5.30
MML-0233	*K. sima*	L	117.2	-7.75	-19.0	10.2	3.20	6.12
MML-0233		R	115.1	-7.75	-15.3	6.72	3.60	3.36
PA636	*K. sima*	L	158.9	-11.3	-25.0	14.4	6.58	9.44
PA636		R	142.6	-11.7	-11.7	11.0	4.42	6.55
PA716	*K. sima*	L	168.8	-5.33	-14.0	16.2	9.19	7.97
PA716		R	161.0	-5.33	-12.0	18.1	8.37	8.58
CMA-01-04B	*K. breviceps*	L	n/a	n/a	n/a	n/a	n/a	n/a
CMA-01-04B		R	97.5	-11.0	-5.00	9.76	4.99	4.30
SP371	*K. breviceps*	L	n/a	-4.75	-9.75	15.1	5.47	25.1
SP371		R	215.0	-9.25	-5.25	15.1	4.28	29.0
SP378	*K. breviceps*	L	180.1	-5.00	-4.00	27.9	6.79	25.2
SP378		R	212.8	-4.33	-4.25	15.7	3.22	17.2
GA1214	*T. truncatus*	L	182.3	-13.0	-32.0	27.7	3.17	18.3
GA1214		R	191.2	-23.0	-13.0	18.6	4.72	17.4
GA1248	*T. truncatus*	L	194.5	n/a	-7.33	16.8	6.29	23.0
GA1248		R	189.0	n/a	-9.67	21.4	5.28	21.7
GA1289	*T. truncatus*	L	196.3	-9.33	-12.7	20.5	10.2	24.2
GA1289		R	245.8	-11.7	-8.33	19.1	4.90	26.4
PA680	*T. truncatus*	L	189.6	-22.0	-15.0	14.2	4.47	15.8
PA680		R	193.0	-22.0	-12.0	12.5	4.79	17.6
PA692	*T. truncatus*	L	200.9	-6.67	-12.0	19.0	7.95	28.7
PA692		R	192.2	-6.67	-9.67	21.5	5.40	28.8
PO432	*T. truncatus*	L	218.3	-9.00	-10.3	17.8	6.36	23.3
PO432		R	196.0	-9.00	-11.0	21.2	4.97	18.2

Table B-18

Stranding identification	Species	Side	PCSA (cm^2)	PMTT (N)	MCSA (cm^2)	MMTT (N)
GA1120	*K. sima*	L	0.62	13.8	0.57	12.8
GA1120		R	0.48	10.7	n/a	n/a
MML-0232	*K. sima*	L	0.44	9.8	0.74	16.7
MML-0232		R	0.36	8.0	0.42	9.5
MML-0233	*K. sima*	L	0.49	11.1	0.59	13.3
MML-0233		R	0.28	6.2	0.33	7.4
PA636	*K. sima*	L	0.56	12.6	0.78	17.5
PA636		R	0.43	9.7	0.51	11.5
PA716	*K. sima*	L	0.45	10.0	0.42	9.5
PA716		R	0.50	11.3	0.51	11.5
CMA-01-04B	*K. breviceps*	L	0.42	9.4	n/a	n/a
CMA-01-04B		R	0.42	9.4	0.58	13.0
SP371	*K. breviceps*	L	1.10	24.8	1.77	39.8
SP371		R	1.27	28.6	1.22	27.5
SP378	*K. breviceps*	L	1.32	29.7	5.45	122.6
SP378		R	0.76	17.1	1.42	31.9
GA1214	*T. truncatus*	L	0.95	21.3	n/a	n/a
GA1214		R	0.86	19.3	n/a	n/a
GA1248	*T. truncatus*	L	1.12	25.1	0.94	21.2
GA1248		R	1.08	24.4	0.83	18.7
GA1289	*T. truncatus*	L	1.17	26.2	0.44	9.9
GA1289		R	1.01	22.8	0.45	10.1
PA680	*T. truncatus*	L	0.79	17.7	1.45	32.6
PA680		R	0.86	19.4	1.45	32.6
PA692	*T. truncatus*	L	1.35	30.4	1.77	39.8
PA692		R	1.41	31.8	1.65	37.1
PO432	*T. truncatus*	L	1.01	22.6	0.84	18.9
PO432		R	0.88	19.7	0.78	17.6

Table B-19

Stranding identification	Species	Side	Length (mm)	Parasagittal angle	Transverse angle	Height (mm)	Width (mm)	Mass (g)
GA1120	*K. sima*	L	139.4	n/a	n/a	32.8	12.0	38.1
GA1120		R	n/a	n/a	n/a	n/a	n/a	34.9
MML-0232	*K. sima*	L	n/a	n/a	n/a	29.4	11.0	n/a
MML-0232		R	n/a	n/a	n/a	30.5	12.0	n/a
MML-0233	*K. sima*	L	92.2	n/a	n/a	33.7	12.0	30.2
MML-0233		R	112.1	n/a	n/a	25.5	14.1	35.1
PA636	*K. sima*	L	184.9	148.7	-6.00	34.4	16.3	74.2
PA636		R	187.4	n/a	n/a	30.8	14.8	n/a
PA716	*K. sima*	L	n/a	n/a	n/a	37.9	13.8	n/a
PA716		R	154.7	147.7	-6.67	38.2	16.9	76.3
CMA-01-04B	*K. breviceps*	L	134.6	159.7	-1.67	15.6	7.17	15.8
CMA-01-04B		R	120.8	157.7	-3.00	19.8	6.89	13.8
SP371	*K. breviceps*	L	242.5	148.0	-18.5	37.5	10.5	93.1
SP371		R	240.0	147.8	-6.75	18.7	12.2	53.4
SP378	*K. breviceps*	L	n/a	n/a	n/a	n/a	n/a	n/a
SP378		R	n/a	n/a	n/a	n/a	n/a	n/a
GA1214	*T. truncatus*	L	n/a	n/a	n/a	n/a	n/a	n/a
GA1214		R	n/a	n/a	n/a	n/a	n/a	n/a
GA1248	*T. truncatus*	L	152.5	151.0	-2.67	20.4	8.82	23.0
GA1248		R	153.2	143.7	-2.33	23.6	9.35	24.8
GA1289	*T. truncatus*	L	135.6	158.0	3.67	20.7	11.3	25.0
GA1289		R	133.0	153.3	3.33	25.2	9.36	23.9
PA680	*T. truncatus*	L	154.6	86.0	-8.00	21.7	13.7	27.5
PA680		R	167.5	n/a	n/a	n/a	n/a	30.1
PA692	*T. truncatus*	L	185.3	140.0	0.00	21.9	9.01	35.7
PA692		R	180.7	140.0	n/a	22.1	9.30	33.3
PO432	*T. truncatus*	L	138.0	151.0	0.00	27.0	9.10	25.9
PO432		R	161.8	151.0	0.00	23.6	8.21	30.6

Table B-20

Stranding identification	Species	Side	PCSA (cm^2)	PMTT (N)	MCSA (cm^2)	MMTT (N)
GA1120	*K. sima*	L	2.58	58.0	3.18	71.6
GA1120		R	2.36	53.1	n/a	n/a
MML-0232	*K. sima*	L	n/a	n/a	3.99	89.8
MML-0232		R	n/a	n/a	4.06	91.3
MML-0233	*K. sima*	L	3.10	69.6	4.13	93.0
MML-0233		R	2.95	66.4	3.76	84.5
PA636	*K. sima*	L	3.79	85.2	4.63	104.2
PA636		R	3.74	84.1	3.90	87.7
PA716	*K. sima*	L	4.65	104.7	3.98	89.6
PA716		R	4.65	104.7	4.86	109.4
CMA-01-04B	*K. breviceps*	L	1.10	24.8	1.17	26.3
CMA-01-04B		R	1.08	24.2	1.27	28.6
SP371	*K. breviceps*	L	3.62	81.5	6.13	137.9
SP371		R	2.10	47.2	n/a	n/a
SP378	*K. breviceps*	L	n/a	n/a	n/a	n/a
SP378		R	n/a	n/a	n/a	n/a
GA1214	*T. truncatus*	L	n/a	n/a	n/a	n/a
GA1214		R	n/a	n/a	n/a	n/a
GA1248	*T. truncatus*	L	1.42	32.0	1.56	35.1
GA1248		R	1.52	34.3	2.22	50.0
GA1289	*T. truncatus*	L	1.74	39.2	4.68	105.3
GA1289		R	1.69	38.1	3.92	88.2
PA680	*T. truncatus*	L	1.68	37.8	2.99	67.3
PA680		R	1.70	38.1	2.85	64.1
PA692	*T. truncatus*	L	1.82	40.9	2.48	55.8
PA692		R	1.74	39.1	2.43	54.7
PO432	*T. truncatus*	L	1.77	39.8	1.84	41.4
PO432		R	1.79	40.2	1.70	38.3

Table B-21

Stranding identification	Species	Side	Length (mm)	Parasagittal angle	Transverse angle	Height (mm)	Width (mm)	Mass (g)
GA1214	*T. truncatus*	L	n/a	n/a	n/a	n/a	n/a	n/a
GA1214		R	n/a	n/a	n/a	n/a	n/a	n/a
GA1248	*T. truncatus*	L	55.0	141.3	15.7	5.61	29.9	4.17
GA1248		R	50.7	133.7	16.3	3.86	27.7	3.29
GA1289	*T. truncatus*	L	45.7	137.3	35.3	4.62	36.1	4.30
GA1289		R	39.4	130.3	25.3	4.59	26.8	3.02
PA680	*T. truncatus*	L	49.5	153.0	26.0	1.79	43.8	5.28
PA680		R	62.3	130.0	28.0	3.83	44.1	5.93
PA692	*T. truncatus*	L	67.6	143.7	5.33	3.60	42.1	6.04
PA692		R	68.2	143.7	11.0	3.80	43.8	5.32
PO432	*T. truncatus*	L	63.5	149.3	18.3	4.11	38.5	7.07
PO432		R	51.1	138.0	10.3	3.86	39.2	5.82

Table B-22

Stranding identification	Species	Side	PCSA (cm^2)	PMTT (N)	MCSA (cm^2)	MMTT (N)
GA1214	*T. truncatus*	L	n/a	n/a	n/a	n/a
GA1214		R	n/a	n/a	n/a	n/a
GA1248	*T. truncatus*	L	0.72	16.1	0.980	22.1
GA1248		R	0.61	13.8	1.02	23.0
GA1289	*T. truncatus*	L	0.89	20.0	n/a	n/a
GA1289		R	0.72	16.3	n/a	n/a
PA680	*T. truncatus*	L	1.01	22.6	2.09	47.0
PA680		R	0.90	20.2	2.09	47.0
PA692	*T. truncatus*	L	0.84	19.0	1.64	36.9
PA692		R	0.74	16.6	1.57	35.3
PO432	*T. truncatus*	L	1.05	23.6	1.84	41.4
PO432		R	1.07	24.2	1.45	32.6

VITA

Brian Edward Bloodworth was born the son of Dr. and Mrs. K. E. Bloodworth of Helotes, Texas. After graduating from Junction City High School in Junction City, Kansas in 1996, he enrolled in the Bachelor of Science program at Texas A&M University at Galveston majoring in marine biology. During this time, he became the State Lab Coordinator of the Texas Marine Mammal Stranding Network. He graduated in 2000 and was employed in a genetics and biochemistry project at the University of Texas Medical Branch at Galveston before enrolling in the Wildlife and Fisheries Sciences department of Texas A&M to pursue a Master's of Science degree in 2002. He can be contacted in care of Dr. Christopher D. Marshall, Department of Marine Biology, Texas A&M University at Galveston, 5007 Ave. U, Galveston, Texas 77551 USA.